

General Disclaimer

One or more of the Following Statements may affect this Document

- This document has been reproduced from the best copy furnished by the organizational source. It is being released in the interest of making available as much information as possible.
- This document may contain data, which exceeds the sheet parameters. It was furnished in this condition by the organizational source and is the best copy available.
- This document may contain tone-on-tone or color graphs, charts and/or pictures, which have been reproduced in black and white.
- This document is paginated as submitted by the original source.
- Portions of this document are not fully legible due to the historical nature of some of the material. However, it is the best reproduction available from the original submission.

Electrostatic Protection
of the
Solar Power Satellite
and
Rectenna

Report for
NASA Contract NAS8-33023
Prepared for the Marshall Space Flight Center
by
Rice University
Houston, Texas 77001

March 1980

J. W. Freeman
J. W. Freeman, P.I.

A. A. Few, Jr.
A. A. Few, Jr., Co-P.I.

Prepared by:

John W. Freeman
Arthur A. Few, Jr.
Patricia H. Reiff
David Cooke
Jerry Bohannon
Bob Haymes

(NASA-CR-161438) ELECTROSTATIC PROTECTION
OF THE SOLAR POWER SATELLITE AND RECTENNA
(Rice Univ.) 157 p HC A08/MF A01 CSCL 22B

N80-23348

G3/15

Unclassified
19464

Part I

PROTECTION OF THE SOLAR POWER SATELLITE

Abstract

This report examines theoretically several features of the interactions of the Solar Power Satellite (SPS) with its space environment. We calculate the voltages produced at various surfaces due to space plasmas and the plasma leakage currents through the kapton and sapphire solar cell blankets. At geosynchronous orbit (GEO), this parasitic power loss is only 0.7%, and is easily compensated by oversizing. At low-earth orbit, (LEO), the power loss is potentially much larger (3%), and anomalous arcing is expected for the EOTV high voltage negative surfaces. Preliminary results of a three-dimensional self-consistent plasma and electric field computer program are presented, confirming the validity of the predictions made from the one-dimensional models. Lastly, the report considers magnetic shielding of the satellite, to reduce the power drain and to protect the solar cells from energetic electron and plasma ion bombardment. We conclude that minor modifications can allow the SPS to operate safely and efficiently in its space environment. The SPS design employed in this study is the Jan 25, 1978 MSFC baseline design utilizing GaAs solar cells at CR-2 and an aluminum structure. Subsequent design changes will substantially alter the basic conclusions in this report.

Introduction

Space is by no means empty. It contains light, magnetic fields and both neutral and charged particles. The light energy is the raison d'etre for space power generation; but it can also eject photoelectrons from satellite surfaces, giving the surface a positive charge and giving it an effective conductivity (Pelizzari and Criswell, 1978).

Magnetic field strengths in the earth's vicinity range from 6×10^{-5} T (0.6 Gauss) at the earth's poles to 2×10^{-9} T (2γ) in the neutral sheet in the magnetotail ($1\gamma = 10^{-5}$ Gauss). At the geosynchronous orbit, the magnetic field strength is roughly 1×10^{-7} T (100 γ). A magnetic field of this strength causes no threat per se to spacecraft operations; however, it plays a fundamental role in trapping energetic particles. These trapped particles respond not only to the Earth's magnetic field, but spacecraft fields as well, especially for spacecraft large in comparison to particle gyroradii (Reiff, 1976; Reiff and Burke, 1976).

Neutral particles have little effect on spacecraft operations above ~ 600 km; however, neutrals can charge-exchange in the EOTV thruster beam (see below).

Charged particle populations at synchronous orbit are of several types and are illustrated in Figure 1. The innermost region is the plasmasphere, a torus-shaped locus of relatively dense ($\sim 100/\text{cm}^3$), cool ($kT \sim 1$ eV) plasma that has evaporated from the ionosphere. Because of the low energies of the plasmaspheric ions, they are considered harmless (Reasoner et al., 1976); however, they can be accelerated by spacecraft electric fields to energies high enough to do damage (tens of kilovolts). Imbedded in the plasmasphere are the radiation belts, regions of very low density but quite high energy (tens to hundreds of kilovolts) trapped radiation. This radiation can cause hazards to men and solar cells.

The remaining plasma population that can penetrate to geosynchronous orbit is the plasma sheet (Fig. 1). This tenuous plasma ($0.1-1/\text{cm}^3$) is considerably warmer (kT on the order of kiloelectron volts) than the plasmasphere (Garrett and DeForest, 1979). In addition, its presence at geosynchronous orbit is associated with substorm activity, when both the fluxes and energies are higher. It is this kind of plasma that contributes most strongly to spacecraft charging and its concomitant disruption of satellite systems (Inouye, 1976).

This report concentrates on spacecraft charging and its effects on solar power satellite (SPS) systems, in particular the NASA/Marshall Space Flight Center (MSFC) baseline design (Hanley, 1978). "Worst case" plasma environments are used to determine possible charging hazards. Spacecraft charging is the principal focus of this paper since its effects can be severe: arc generation from exceeding breakdown voltages, direct electrical component damage from transients, disruption of logic and switching circuits from electromagnetic interference, change of reflective or thermal control surfaces due to the attraction of outgassed contaminants or pitting, and shock hazards for extravehicular and docking activities (see DeForest, 1972; Pike and Bunn, 1976; Shaw et al., 1976).

We will show that, under substorm conditions, the kapton substrate contemplated for use as a support blanket for the reflectors and solar cells will be subjected to near-breakdown voltage. Additional kapton insulation seems unfeasible because of weight considerations. The alternatives, higher conductivity substrates or conducting leads to the surfaces, seem more reasonable since the resulting parasitic currents are not excessive. The paper also will discuss the optimum point for grounding the spacecraft to the solar panels and outlines a method of using judicious routing of bus-bar currents to shield the satellite from particle bombardment. Although it is possible to use a similar method to magnetically align the satellite with the Earth's magnetic field (counteracting gravity-gradient torques), the fields required seem unreasonably large.

Spacecraft Charging

A body immersed in a plasma will acquire a net charge from unequal fluxes of plasma particles. For most plasmas, the electron and ion densities N_e and N_i are roughly equal, and the electron and ion temperatures T_e and T_i are comparable. Thus the electron flux J_e (proportional to $N_e \sqrt{kT_e/M_e}$) is generally much larger than the ion flux J_i , and the body acquires a negative charge sufficient to bring the currents into balance. For stationary, isothermal, singly-charged plasmas, the equilibrium unlit body potential is roughly $(kT_e/e)\ln(J_e/aJ_i)$ (Whipple, 1965), where a is a parameter (of order unity) depending on the thickness of the sheath. Exposing the body to sunlight causes photoelectrons to be ejected. For most substances, the photoelectron current is on the order of one to four nanoamps per square centimeter. Since this is comparable to or larger than most space plasma electron currents, the surface will tend to acquire a small positive charge. The actual equilibrium potential will

depend on the details of the ion and electron distribution function, however (Whipple, 1976). The fluxes to a sunlit plate immersed in a plasma are shown schematically in Fig. 2. The lit side will tend to charge slightly positive, and the dark side negative.

The NASA MSFC baseline design (Hanley, 1978) is shown in Fig. 3. The surfaces on the satellite are divided into two types: active and passive, depending on whether or not voltages appear on the surface as a result of the satellite's own power supply. Passive surfaces include the solar reflectors and structural members. Active surfaces include the solar cells, interconnects, and bus bars. Active surfaces may attract or repel the ambient ions or electrons depending on the polarity of the surface voltage. Currents reach the passive surfaces only by photoemission and the thermal motion of ions and electrons. (We ignore backscattered and secondary electrons.)

Calculation of Potentials

We make the simplifying assumption of a thin sheath (or 1-dimensional) approximation, i.e., the area collecting plasma is the actual geometrical area of the satellite (no focussing considered). The ambient electron and ion currents, therefore are, simply the thermal currents, given by

$$J_{i,e} = \frac{N_e}{4} \left(\frac{8kT}{\pi M} \right)^{1/2} \quad (1)$$

where N , e , T , and M are the number density, charge, temperature and mass for electrons or protons, depending on which current is calculated.

Parker (1979) has addressed the problem of a large flat-plate solar collector in space. He has found that the thin-sheath approximation is not valid at geosynchronous orbit for active structures. However, in the MSFC design, the passive, grounded reflecting panels form a trough in which the solar cells lie. Since the reflectors are conducting, they have a tendency to confine electric fields from the solar cells within the trough. This reduces the thick-sheath focussing effect because the electric fields do not penetrate significantly into space above the trough, and the reflectors themselves are barriers against plasma fluxes entering from the sides of the trough. Later in the paper we verify this assumption by showing results from a modified version of Parker's PANEL program for the special geometry of the MSFC design.

The analytic calculations below assume, for simplicity,



an intermediate sheath approximation; i.e., no focussing of outside plasma is considered, yet the sheath is large enough that photoelectrons from the reflectors can impact the solar cell, and vice versa.

For GEO, our assumed "worst case" plasma conditions are: $N_e = N_i = 2/cm^3$, $kT_e = 5 \text{ keV}$ and $kT_i = 10 \text{ keV}$ (Inouye, 1976). This yields $J_e = 3 \times 10^{-10} \text{ A/cm}^2$ and $J_i = 1 \times 10^{-11} \text{ A/cm}^2$.

The photoelectron current density was calculated by integrating the product of the photoelectron yield function for synthetic sapphire and the solar spectrum; the resulting photocurrent density J_{pe} is $3 \times 10^{-11} \text{ A/cm}^2$. A similar calculation for aluminum yields roughly the same photoelectron current density.

It is apparent, then, that the photoelectron current will usually dominate for all sunlit surfaces at GEO. The equilibrium potential for such surfaces will be on the order of a few times the average photoelectron energy, from about 1 to 100 V positive, such as is found on the dayside of the moon (Reasoner and Burke, 1972; Freeman and Ibrahim, 1975). Passive sunlit surfaces will attain this voltage; however, for active surfaces, the finite conductivity of the cover surfaces (kapton and sapphire) will prevent this voltage from being obtained, i.e., the surface potential will more nearly follow that of the underlying solar cell.

Nightside potentials are estimated from Chopra's (1961) equation:

$$\phi \approx -\frac{kT_e}{2e} \ln \left(\frac{M_i T_e}{M_e T_i} \right) \quad (2)$$

For the "worst case" described above, this implies a dark-side potential of -17,000 V. Secondary electron emission or backscattering will reduce this potential somewhat. Again, passive surfaces will attain this voltage, but most active surfaces will be more nearly the potential of the underlying solar cell.

The most vulnerable active surfaces on the satellite are the solar cells because the ohmic contacts are separated from the plasma by only tens of micrometers of shielding. Figure 4 shows the dimensions and structure of the solar cell selected in the MSFC design. The GaAlAs cell is supported from below by a kapton blanket and is covered with synthetic sapphire. The sapphire coverglass is 20 μm thick and the kapton blanket is 25 μm thick.

For our study, the solar cell was idealized as a sapphire - active region - kapton sandwich as shown in Fig. 5. Plasma ions were assumed to be attracted to the negatively biased portion of the solar array and plasma electrons to the positively biased portion. Photoelectrons were assumed to leave the negative surface and be attracted to the positive surface. Secondaries were neglected. The currents used were those described previously; we assume a steady state condition. In this case the voltages across the sapphire and kapton dielectrics are the photoelectron and plasma currents multiplied by the resistance of the dielectrics. The assumed resistivity of sapphire is 10^{12} ohm-cm. Based on the measurements of Kennerud (1974) we have approximated the resistivity of kapton by

$$\rho = 9.2 \times 10^{16} \exp -[E/1.1 \text{ KV/mil}] \text{ ohm-cm},$$

where E is the electric field across the kapton in KV/mil. The transcendental equation for the potential difference, V, through the 1-mil kapton layer is $\ln [V/K] = -V/1100$, where K is proportional to the current ($K = 9 \times 10^{16} \times \text{thickness (cm)} \times \text{current (A/cm)}$). This equation was solved numerically. The resulting voltages are shown on Fig. 5: a drop of 949 V through the ion-attracting side, and a drop of 3.3 KV through the electron-attracting side. In no case are the breakdown voltages exceeded; however, the voltage on the positive array is within a factor of 2 of the breakdown voltage. For an electron current ten times larger (which can certainly occur within the satellite's life-span), the voltage drop is 5.4 KV, which is near breakdown. For this reason, we recommend replacing kapton with a higher conductivity material, or else providing a current path from the solar cell to the back side. Conductive coatings will also help reduce spot arcing (McCoy and Konradi, 1979).

Kennerud (1974) and others have found anomalous arcing when solar panels are held at high voltage negative in a plasma. Typical voltages and currents required for such anomalous arcing to take place are 400 volts at 1×10^{-7} A/cm². Our expected ion currents to the negative portion of the solar array at GEO are 1×10^{-11} A/cm². Therefore, we do not anticipate anomalous arcing in the GEO environment.

The MSFC design calls for the reflectors to be constructed from 0.5 mil (12.5 μm) kapton covered with a 400 A film of aluminum. We expect the aluminized front side potential to be fixed at 1 to 100 volts positive by photo-electron emission. Using the same analysis that was applied to the kapton solar cell blanket, we calculate the reflector back side voltage to be approximately -1.7 kV for our standard "worst case" condition, and -2.7 kV for a ten times

larger electron current. The breakdown voltage for 1/2 mil kapton is 3.1 kV, which could be reached with only slightly more severe plasma conditions. Clearly, the backside must also be conducting and electrically connected to the front, or the kapton must be replaced with a higher conductivity material. A summary of the expected voltages on various surfaces during sunlit and eclipse conditions is shown on Fig. 6. Note that during eclipse the entire satellite may charge to high voltage negative. This should be countered by the use of a hot filament electron emitter to bleed electrons from the spacecraft.

Optimizing the Grounding Point

The currents between the satellite and the plasma will adjust until the net current is zero. This means that the flow of current to the positively biased areas must equal that from the negatively biased areas. In a flat plate collector, the balance is between plasma electron currents to the positive portions and plasma ion currents to the negative portions of the array. Since the plasma electron currents are so large, the plate will "float" substantially negative, i.e., the area of the collector with negative potential is much larger than the corresponding positive potential area (Parker, 1979).

In the MSFC design, however, the large aluminum reflectors are also sources and sinks of photoelectrons. Photoelectrons from the reflectors will be attracted to positive portions of the solar cell array and photoelectrons from the negative portions of the solar cell array will be attracted to the neighboring reflector (Figure 7). These electrons will "hop" along the surface (Pelizzetti and Criswell, 1978), adding to the power drain. Thus the photoelectron current becomes the dominant parasitic current, at least in all but the most intense substorm environments.

The large aluminum reflectors make a convenient spacecraft ground, since the sunlit sides will remain a few volts positive with respect to space. To minimize the power drain, the solar cell array should drive no new currents through the reflectors to the plasma. Thus the reflector "ground" should be tied to the solar cells in an optimum way. Accurate calculation of the 3-dimensional electric field pattern and resultant power drain including effects of the space charge and secondaries is a formidable task; an oversimplified argument follows. If A_- is the solar cell area that is negative and A_+ is the solar cell area that is positive, current balance requires

$$(A_-) (J_{pe} + 2J_i) = (A_+) (J_{pe} + 2J_e) \quad (3)$$

or,

$$A_-/A_+ = (J_{pe} + 2J_e)/(J_{pe} + 2J_i).$$

Here we assume that the photoelectron flux from the reflectors to the positive segments is approximately the same as the photoelectron flux from the negative segments to the reflectors. For low plasma-current regions, (e.g., the plasmasphere or the quiet plasmashell) or for cases in which the plasma current is shielded from the surfaces magnetically, the ratio approaches unity. Even for our "worst case," the ratio is only 1.17. Therefore, we recommend grounding the midpoint of the string to the reflectors. On the other hand, at low Earth orbit plasma electron and ion ram fluxes dominate, and the grounding point must be more carefully calculated.

With the ground point determined, the parasitic load can be calculated. The principal parasitic current at GEO is from photoelectrons (Fig. 7), and is calculated to be about 3000 A. Coupled with an average potential drop of 11375 V, this implies a power loss of 34 MW, which is only 0.7% of output power, and is easily manageable by slight oversizing. This percentage power loss is comparable to that (~ 0.1%) from a flat-plate collector (Parker, 1979). Thus optimizing the grounding point at GEO is not critical. As discussed later, however, at LEO optimization could be very important.

Currents at Low-Earth Orbit

An integral part of the SPS concept is the Earth-Orbit Transfer Vehicle (EOTV) which will transfer the SPS to GEO. It is expected to employ a high-voltage solar cell array and to operate primarily in the low-Earth orbit (LEO) environment where the plasma currents are considerably different than GEO. At 400 km altitude, the dominant ion is O^+ with a number density of $10^6/cm^3$ and a temperature of 2000 K (Johnson, 1965). Thus the thermal ion current will be $7 \times 10^{-9} A/cm$ and the thermal electron current will be $3 \times 10^{-7} A/cm$. For these currents, the potentials on the EOTV will be comparable those for which Kennerud (1974) found arcing; therefore, one must expect arcing to take place on negatively-biased surfaces unless a lower-voltage array is used. Indeed, arcing has been observed from insulated surfaces in a LEO simulation vacuum tank test (McCoy and Konradi, 1979). Alternatively, the array could be biased with a minimum of negative surface (grounding the lowest end of the string to the reflectors), but that would be far from the optimum grounding scheme, and would increase parasitic losses by a factor of three.

Spacecraft motion implies a substantial though varying ram flux which will cause an additional parasitic current drain of as much as $2 \times 10^{-7} A/cm^2$. Coupled with the cur-

rent losses due to the thermal currents, the power loss could be as high as ~3%. As noted, however, arcing probably will occur at much lower potentials than those for which 3% power loss would be observed. Parker (1979) has pointed out that sheath and wake effects also could substantially alter the satellite potentials and current flow.

EOTV Parasitic Load Due to Thurster Charge-exchange Ions

An additional source of parasitic current for the EOTV is created by charge-exchange of ionized neutral gas from the thrusters with the energetic ions from the main thruster ion beam. This results in "thermal" ions which may drift into the Langmuir sheath electric field region surrounding the solar cell array. Once into the field they will be accelerated toward the solar cells and produce a parasitic load.

Following an approach outlined by H. R. Kaufman (NASA CR-135099) we have estimated the resulting parasitic load to the EOTV solar array to be 174 MW or 52% (Freeman and Few, 1979). This load is clearly unacceptable but it can easily be mitigated by placing a shield between the thrusters and the solar array. This shield can consist of an aluminized kapton sheet stretched across the end of the EOTV. The shield will need to have a height comparable to the dimensions of the Langmuir sheath, about 500 m. Additionally the low voltage edge of the solar cell array should be located toward the outside. Similar shields should be considered adjacent to the ACS thrusters on the SPS itself.

Non-Steady State

Until now it has been assumed that the charging currents from the plasma are steady. This approach is supported by a study of the time dependent charging of a three-axis stabilized spacecraft by Massaro et al., (1977). For all the surfaces modeled, they found that the greatest differential voltages occurred in the steady state limit, although nearly instantaneous changes in absolute potential were observed. However, in order to evaluate the effects of non-steady charging, we calculated the RC time constant or discharge time of the relevant insulators, sapphire and kapton. The RC decay time is $\rho\epsilon$ where ρ is the resistivity and ϵ the permittivity. For kapton this implies a time constant of 1 hr; for sapphire, 1 sec. Large magnetospheric changes can occur with 1 min - 1 hr time constants (McIlwain, 1974; Inouye, 1976). Therefore, high voltages can build up on the kapton in time intervals short compared to the discharge time. Transient charging is not expected to cause differential charging in excess of the steady state predictions, nevertheless, the large kapton time constant reinforces the previous conclusion that kapton should be replaced with a higher conductivity material.

3-Dimensional Model

All of the foregoing analysis on parasitic loads, plasma induced voltages, etc., is based on one-dimensional plasma theory. More precise results require a three-dimensional self-consistent computer model which takes into account all plasma sources and interactions with reflectors simultaneously. A computer program, "PANEL" written by Dr. Lee Parker (Parker, 1979), provided a convenient starting point for our model of the SPS environment. Preliminary results will be presented here. They are preliminary since we have not yet included the photo-electron current (which we showed to be important), nor have we as yet included space charge effects. Nevertheless, the results demonstrate several important features of the sheath around the SPS troughs.

PANEL utilizes a three-dimensional grid where the satellite is modeled by fixing potentials at selected grid points. Laplace's equation is then satisfied by relaxing the free space potentials until Gauss's law is satisfied for a box surrounding each point. The currents and power losses are obtained by numerically performing the integral

$$J = \int_0^\infty dv \int_0^{\pi/2} d\theta \int_0^{2\pi} d\phi f(v, \theta, \phi) v^3 \cos\theta \sin\theta$$

where J is the current density, and f is the distribution function. The problem is then to evaluate f . For a collisionless steady state plasma, the Vlasov equation

$$\vec{v} \cdot \vec{\nabla}f + \frac{1}{m} \vec{F} \cdot \vec{\nabla}_v f = 0, \text{ states that a distribution function}$$

is constant along a particle's path in phase space. If f is written in terms of a particle's total energy ($E = T + V$, the kinetic plus potential energy), f will be constant in E along the path in real space. The integral for J is then transformed into a sum using the method of gaussian quadratures which picks key values of E , θ , and ϕ . These values represent trajectories that are traced backwards to either source or nonsource regions to determine the value of f . Once the current is known it is multiplied by the local potential to determine the power loss at that point.

PANEL is a Laplacian calculation since space charge effects are not included in the electrostatic potential calculation. The next phase in the development of PANEL is to calculate the charge density for each point in space by evaluating the integral

$$N = \int_0^\infty dv \int_0^{\pi/2} d\theta \int_0^{2\pi} d\phi f(v, \theta, \phi) v^2 \sin\theta$$

in the same manner as described for the current calculation. Then PANEL must iterate between the potential relaxation routine and the density calculation since the density calculation depends upon the potential structure for accurate trajectories. This is known as the inside-out method (Parker, 1977) because trajectories are traced backwards in time.

Figure 8 illustrates the three dimensional grid used to model two interior panels of a trough. Not shown are grid points at the intersection of all integer x and y values and even values of z . One unit of grid spacing corresponds to 85.0 meters, giving model dimensions of 765 m X 425 m. Fixed voltages are indicated on the figure. The assumed plasma

conditions are $N_i = N_e = 2/\text{cm}^3$, $kT_i = 10 \text{ keV}$, $kT_e = 5 \text{ keV}$. For these conditions, the random thermal current densities are, as before:

$$J_{\text{th},i} = 1.25 \times 10^{-7} \text{ A/m}^2$$

$$J_{\text{th},e} = 3.79 \times 10^{-6} \text{ A/m}^2$$

The dimensionless numbers at selected points on the panels are ratios of local average electron current densities to the random electron thermal current. For the two panels modeled, PANEL traced 864 trajectories per grid square of surface. The resulting total current collected and power loss are $6.64 \times 10^{-2} \text{ A}$, and $5.66 \times 10^2 \text{ W}$ for protons and 2.25 A and $2.72 \times 10^4 \text{ W}$ for electrons. Calculated potential patterns in the $x = 0$ plane and $y = 3$ plane are shown in Figs. 9 and 10, respectively. Note that potentials of only 1-2 kV extend beyond the upper limits of the trough, justifying our earlier "intermediate sheath" approximation.

Photoelectrons from the reflectors and backscattered and secondary electrons undoubtably will be important contributor to the power loss but have not yet been modeled.

Magnetic protection of the SPS

The SPS of necessity contains bus bars of current 10^5 A , routed between the solar panels and the microwave antennae. With judicious routing of these bus bars, the SPS can create its own protective magnetic barrier, screening out all the low energy ($\sim 100 \text{ eV}$) plasmaspheric plasma (which can cause power drain), and most of the energetic electrons. Parker and Oran (1979) have shown that this idea is feasible with nominal bus-bar currents. We propose modified bus-bar currents to prevent spacecraft fields from merging with the earth's magnetic field. Merging can have two harmful effects:

- 1) It can channel energetic particles trapped in the Earth's magnetic field towards sensitive areas of the SPS.
- 2) It can energize the high density plasmaspheric plasma that would otherwise be harmless.

Previous spacecraft were small in size compared to particle gyroradii, so magnetic effects were not important. The size of the SPS, however, is comparable to particle gyroradii, so magnetic effects must be taken into account. (At geosynchronous orbit, a 2 eV proton or 3 keV electron has a gyroradius of 2 km; a 50 eV proton or 80 keV electron has a gyroradius of 10 km.) In the following, in order to estimate these effects (i.e., to repel trapped particles and to minimize energy released in magnetic merging) we assume

that it is important to have spacecraft magnetic fields parallel to sensitive areas (e.g., solar cells) and aligned with the Earth's magnetic field. (Even magnetic fields perpendicular to the surface can be beneficial, however, and have been considered in Parker and Oran, 1979).

A solenoidal bus-bar winding yields the best magnetic field configuration: at a distance, the field approaches that of a dipole, and in the vicinity of the satellite the field is parallel to the solar panels. The windings for the solenoid should enclose as much area as feasible. This will have two benefits: it will maximize the overall dipole moment while minimizing the bus bar length and thus IR losses, and will minimize the internal field. On the other hand, for spatial uniformity, one should have a least one turn per kilometer. Some possible cross-sections are shown in Fig. 11. This figure is a view from the north end of three types of trough-like SPS design and shows one turn of the helical winding each.

The field of the SPS must have sufficient rigidity to successfully deflect the species desired to be excluded. Table 1 show magnetic moments μ required for various tasks. Two possible orientations of the SPS's dipole moment are compared: parallel or antiparallel to the Earth's dipole moment. A parallel orientation, since it adds to the local magnetic field, is more efficient at shielding the SPS from particle bombardment; however, the opposite orientation is dynamically more stable, since the SPS's moment will tend to align with the Earth's magnetic field. In fact, the moment may be used to balance gravity-gradient torques if the dipole moment is large enough. For a (uniform) body 22 km long and 4 km wide of mass 5×10^7 kg, the moment of inertia about an axis perpendicular to the length of the satellite would be 2×10^{12} kg-m². The daily + 10 deg tilt of the geosynchronous magnetic field would cause a torque on the satellite of ($\mu \times B$) = 1.7×10^4 Nt-m, for a $\mu = 10^{12}$ A-m² (corresponding to 0.9 Nt of force on each end). Since the satellite is so massive, this torque will result in a daily sinusoidal tilting motion of the satellite of amplitude $\sim 10^{-5}$ degrees, completely negligible. A 10 deg tilt of the satellite toward the Earth, in contrast, will cause a gravity-gradient torque of 2.7×10^6 Nt-m, or 125 Nt at each end, requiring a magnetic moment of 1.5×10^{14} A-m² to balance it. Then, however, the 10 deg misalignment between the spin axis and the dipole axis of the Earth would become more important. In addition, the magnetic fields in the SPS center would be quite large (90 G.). The internal field is sensitive to the exact configuration, and can vary by a factor of two or so depending on the area and number of turns per km. The rigidity, on the other hand, is not too sensi-

tive on the exact configuration, being mainly a function of overall magnetic moment.

One reasonable magnetic field configuration is shown in Figs. 12 ~ 14. The dipole moment assumed for these figures is the low-field case, 10^{11} A-m^2 per km, 21 km total. All components of the field are, of course, linear in the dipole moment. This model superposes 21 dipoles at 1 km intervals (simulating one turn per km). Figure 12 shows vector magnetic fields for one quadrant; Fig. 13 shows contours of constant $|B|$, and Fig. 14 shows magnetic field components. Here the z -component is measured along the long axis and the ρ component is measured from the long axis. The center of the SPS is the lower left corner ($z = 0, \rho = 0$). Only one quadrant is shown because of symmetry: $B_z(z) = B_z(-z)$; $B_\rho(z) = -B_\rho(-z)$. The field is similar to that of a solenoid and is nearly parallel to the long sides of the SPS (and therefore to the solar cells), converging at the SPS's north and south ends. (The SPS is aligned north-south to minimize the shadowing of one SPS on another in the equinox seasons.)

The field in Figs. 12 - 14 is strongest at the ends and weakest in the center; therefore, fewer wraps (or, more likely, less current per wrap) could be used at the ends and still obtain the same overall rigidity. A field of 100 extends to over 7 km from the center, and a field of 20 extends to 19 km. The overall rigidity at $\rho = 1 \text{ km}, z = 0 \text{ km}$ is roughly $2000 \text{Y - km (G-cm)}$. With a magnetic field of this orientation and strength, ions $< 100 \text{ eV}$ (including all the plasmaspheric plasma) and electrons $< 30 \text{ keV}$ (most of the plasma sheet electron fluxes) are excluded. Higher dipole moments would yield more shielding (see Table 1). Thus, it appears that magnetic protection is feasible. Because of the convergence of the field, particle fluxes will have a tendency to strike only the ends of the long axis of the SPS. Simply capping the ends of the SPS, then, will be sufficient to protect electronics and humans inside from the lower-energy particles. Such capping is also useful to prevent the plasma from the ion engines from returning to the satellite, causing a significant power drain (Freeman and Few, 1979).

Conclusions

The SPS will certainly interact with its plasma environment. It appears that, with relatively minor modifications to the NASA MSFC baseline design, these interactions will not significantly impair SPS operations. The conclusions and recommendations of this study include:

- 1) Arcing is likely to occur on kapton surfaces (the solar reflectors and the solar cell back surface blanket)

during substorms unless the kapton is replaced by a lower resistivity material ($\rho < 10^{13}$ ohm-cm) or current paths from the surfaces to the solar cells are provided.

2) The SPS parasitic load under normal conditions will be about 34 MW (for a 5 GW array) at geosynchronous orbit. This 0.7% power loss should be accommodated by oversizing.

3) The optimum grounding point at GEO for the SPS solar cell array is approximately the midpoint on the voltage string. At LEO, arcing considerations demand that the string be biased mostly positive, although the optimum configuration to minimize power loss would be substantially negative (see conclusion 5).

4) The solar cells may require conductive coatings. The reflector panels may require current paths linking the front and back sides. Laboratory tests in a substorm simulator on realistic solar panels are recommended to determine the actual arcing probability.

5) Severe arcing problems are expected for negative portions of the EOTV solar cell array at LEO. Overcoming this problem by biasing the array as positive as possible will result in high parasitic loads (power losses on the order of 3%). Only a low voltage EOTV solar array should be used.

6) The SPS will occasionally charge to about -20 kV during eclipses. An active discharge method such as a hot filament electron emitter should be provided.

7) A shield should be placed across the ends of the EOTV to prevent thruster ion feedback to the solar array. Similar shields may be required on the SPS.

8) Three-dimensional computer modeling of the SPS electric field pattern and plasma currents is underway. The model shows that, for the grounding scheme used here, spacecraft electric fields extend only slightly beyond the reflectors.

9) Active magnetic plasma shielding is possible through judicious routing of bus-bars; power drain from additional lengths of bus-bars has not been calculated yet.

10) It is possible to use the internal magnetic field to align the satellite (counteracting gravity-gradient torques), but it would require an unreasonably large magnetic moment (1.5×10^{14} A-m²).

Acknowledgments

The authors thank Dr. Lee Parker for consultation and the use of the computer program "PANEL." In addition, we have benefited from discussion with Dr. James McCoy. This work was supported by NASA under grant NAS8-33023.

The computer program PANEL is attached as appendix A.

References

- Burke, W. J., Reiff, P. H., and Reasoner, D. L., "The Effect of Local Magnetic Fields on the Lunar Photoelectron Layer While the Moon Is in the Plasma Sheet," Geochemica Cosmochimica Acta, Suppl. 6, Vol. 3, 1975, pp. 2985-2997.
- Chopra, K. P., Reviews of Modern Physics, Vol. 33, 1961, p. 153.
- DeForest, S. E., "Spacecraft Charging at Synchronous Orbit," Journal of Geophysical Research, Vol. 77, February, 1972, pp. 651-659.
- Freeman, J. W. and Few, A. A., "Electrostatic Protection of the Solar Power Satellite And Rectenna," final report, NASA contract NAS8-33023, Rice University, Houston, Texas, May 1979.
- Freeman, J. W. and Ibrahim, M., "Lunar Electric Fields, Surface Potential And Associated Plasma Sheets, The Moon, Vol. 14, 1975, pp. 103-114.
- Garrett, H. B. and DeForest S. E., "Analytic Simulation of the Geosynchronous Plasma Environment," Planetary Space Science, Vol 26, (in press), 1979.
- Hanley, G. M., "Satellite Power Systems (SPS) Concept Definition Study," final report for NASA contract NAS8-32475, Rockwell International Report #5078-AP-0023, Cincinnati, 1978.
- Inouye, G. T., "Spacecraft Potentials in A Substorm Environment," Progress in Astronautics and Aeronautics: Spacecraft Charging by Magnetospheric Plasmas, ed. by A. Rosen, AIAA, New York, 1976, pp. 103-120.
- Johnson, F. S (ed). Satellite Environment Handbook, Stanford University Press, Stanford, California, 1965.
- Kennerud, K. L., "Final Report High Voltage Solar Array Experiments," Boeing Aerospace Corp., Seattle, Wash., Rept. No. CR121280, 1974.
- Massaro, M. J., Green, T., and Ling, P., "A Charging Model for Three-axis Stabilized Spacecraft," Proceedings of the Spacecraft Charging Technology Conference, edited by C. P. Pike and R. R. Lovell, Air Force Rept. AFGL-TR-77-0651, 1977, pp. 237-267.

McCoy, J. E. and Konradi, A., "Sheath Effects Observed on A 10 Meter High Voltage Panel in Simulated Low Earth Orbit Plasma," Space Craft Charging Technology-1978, edited by R. C. Finke and C. P. Pike, NASA CP 2071, 1979, pp. 315-340.

McIlwain, C. E., "Substorm Injection Boundaries," Magnetospheric Physics, edited by B. M. McCormac, D. Reidel, Hingham, Mass., 1974, p. 143.

Mizera, P. F. and Fennell, J. F., "Satellite Observations of Polar, Magnetotail Lobe, and Interplanetary Electrons at Low Energies," SAMSO Rept TR-78-6, 1978.

Parker, L. W., "Plasma Sheath Effects and Voltage Distributions of Large High-power Satellite Solar Arrays," Spacecraft Charging Technology-1978, edited by R. C. Finke and C. P. Pike, NASA CP 2071, 1979, pp. 341-357.

Parker, L. W. and Oran, W. A., "Magnetic Shielding of Large High-power-satellite Solar Arrays Using Internal Currents," Spacecraft Charging Technology-1978, edited by R. C. Finke and C. P. Pike, NASA CP 2071, 1979, pp. 376-387.

Parker, L. W., "Calculation of Sheath and Wake Structure about A Pillbox-shaped Spacecraft in A Flowing Plasma," Proceedings of the Spacecraft Charging Technology Conference, edited by C. P. Pike and R. R. Lovell, Air Force Report AF6L-TR-77-0051, 1977, pp. 331-336.

Pelizzari, M. A. and Criswell, D. R., "Differential Photoelectric Charging of Nonconducting Surfaces in Space," Journal of Geophysical Research, Vol. 83, November, 1978, pp. 5233-5244.

Pike, C. P. and Brun, M. H., "A Correlation Study Relating Spacecraft Anomalies to Environmental Data," Progress in Astronautics and Aeronautics: Spacecraft Charging by Magnetospheric Plasmas, edited by A. Rosen, AIAA (New York), 1976, pp. 45-60.

Reasoner, D. L. and Burke, W. J., "Characteristics of the Lunar Photoelectron Layer," Journal of Geophysical Research, Vol. 77, December, 1972, pp. 6671.

Reasoner, D. L., Lennartsson, W., and Chappell, C. R., "Relationship Between ATS-6 Spacecraft-charging Occurrences and Warm Plasma Encounters," Progress in Astronautics and Aeronautics: Sapcecraft Charging by Magnetospheric Plasmas, edited by A. Rosen, AIAA, New York, 1976, pp. 89-101.

Reiff, P. H., "Magnetic Shadowing of Charged Particles by An Extended Surface," Journal of Geophysical Research, Vol. 81, July, 1976, pp. 3423-3427.

Reiff, P. H. and Burke, W. J., "Interactions of the Plasma Sheet with the Lunar Surface at the Apollo 14 Site," Journal of Geophysical Research, Vol 81, September, 1976, pp. 4761-4764.

Shaw, R. R., Nanevicz, J. W., and Adamo, R. C., "Observations of Electrical Discharges Caused by Differential Charging," Progress in Astronautics and Aeronautics: Spacecraft Charging by Magnetospheric Plasmas, edited by A. Rosen, AIAA, New York, 1976, pp. 61-79.

Whipple, E. C., Jr., "The Equilibrium Electric Potential at A Body in the Upper Atmosphere and in Interplanetary Space," NASA T. N. X-615-65-296, 1965.

Whipple, E. C., Jr., "Theory of the Spherically Symmetric Photoelectron Sheath: A Thick Sheath Approximation and Comparison with ATS6 Observation of a Potential Barrier," Journal of Geophysical Research, Vol. 81, February, 1976, pp. 601-607.

FIGURE CAPTIONS

Fig. 1 Sketch of the Earth's magnetosphere (from Mizera and Fennell, 1978).

Fig. 2 Schematic of plasma and photoelectron currents.

Fig. 3 Sketch of the MSFC January 25, 1978, baseline design (from Hanley, 1978).

Fig. 4 Cross-section of a proposed GaAlAs solar cell (from Hanley, 1978).

Fig. 5 Idealization of the solar cell blanket, used in calculations of electrostatic potential, for the "worst case" plasma fluxes.

Fig. 6 Summary of voltages on the reflectors and solar cells surfaces, for solar cells at large positive voltages (top), large negative voltages (middle), and during eclipse (bottom). (Midpoint of the solar cell voltage string is assumed to be grounded to the sunlit side of the reflectors.)

Fig. 7 Summary of parasitic current densities for the SPS and the parasitic current and power loss total for one half of the Marshall satellite (5 GW system).

Fig. 8 Computer grid used to model 2 panels of the SPS. (Small numbers on the panel surface are the plasma electron currents normalized to random thermal currents.)

Fig. 9 Equipotential contours in the yz plane at $x = 0$ (indicated in Fig. 8).

Fig. 10 Equipotential contours in the xz plane at $y = 3$ (indicated in Fig. 8).

Fig. 11 Recommended current windings for several SPS configurations (view from north end).

Fig. 12 Vector magnetic fields for a solenoidal current configuration, low-field case ($\mu = 10^{11} \text{ A-m}^2$ per km, 21 km total). (Z-axis is along the spacecraft ($z = 0$ is the center), and ρ is measured from the spacecraft axis; only one quadrant is shown, because of symmetry: $B_z(-z) = B_z(z)$; $B_\rho(-z) = -B_\rho(z)$.)

**Fig. 13 Contours of constant
 $|B|$ for the low-field case.
Only one quadrant is shown.**

Fig. 14 Contours of constant B_ρ and B_z , low-field case.

Magnetic Moment Required for SPS Tasks

Task	Rigidity Required	Orientation Of Moment	Internal Field (Gauss)	Required Moment A-m ² /km ²
Shielding 200 eV Protons and 30 keV Electrons	2×10^3	*Parallel Antiparallel	1.3 4	1×10^{11} 3×10^{11}
Shielding 3 KeV Protons and 2 MeV Electrons	8×10^3	*Parallel *Antiparallel	5.3 11	4×10^{11} 8×10^{11}
Shielding 30 KeV Protons 10 MeV Electrons	3×10^4	Parallel *Antiparallel	20 25	1.5×10^{12} 2×10^{12}
Magnetic Alignment (Balance Gravity-Gradient)	N/A	*Antiparallel	92	7×10^{12}

*Recommended Orientation

†Multiply by 21 for total magnetic moment.

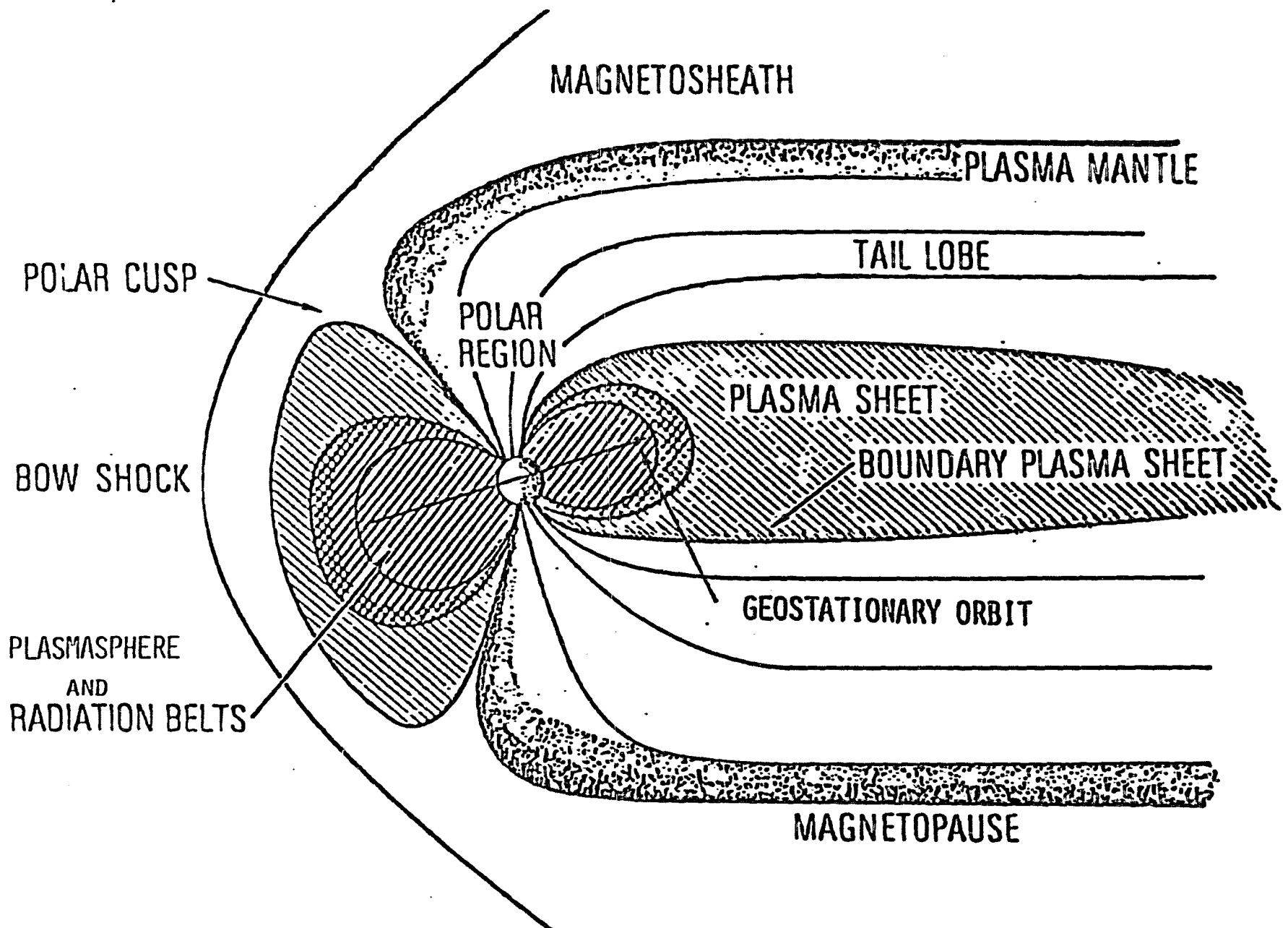


Figure 1

A BODY IN A PLASMA PLUS SUNLIGHT

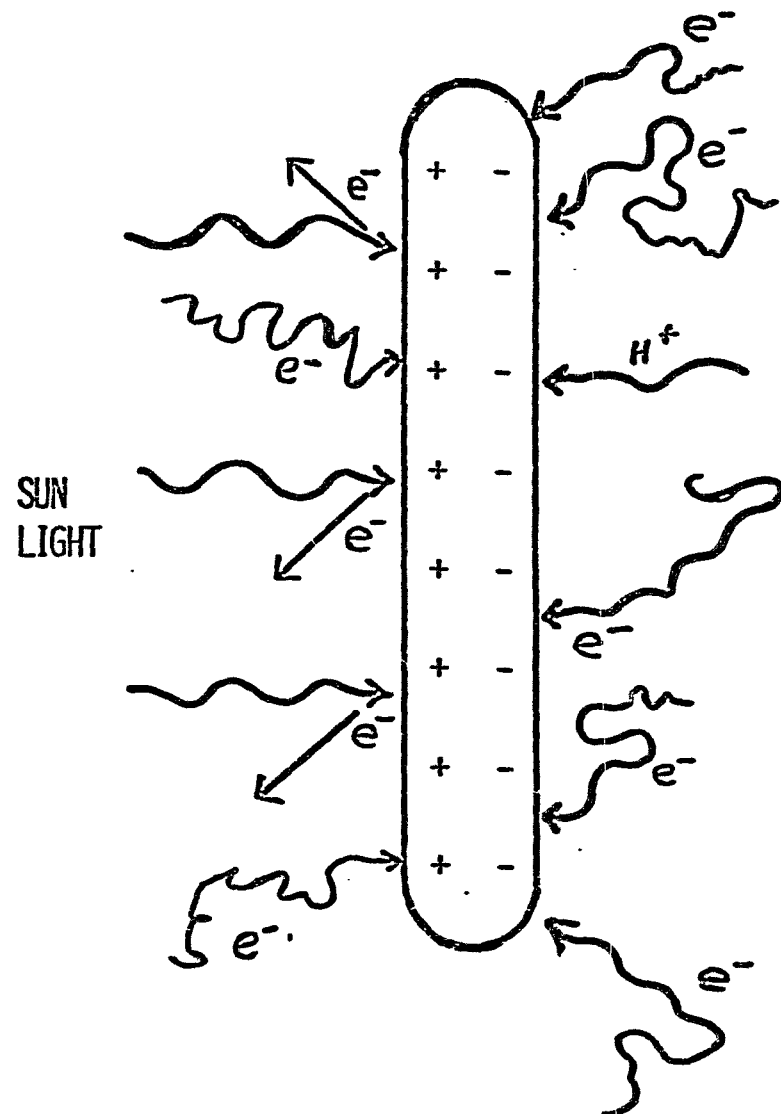


Figure 2

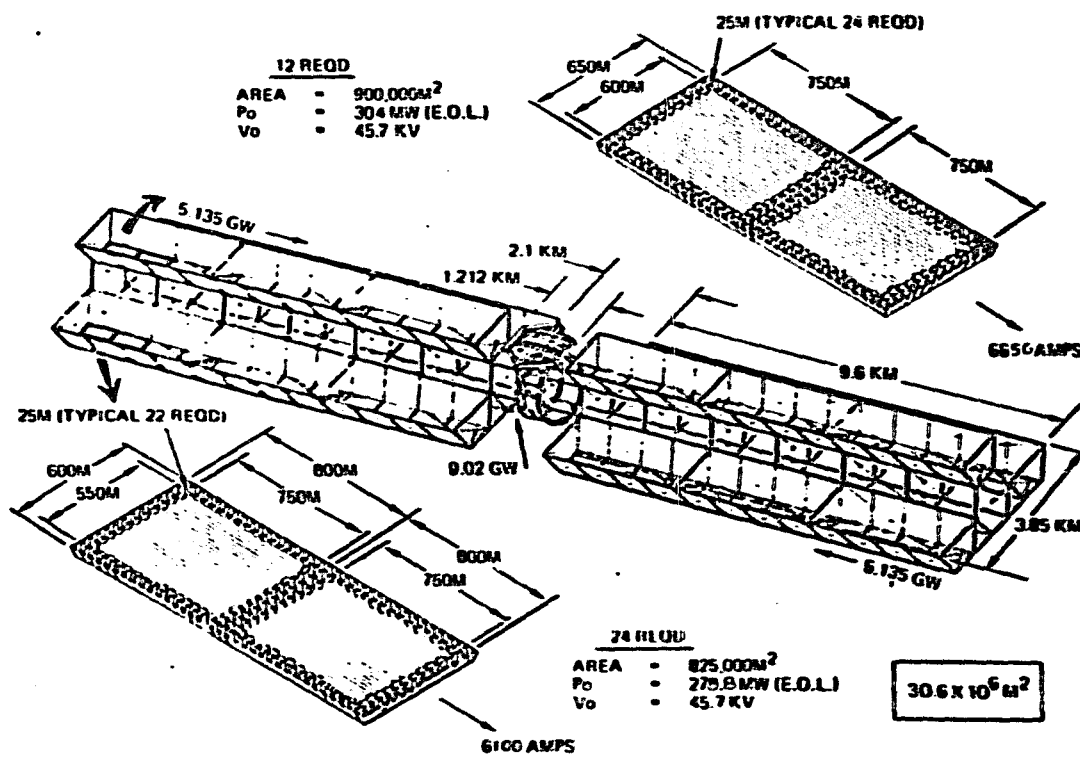


Figure 3

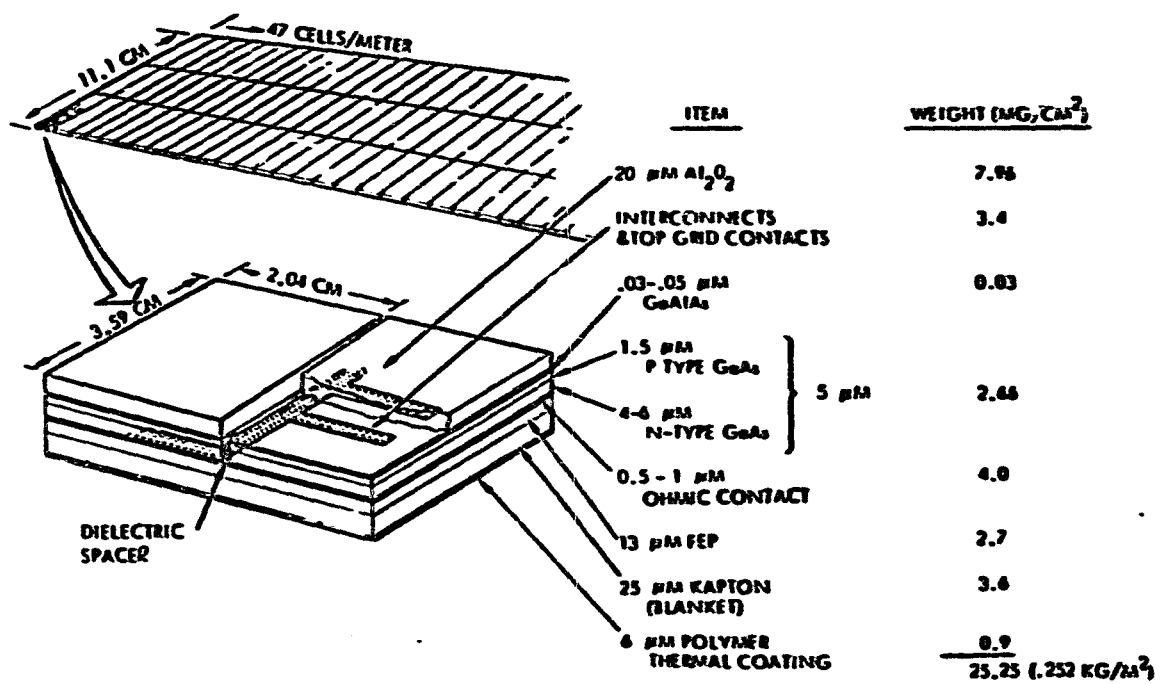
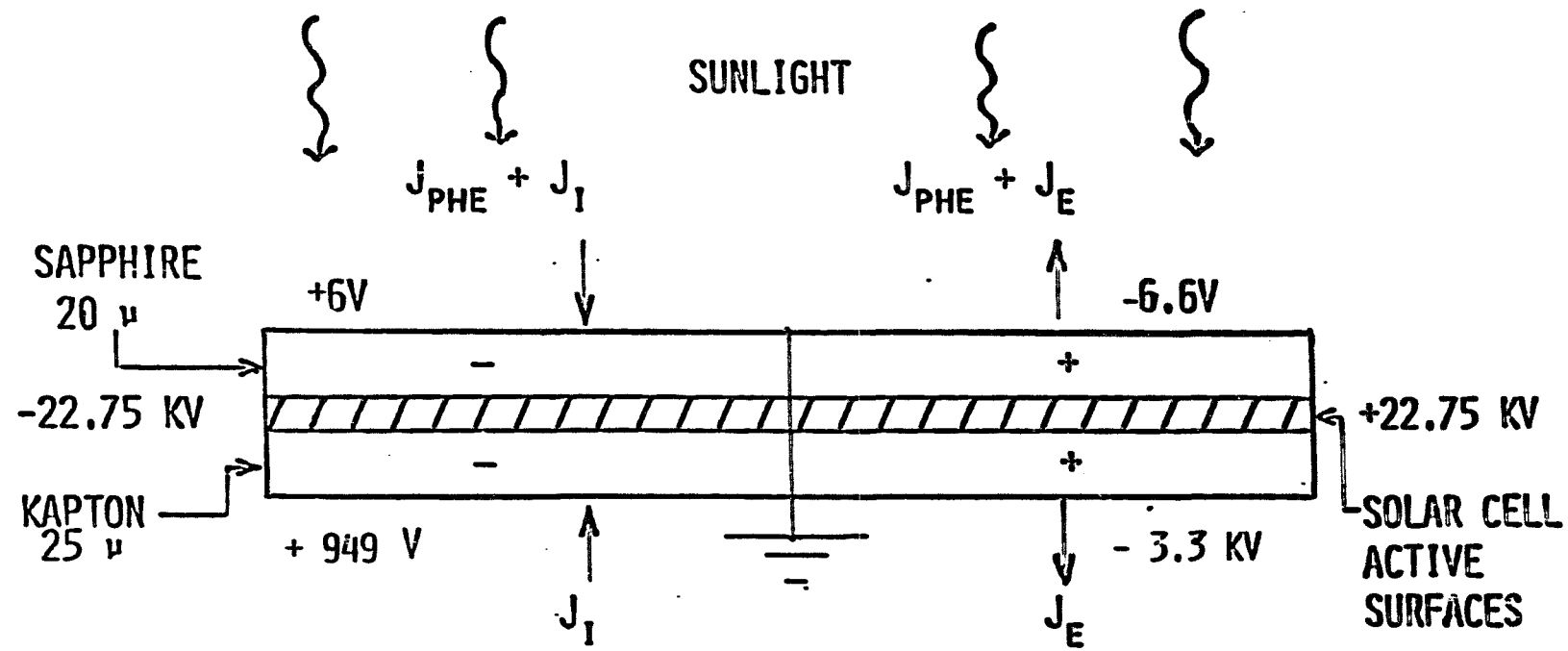


Figure 4

ACTIVE SURFACES (SOLAR CELL BLANKET):



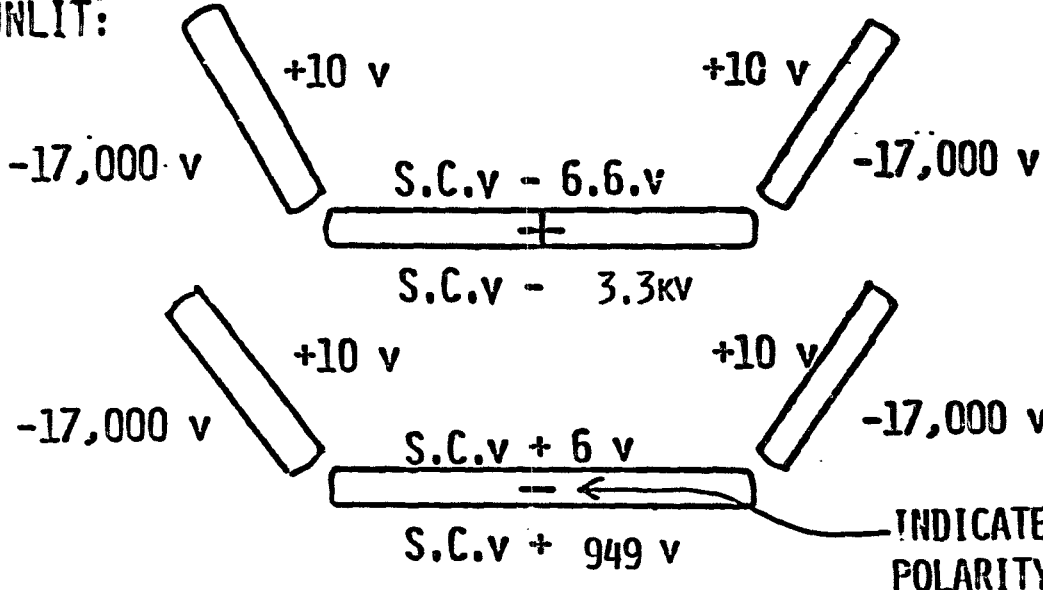
VOLTAGES SHOWN ARE RELATIVE TO THE LOCAL SOLAR CELL VOLTAGE. THEY REPRESENT THE IR DROP ACROSS THE COVER GLASS OR KAPTON BLANKET.

- * THE KAPTON BREAKDOWN VOLTAGE IS ~ 6250 V

Figure 5

SUMMARY OF VOLTAGES:

SUNLIT:



INDICATES SOLAR CELL ARRAY
POLARITY

ECLIPSE:

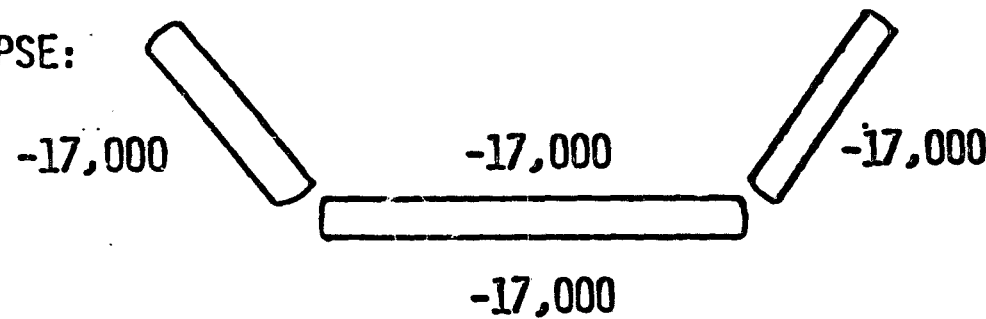


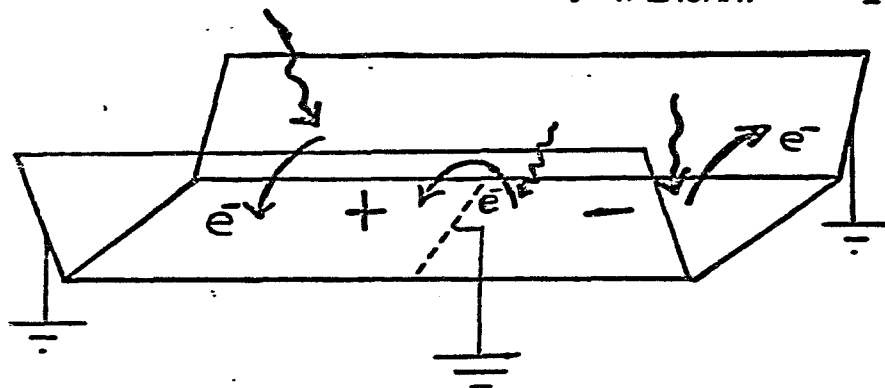
Figure 6

THE VARIOUS CURRENT DENSITIES ARE:

$$J_{PHE} = 3 \times 10^{-9} \text{ AMP}/\text{CM}^2 \text{ (FOR SAPPHIRE)}$$

$$J_E \text{ (PLASMA)} = 3 \times 10^{-10} \text{ AMP}/\text{CM}^2$$

$$J_I \text{ (PLASMA)} = 1 \times 10^{-11} \text{ AMP}/\text{CM}^2$$



PHOTOELECTRON FLOW DIRECTIONS

TOTAL PARASITIC CURRENT:

$$I_P \cong 3000 \text{ AMPS}$$

$$\bar{V} = 11,375 \text{ V}$$

THE PARASITIC POWER IS:

$$P_P \cong 34 \text{ MW}$$

(0.7% OF OUTPUT POWER)

Figure 7

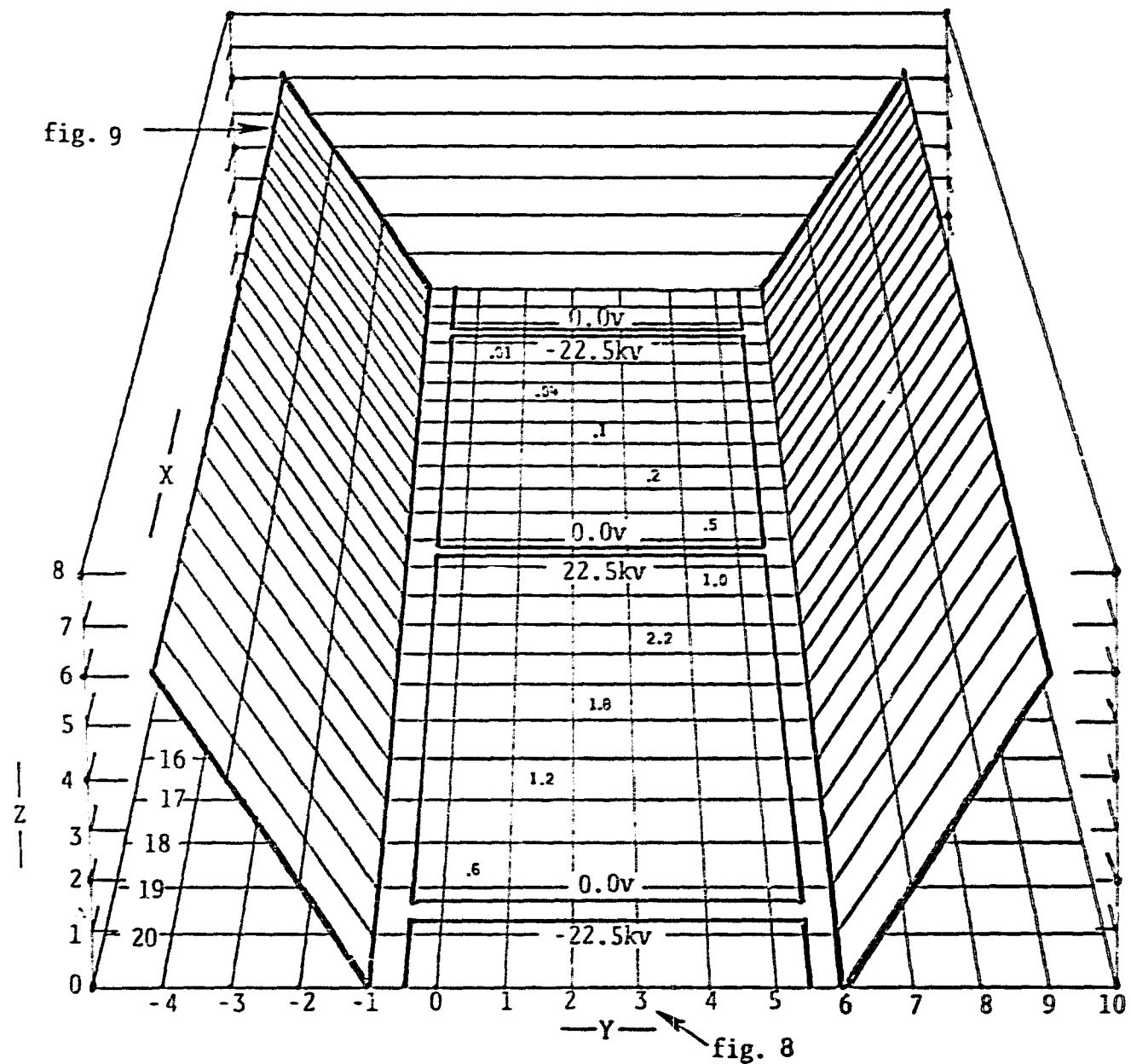
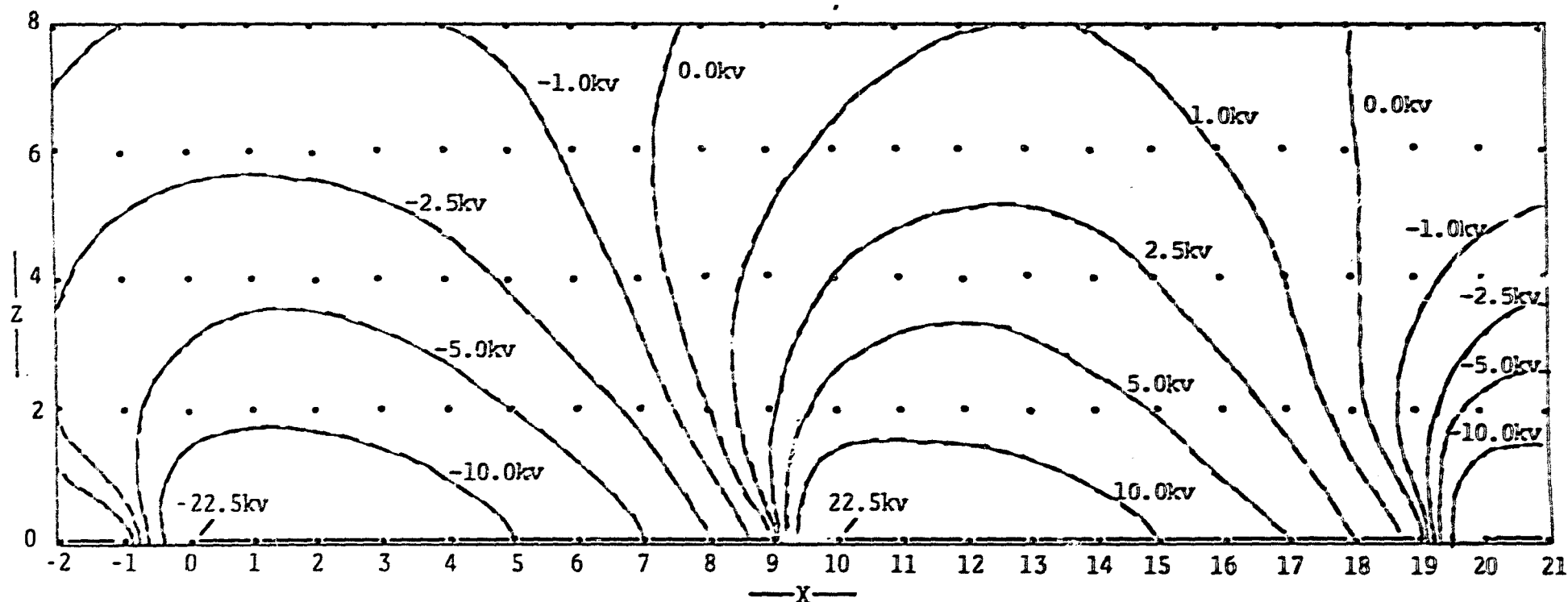
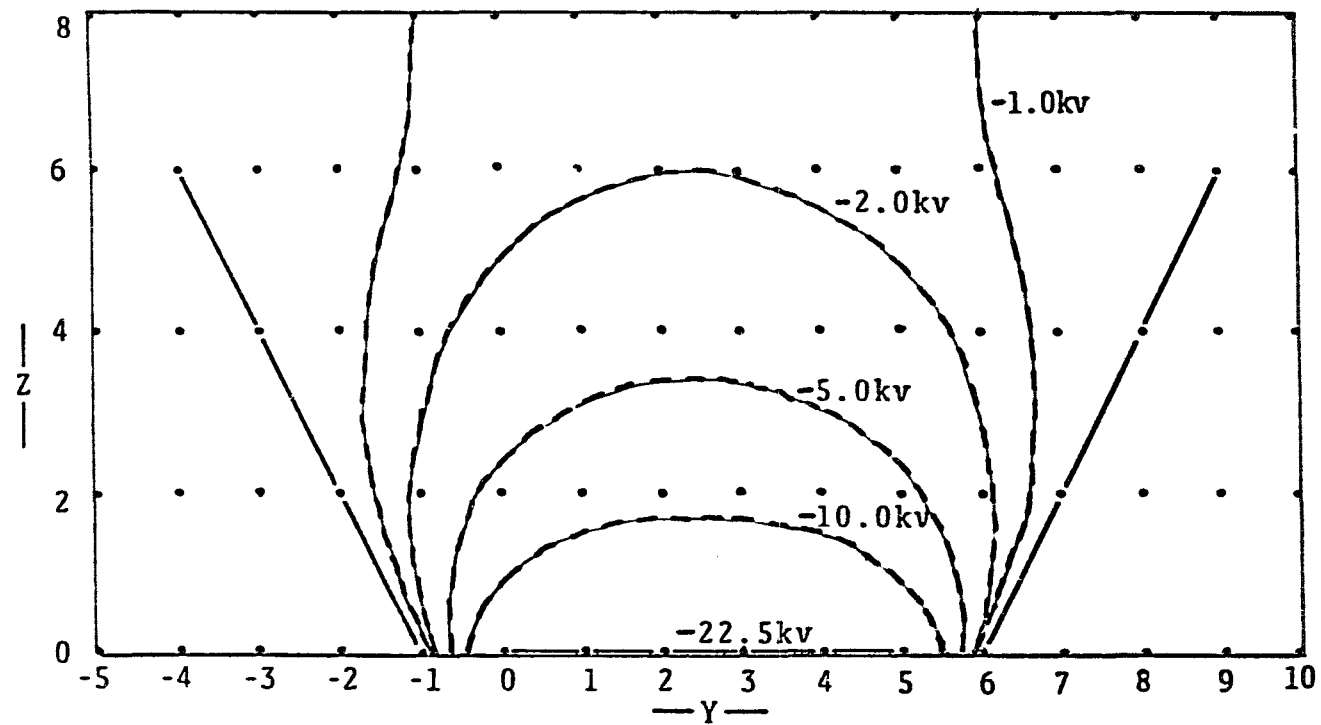


Figure 8



EQUIPOTENTIALS IN THE $Y=3$ PLANE

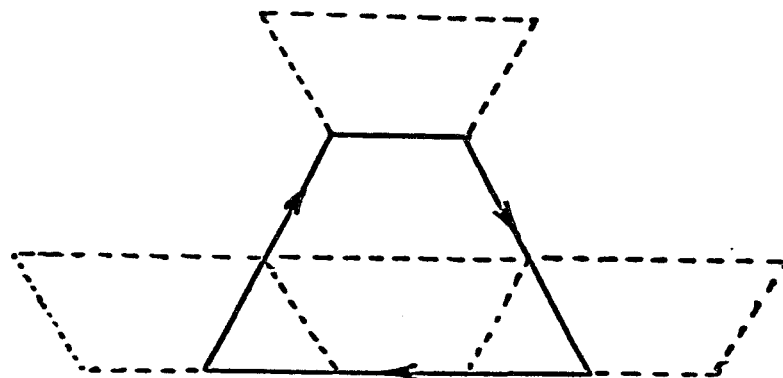
Figure 9



EQUIPOTENTIALS IN THE $X = 0$ PLANE

Figure 10

PREFERRED CONFIGURATION



AREA = $1.6 \times 10^6 \text{ m}^2$

LOOP LENGTH = 5200 M

1-4 TURNS PER KM RECOMMENDED

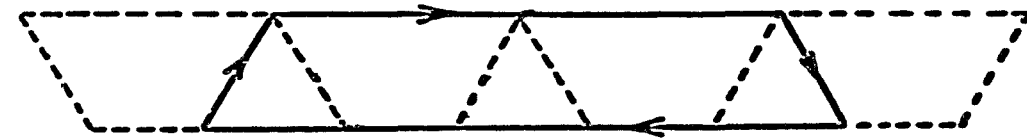
RECOMMENDED BUS BAR CURRENT CONFIGURATIONS



AREA = $9.1 \times 10^5 \text{ m}^2$

LOOP LENGTH = 4300 M

1-6 TURNS PER KM RECOMMENDED



AREA = $2.4 \times 10^6 \text{ m}^2$

LOOP LENGTH = 9500 M

1-2.5 TURNS PER KM RECOMMENDED

Figure 11

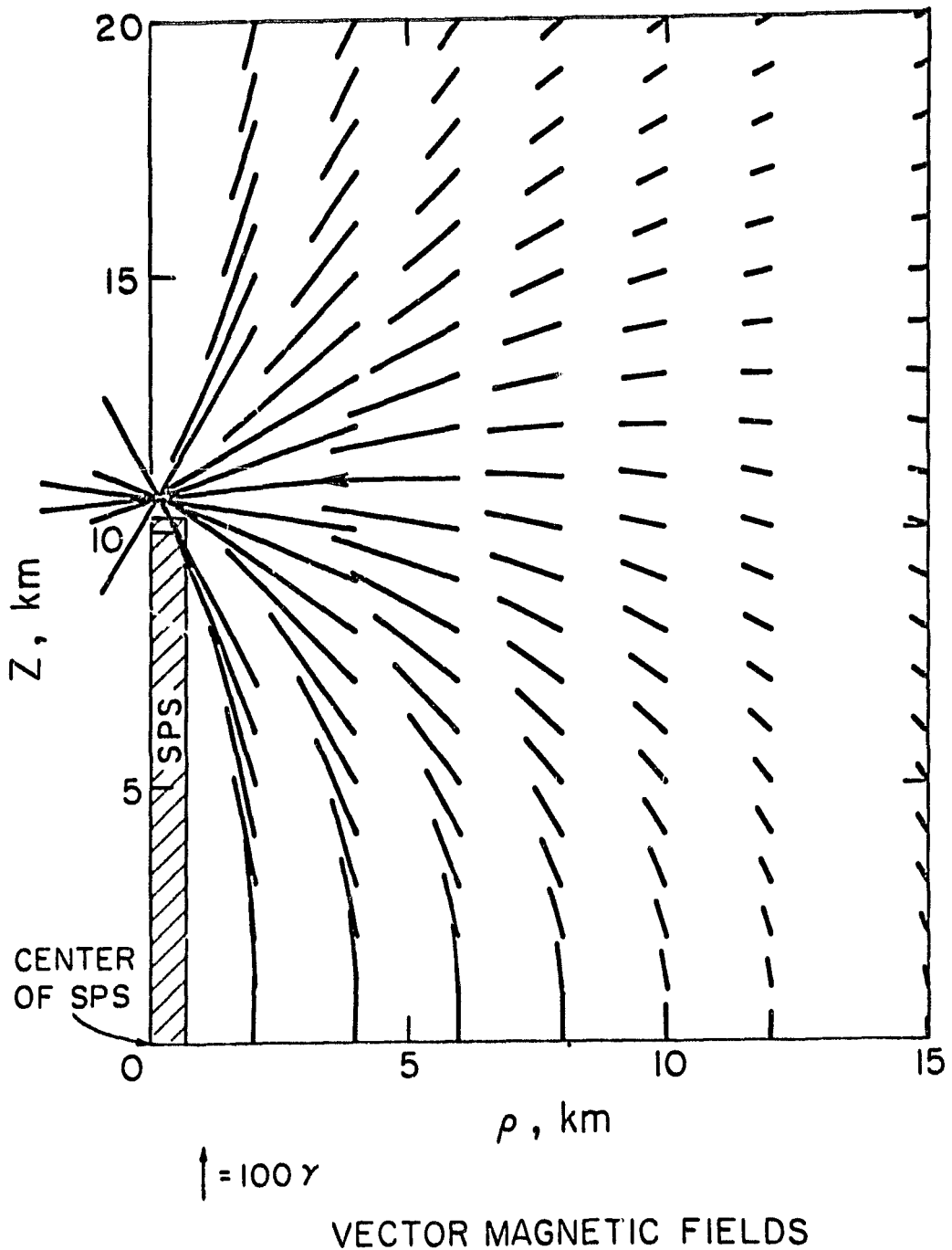


Figure 12

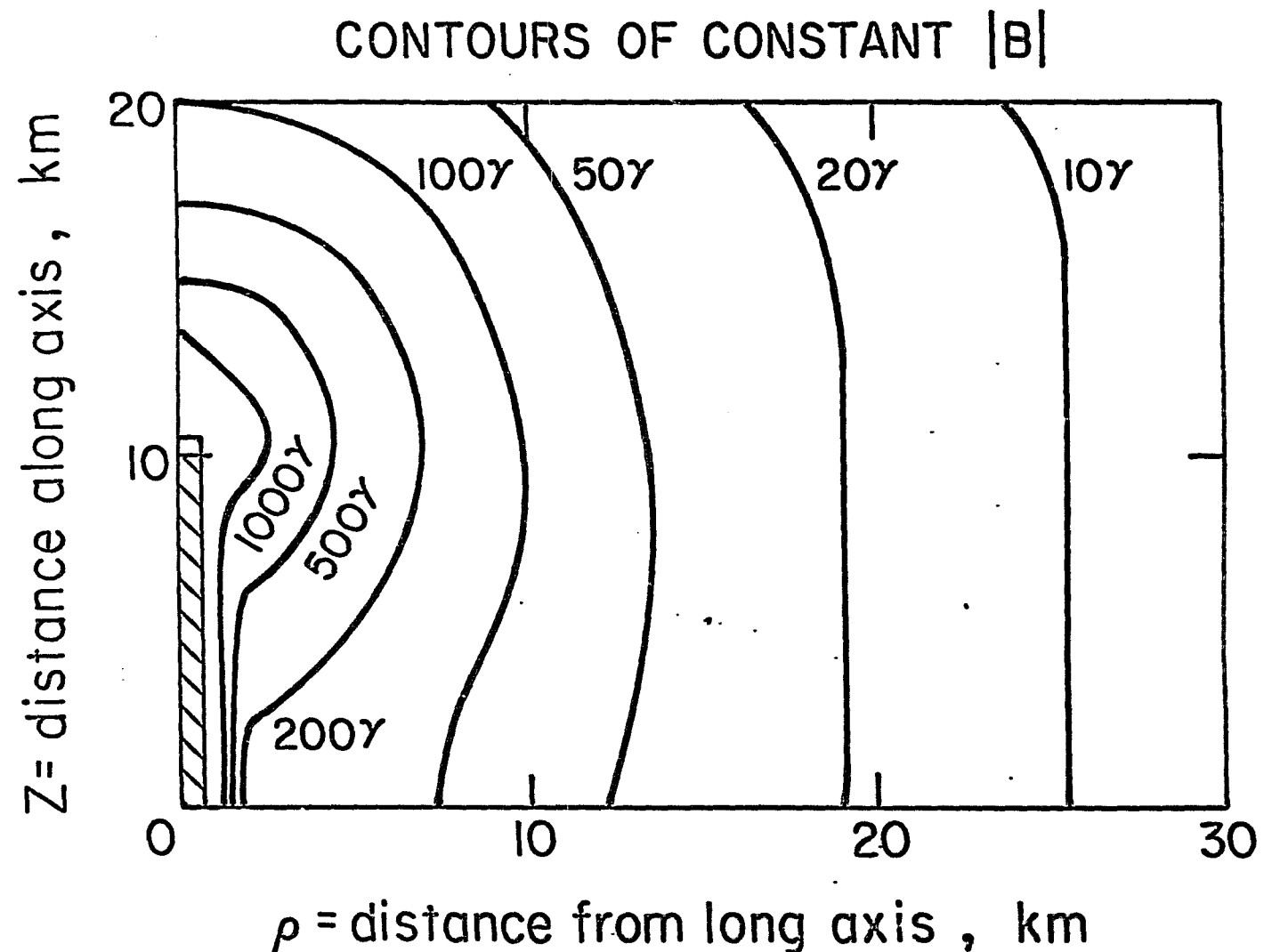


Figure 13

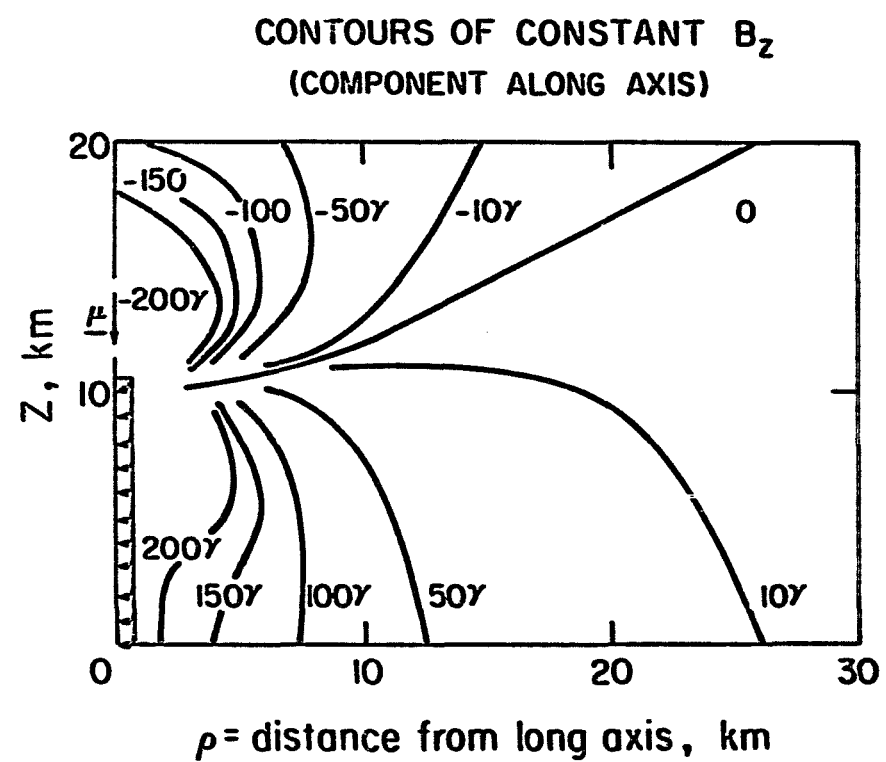
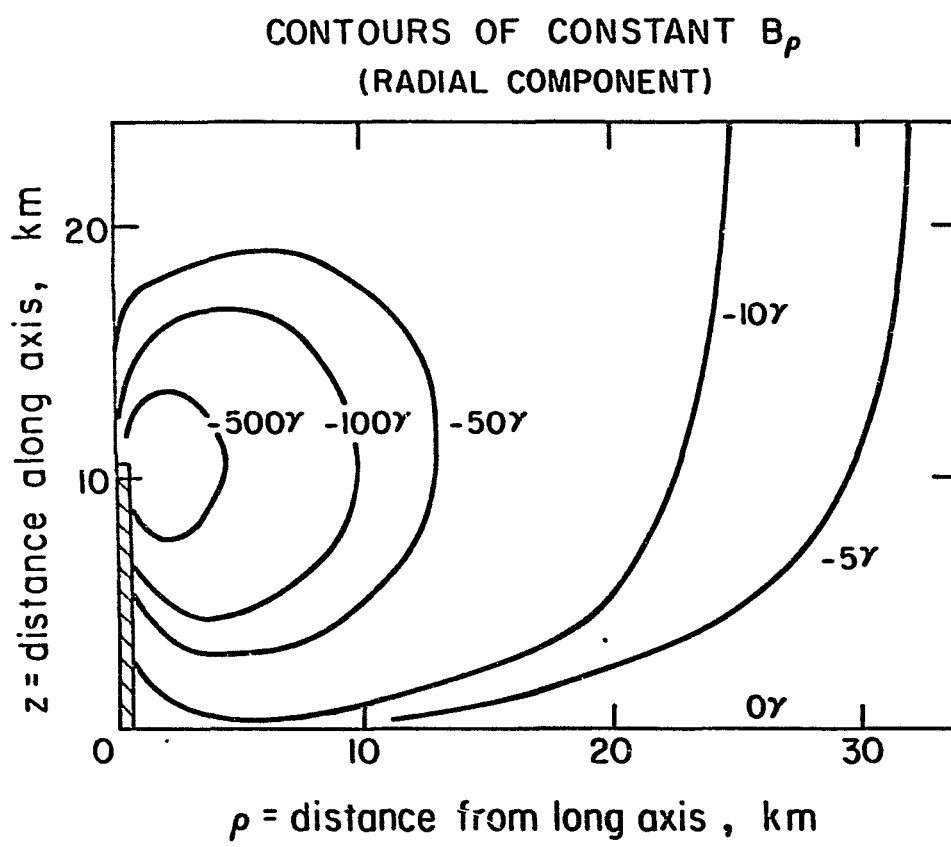


Figure 14

Table of Contents

I.	LIGHTNING ROD PROTECTION CAPABILITIES SUITABLE TO THE RECTENNA.....	1
II.	SIMULATIONS OF LIGHTNING STRIKES TO THE SPS RECTENNA.....	17
III.	GROUNDING CONSIDERATIONS FOR THE PROPOSED LIGHTNING PROTECTION SYSTEM..	28
IV.	MATERIALS AND SPECIFICATIONS FOR LIGHTNING PROTECTION.....	35
V.	ESTIMATE OF POWER LOSS FROM THE BEAM.....	37
VI.	MICROWAVE DIODE FAILURES DUE TO INDUCED CURRENT TRANSIENTS.....	39
VII.	COMPUTER SIMULATION OF ELECTROSTATIC FIELD AROUND AN SPS RECTENNA.....	41
VIII.	COMPUTATION OF LIGHTNING ELECTRIC FIELDS.....	47
IX.	COMPUTATIONS OF DIODE FAILURE.....	57
X.	LIGHTNING PROTECTION FOR SERIES DIODE STRINGS.....	59
XI.	CLOUD-TO-GROUND LIGHTNING DISTRIBUTION IN THE UNITED STATES.....	61

PRECEDING PAGE BLANK NOT FILMED

SUMMARY AND CONCLUSIONS

1. The very high lightning flash density in many parts of the United States and the large size of the SPS rectenna require us to incorporate lightning protection systems in the rectenna design.
2. A distributed lightning protection system is described in this report that will protect the rectenna components from direct lightning strike damage and will, in addition, provide reduced induced lightning effects in the power and control circuits.
3. The proposed lightning protection system should be incorporated as a structural member of the rectenna support system; viewed as such, the lightning protection system will not appreciably increase the total material requirements for the rectenna unless materials are used that are incapable of safely conducting lightning currents.
4. The lightning protection design places the conducting elements so that the microwave shadow cast by protection systems falls along the upper edge of the billboard on which it is mounted (and the lower edge of the next billboard to the north); these shadow areas are only a slight fraction of the collecting area, so the protection elements produce very little, if any, additional power loss to the rectenna as a whole.
5. Individually the microwave diodes are self-protecting with respect to "average" lightning and those near the center of the rectenna are safe from extreme lightning. However, the series connection of the diodes to form 40,000 V strings creates a protection requirement for the string. Standard surge protection practices are necessary for the string.
6. Electric power industries usually attribute 10% of the cost of power transmission equipment to lightning protection requirements. If this factor is not already included in cost estimates, it should be added.

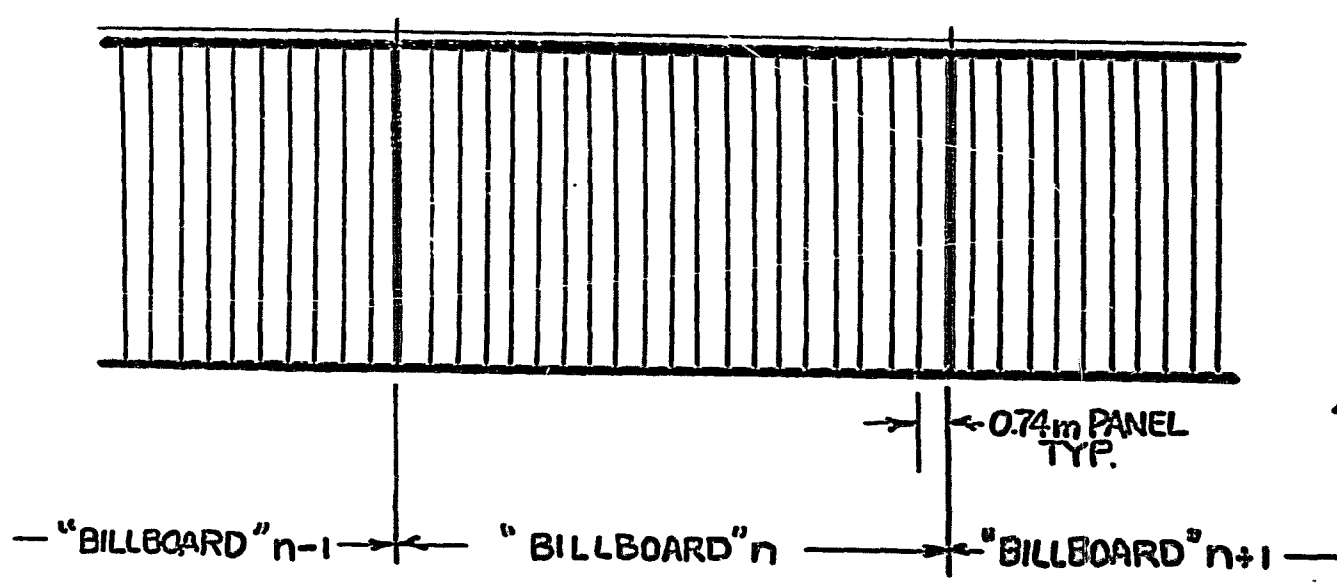
LIGHTNING PROTECTION OF THE RECTENNA

ABSTRACT

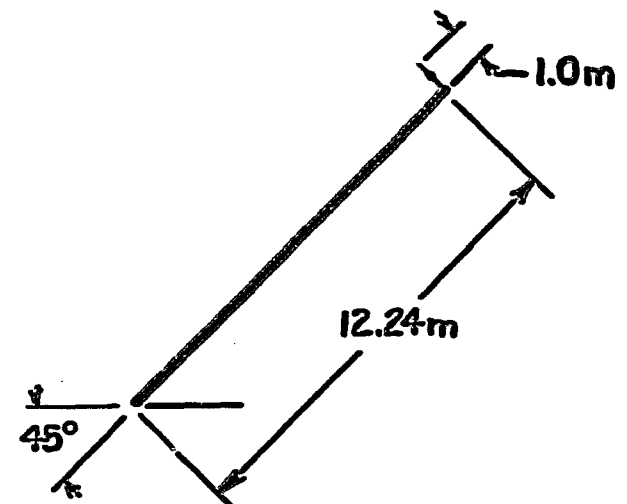
Computer simulations and laboratory tests were used to evaluate the hazard posed by lightning flashes to ground on the SPS rectenna and to make recommendations on a lightning protection system for the rectenna. The distribution of lightning over the lower 48 of the continental United States was determined, as were the interactions of lightning with the rectenna and the modes in which those interactions could damage the rectenna. The studies showed that lightning protection was both required and feasible. Several systems of lightning protection were considered and evaluated. These included two systems that employed lightning rods of different lengths and placed on top of the rectenna's billboards and a third, distributed system. The distributed system is similar to one used by power distribution companies; it consists of short lightning rods all along the length of each billboard that are connected by a horizontal wire above the billboard. The system that not only affords greater protection than the others considered but offers easiest integration into the rectenna's structural design, was the distributed lightning protection system.

SUMMARY OF THE RECOMMENDED LIGHTNING PROTECTION DESIGN

Based upon our research, computer simulations, and laboratory tests with a scale model, we recommend a distributed lightning protection system that employs a horizontal conducting member with points and grounds placed at every bay or billboard (14.69 meters apart). This configuration not only provides greater protection than other configurations that were evaluated, it is more easily integrated into the structural design of the rectenna. The recommended system is shown in Figure 1.



FRONT



SIDE

DISTRIBUTED LIGHTNING PROTECTION SYSTEM

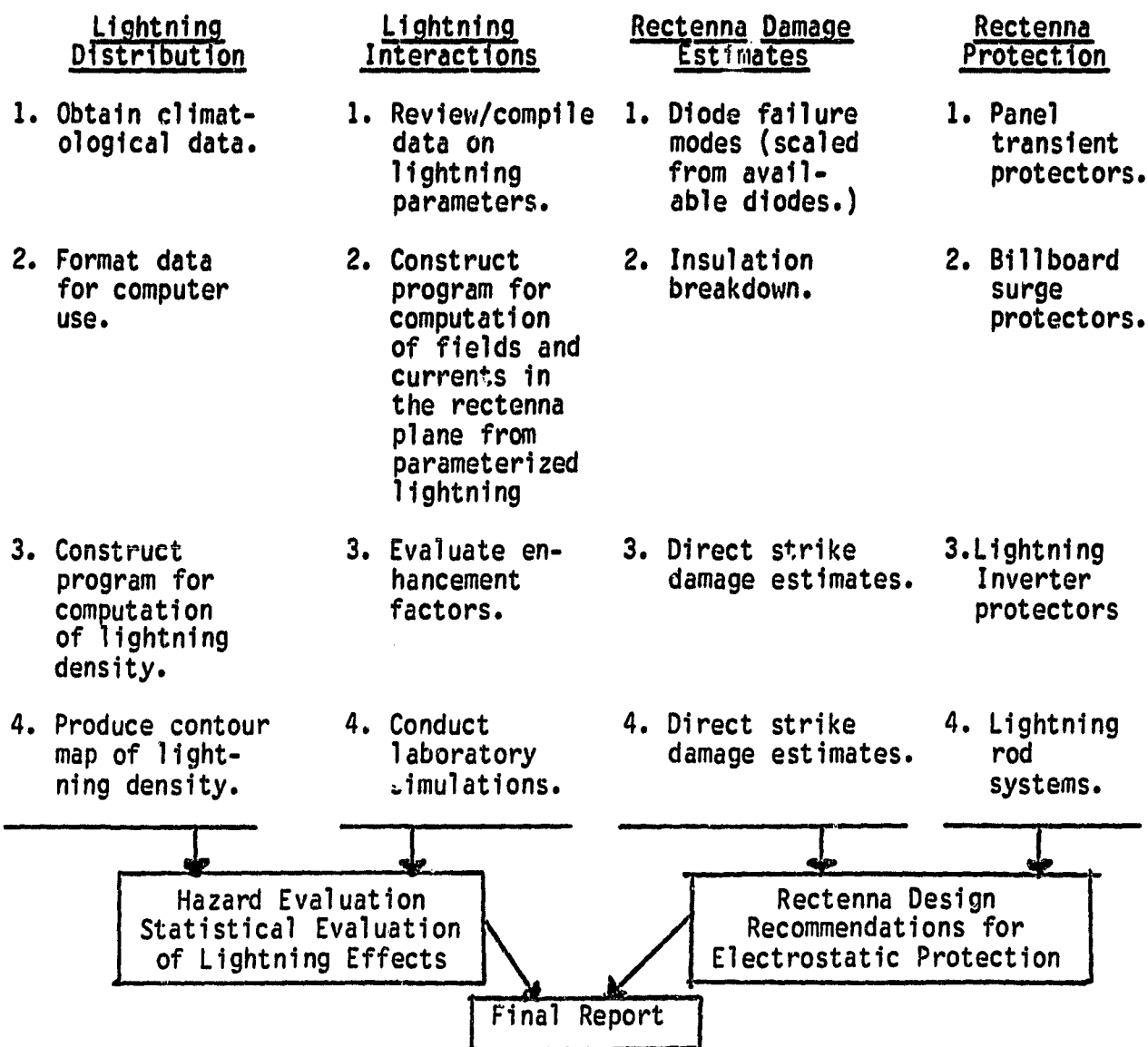
FIGURE

PREFACE

The objectives of this study are to evaluate the hazard posed by lightning flashes to ground on the SPS rectenna and to make recommendations for a lightning protection system that will provide sufficient protection to the rectenna. For purposes of this study, the SPS rectenna design is based upon the data supplied to us by Rockwell International in July, 1978.

This study has four major components, each with several elements of investigation. The components were: lightning distribution; lightning interactions; rectenna damage estimates; rectenna protection. The elements of each component are listed in Table A. The study plan was to proceed from top to bottom evaluating the elements listed in each component; work proceeded in a parallel manner for the four components. The organization of this final report reverses this order by presenting the more important results of the study first, then following this with the material and considerations leading to the conclusions.

TABLE A
Rectenna Electrostatic Protection



The Principal Investigator was J.W. Freeman, Jr., and the principal author of this section of the final report was A.A. Few, Jr. They wish to express their thanks and appreciation to the following co-authors, all of whom were or are associated with Rice University.

J. Bohannon
R.C. Haymes
D. O'Gwynn
M.F. Stewart

I. ANALYSIS OF LIGHTNING ROD PROTECTION CAPABILITIES FOR A CONFIGURATION SUITABLE TO THE RECTENNA

1. Cone of Protection Considerations:

I. 1.1 Definition and Considerations

The capability of a vertical conductor to attract a lightning flash is described by the cone-of-protection, or perhaps more accurately the cone-of-attraction. In theory, any lightning flash that would have entered this cone had the vertical conductor not been in place, will strike instead the conductor and be shunted to the ground. The method by which this process takes place is as follows:

The lightning stepped leader creates high voltages over a wide area on the rectenna because of the large charge on the leader tip. At points on the rectenna where the electric field reaches breakdown values due to local enhancement factors, upward propagating sparks are initiated which move to meet the downward propagating stepped leader. The upward propagating spark which first makes contact with the leader completes the electrical circuit and the lightning flash current will pass through the structure that initiated the successful upward going spark.

The cone of protection is primarily a function of the height of the vertical conductor because of the field-enhancement factor which enables the taller object to initiate the upward spark before lower objects. Other factors enter into the consideration of the cone of protection, such as the charge on the leader tip and the velocity of the leader, because these factors strongly influence the timing of the production of upward sparks and the height at which the spark and leader meet. In general, the results of research into this subject have shown that the larger the leader charge, then the larger the angle β of the associated cone of protection. Since larger leader charges are usually associated with the larger lightning currents, we find a fortunate result that the cone of protection increases with the potential hazard of the lightning flash.

It follows then that the angle β of the cone of protection (See Figure 2) varies with the particular lightning flash. $\beta = 45^{\circ}$ is a very commonly used design angle in the United States and many of the examples in this report employ $\beta = 45^{\circ}$.

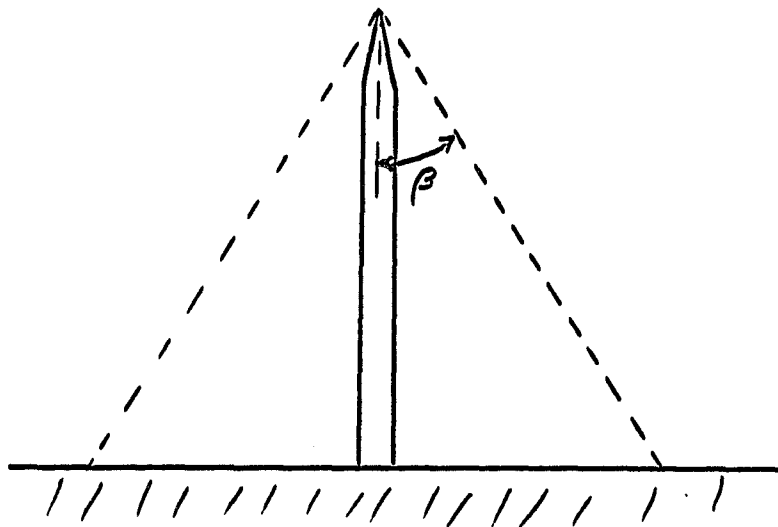


Figure 2

1.2 Distributed Lightning Protection Systems

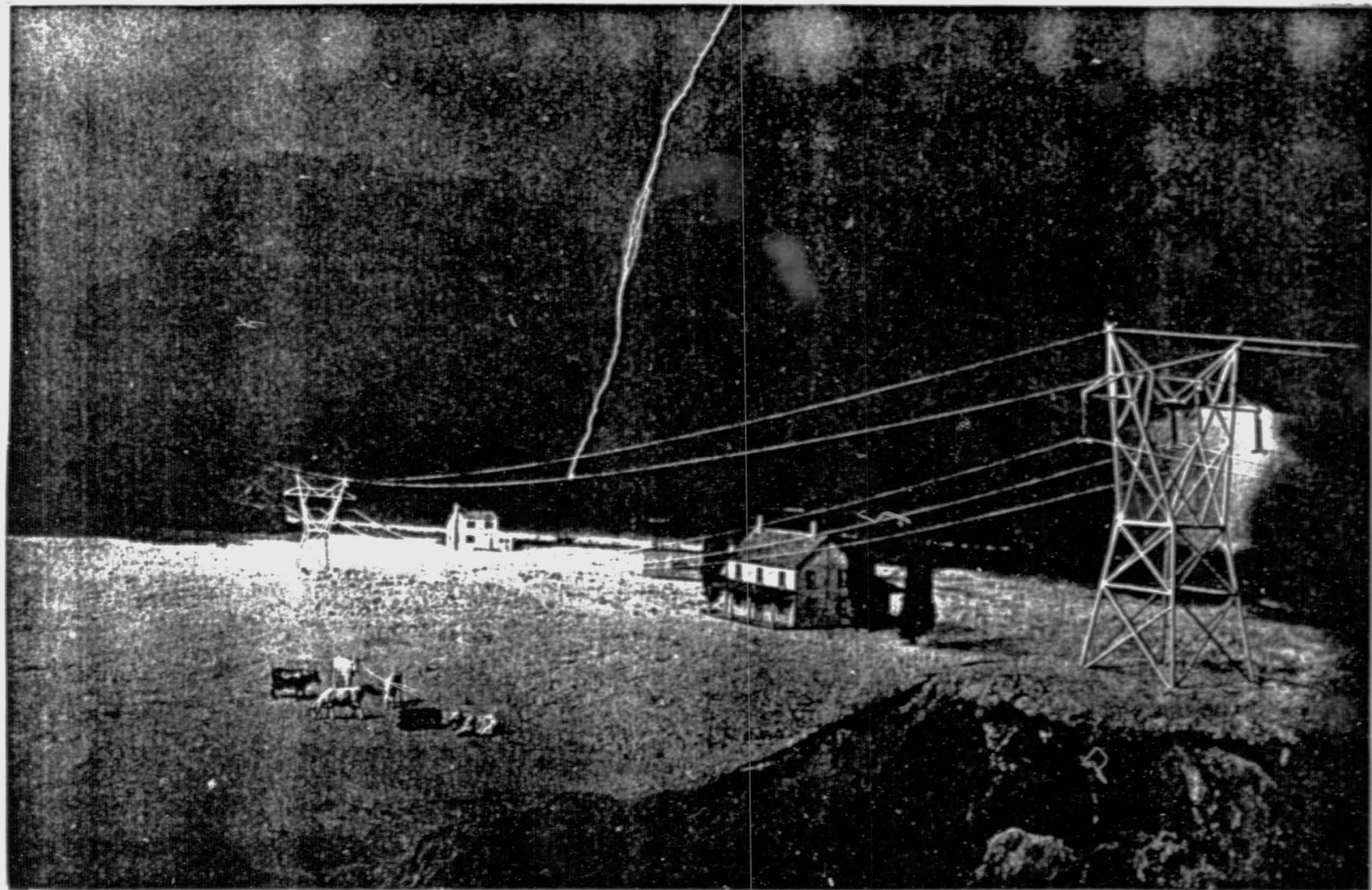
The cone of protection and the experimental data used to evaluate are specifically related to the single elevated point, and in most cases the system under consideration is 10 to 100 meters in height. As will be seen later, lightning protection of the rectenna falls into a class of structures that requires distributed lightning protection tactics. Figure 3 illustrates a distributed system used by power transmission companies. The main point is that the cone of protection concept is of limited usefulness in the total protection problem. We will use it on the panel and billboard scale as a technique to make a comparative assessment of capabilities of various configurations.

2. Lightning Rod Protection Configurations Compatible with the SPS Rectenna

We have considered three different configurations of lightning rod systems in this effort. In the smallest scale system considered each rectenna panel (0.74m in width) had a short lightning rod attached; see upper example in Figure 4. In the medium scale system each rectenna support structure (14.69m apart) or billboard will have an attached lightning rod; see middle example in Figure 4. And, in the distributed protection system, short terminals located on each rectenna support structure (14.69m apart) were connected by horizontal conducting structures; see lower example in Figure 4.

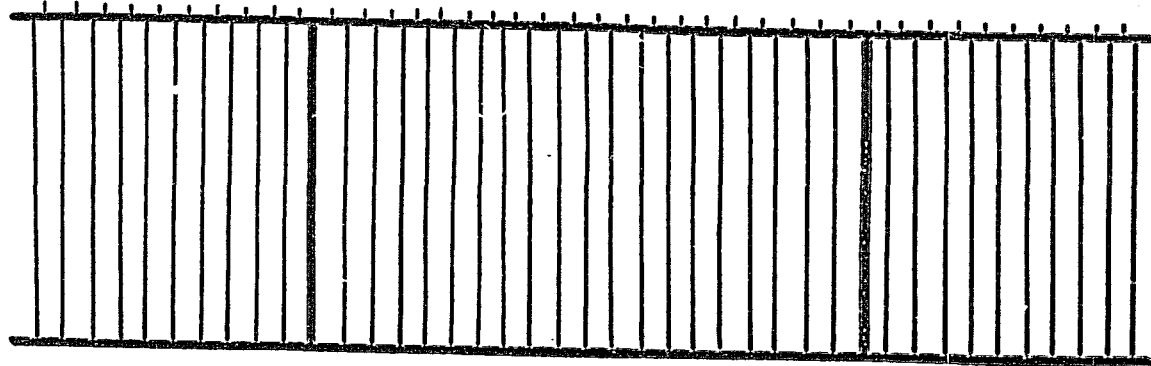
As seen in the analysis of the billboard scale system, it is impractical to seriously consider larger scale systems.

ORIGINAL PAGE IS
OF FLOOR QUALITY

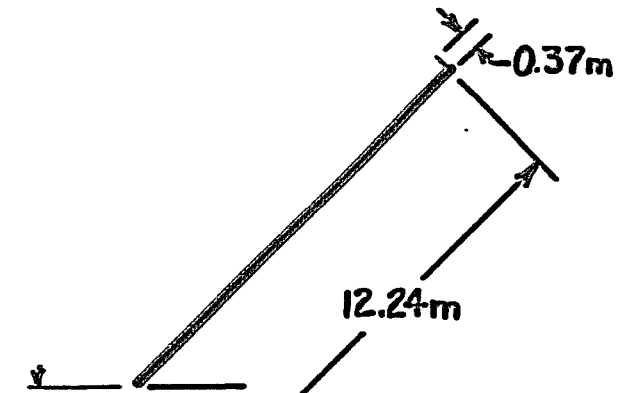
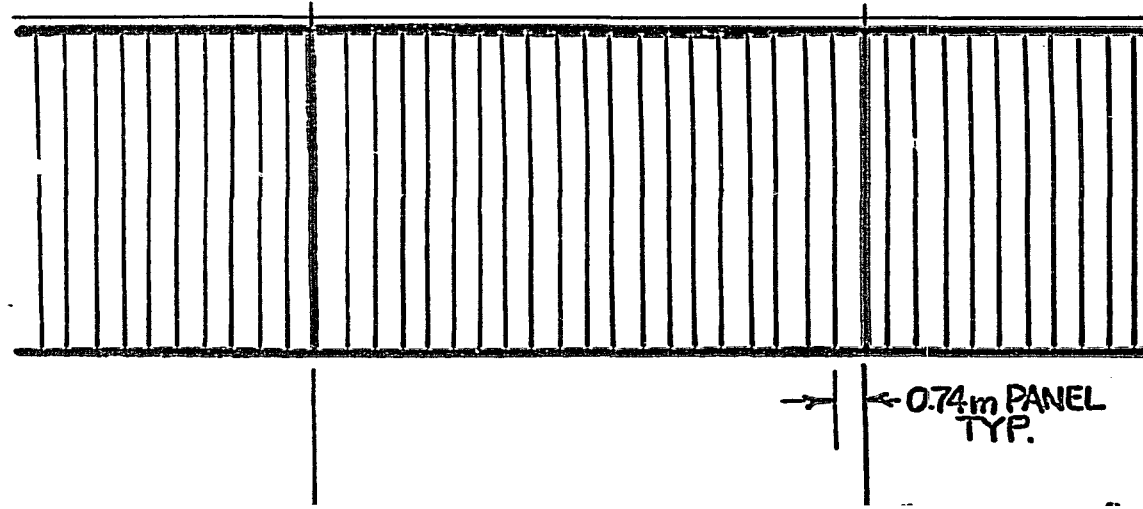
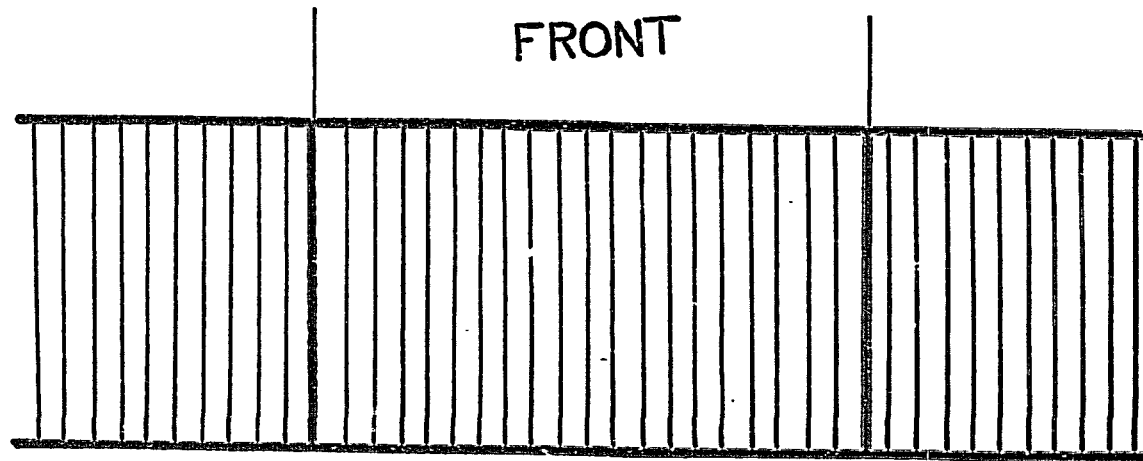


POWER LINES EMPLOY DISTRIBUTED LIGHTNING PROTECTION SYSTEMS. THIS ILLUSTRATION SHOWS A "STATIC" OR GROUNDED PROTECTION WIRE TAKING A STRIKE AND PROTECTING THE POWER LINES BELOW.

FIGURE 3



FRONT



SIDE

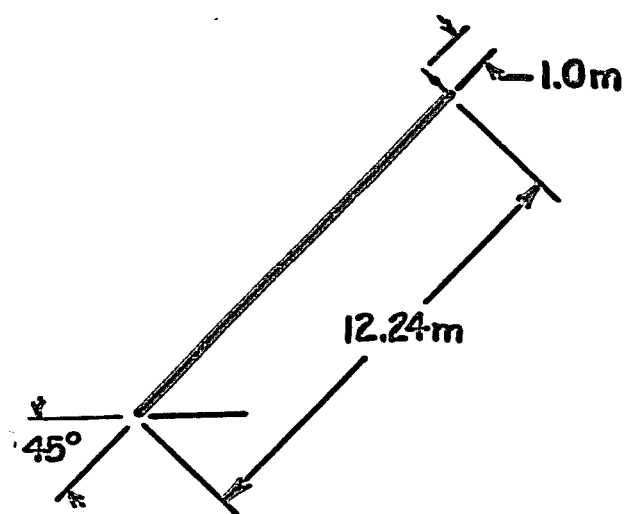
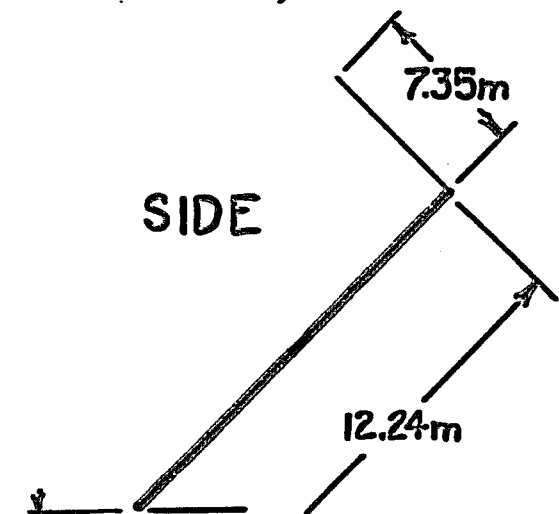
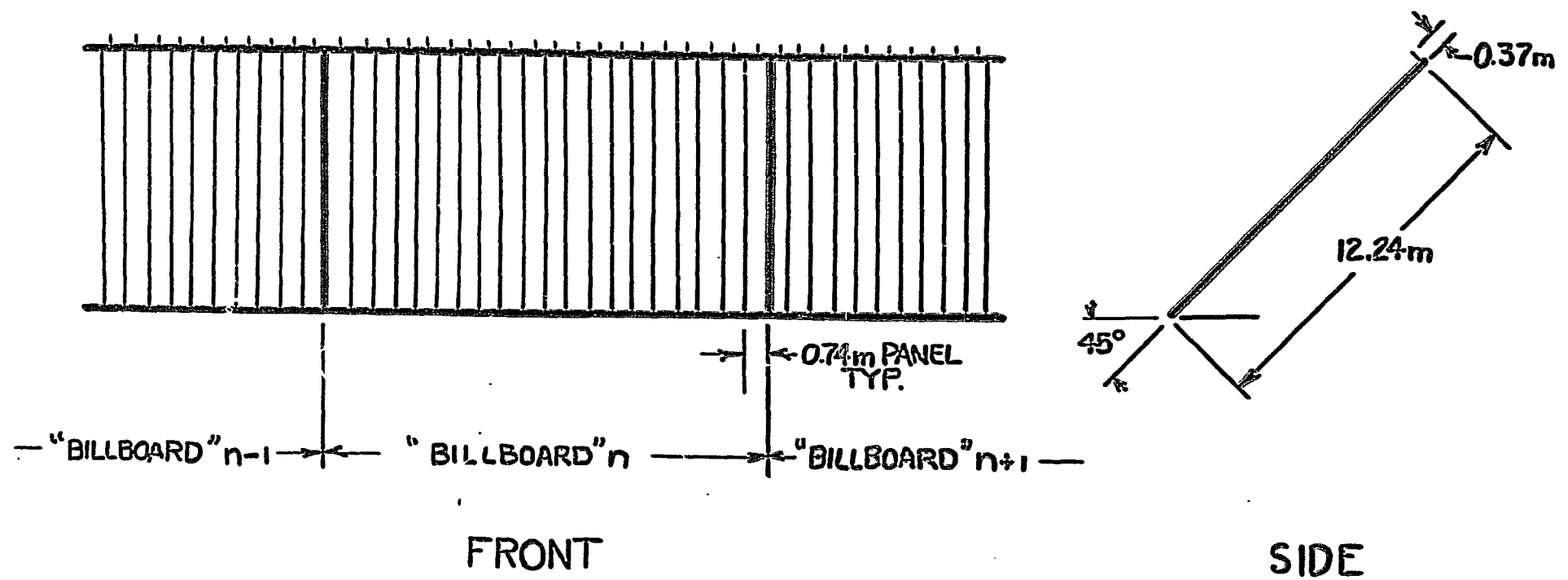


FIGURE A



PANEL SCALE LIGHTNING PROTECTION SYSTEM

FIGURE 5

2.1 Lightning Rod Protection at the Panel Scale

In this system configuration a relatively short lightning rod is positioned at the top of each panel and oriented perpendicular to the panel face (see Figure 5). Conceptually the rod is centered on the top of the panel, but in practice it could be on the panel edge without altering the results of this analysis.

Let α be the inclination of the rectenna. Figure 6 illustrates the case where β , the angle of the cone of protection, is greater than α . This figure applies only to the conditions in the vertical plane that passes through the lightning rod and is perpendicular to the rectenna face. In this particular projection it appears that the short (example 0.74m) lightning rod on the panel provides adequate protection to the rectenna. In other projections we see that there are, however, "holes in the armor."-

Figure 7 is an enlargement (x10) of the lightning rod portion of Figure 6, and defines the parameters to be used in the following discussions. The cone of protection intersects the plane of the rectenna to form conic sections:

- (1) If $\alpha + \beta = 90^\circ$ the intersection is a parabola.
- (2) If $\alpha + \beta < 90^\circ$ the intersection is an ellipse.
(this is the case illustrated in Figures 6 & 7)
- (3) If $\alpha + \beta > 90^\circ$ the intersection is a hyperbola.

If we now look at the intersection of the cone of protection with the panel for the specific cases above, we see the emergence of the protection problem with this type of lightning rod protection configuration. From the geometry of Figure 7 we see that the axis of the cone is at $\ell = L \tan \alpha$ and that the vertex of the conic is at $d = L \tan (\beta - \alpha)$ relative to the top of the panel.

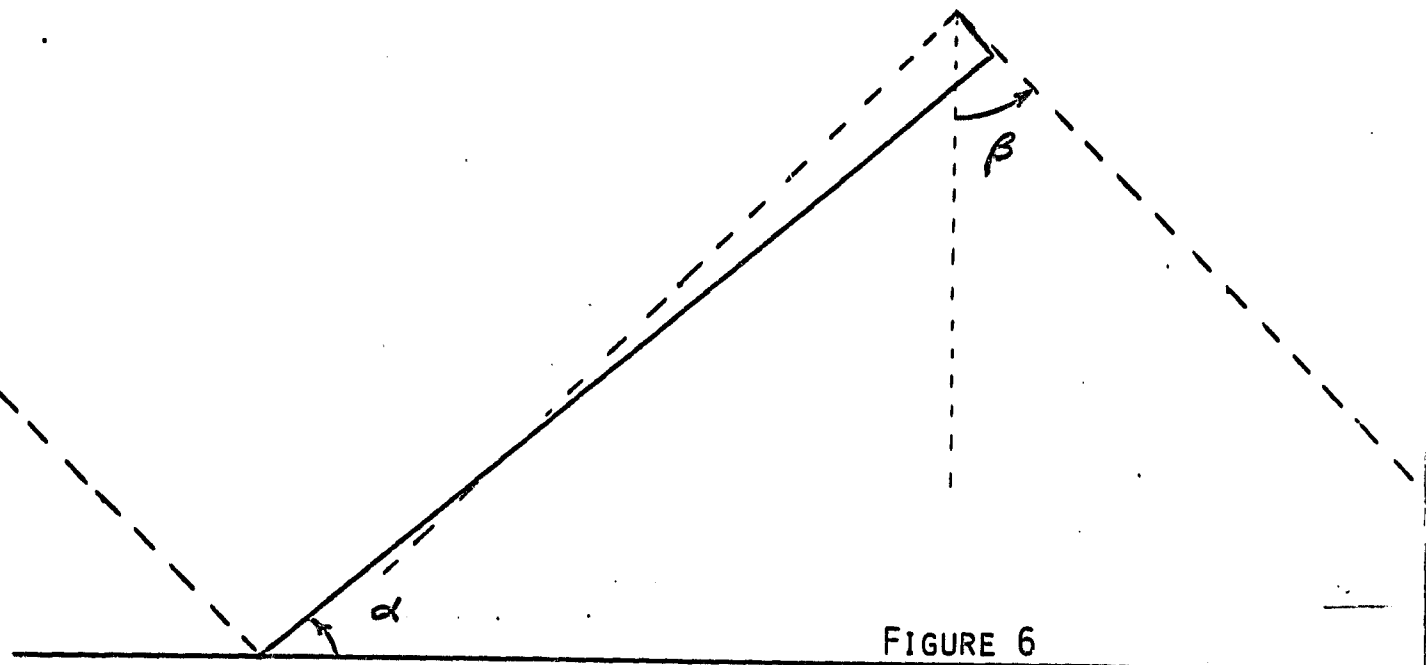


FIGURE 6

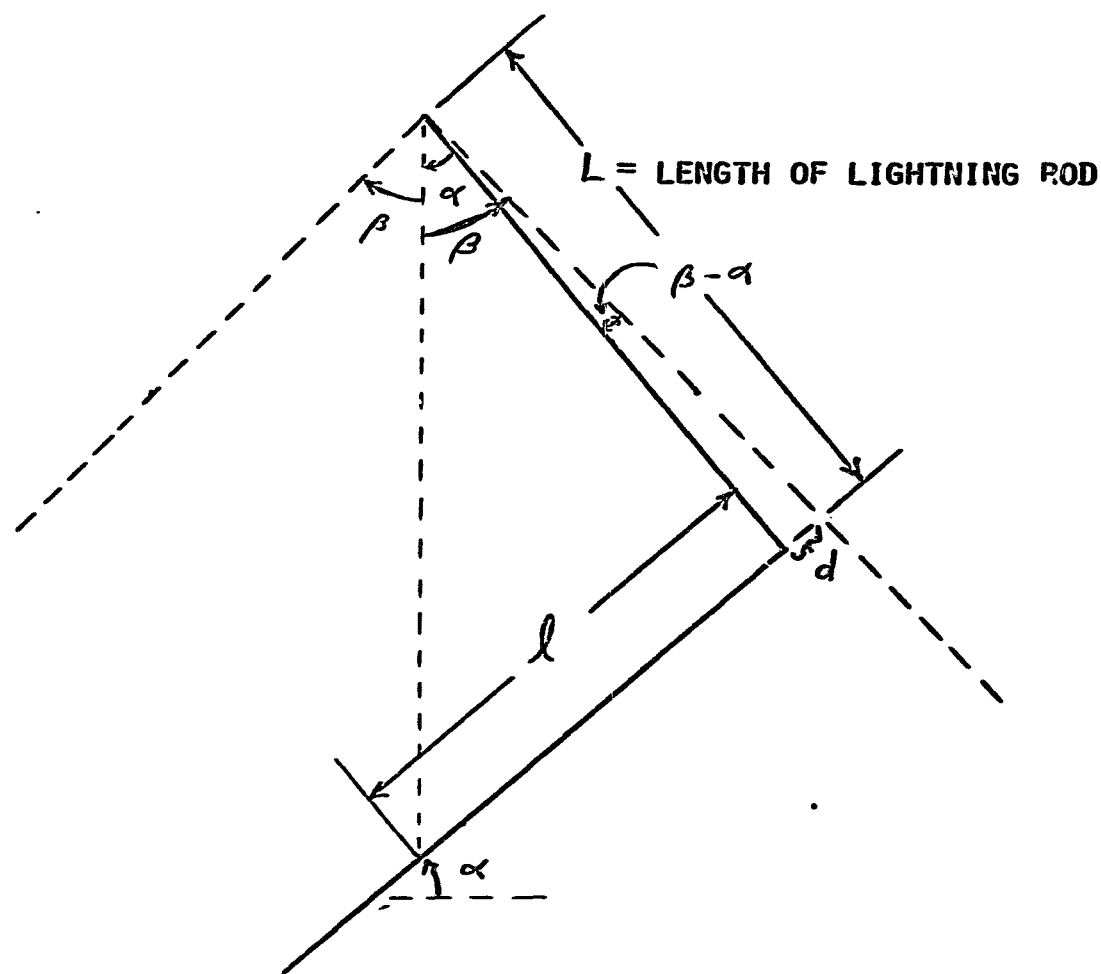


FIGURE 7'

ENLARGED VIEW OF THE UPPER END OF THE
RECTENNA IN FIGURE 7.

In a coordinate system defined in the rectenna plane with the origin at the axis of the cone and the y axis directed north (toward top of rectenna) and the x axis directed east, the equation for conic is:

$$\frac{x^2 \cos^2 \alpha}{L^2 \tan^2 \beta} + \frac{y^2 (\cos^2 \alpha - \sin^2 \alpha \tan^2 \beta) \cos^2 \alpha}{L^2 \tan^2 \beta} + \frac{2y \sin \alpha \cos \alpha}{L} = 1$$

For the parabolic solution this equation reduces to:

$$x^2 = -\frac{2L \sin^2 \beta}{\cos \beta \cos \alpha} \left(y - \frac{L}{2 \cos \beta \cos \alpha} \right)$$

In figure 8 we have plotted the intersection of cones of protection for three lightning rods of lengths 0.185m ($\approx 1/4$ panel width), 0.37m ($\approx 1/2$ panel width), and 0.74m (\approx panel width.)

In these examples the rectenna inclination angle α is taken to be 45° and the cone of protection β is equal to 45° . The resulting intersections are parabolas for the cases depicted in Figure 8. For the parabolic solution the cone of protection is parallel to the face of the rectenna in the vertical plane bisecting the panel (The view of Figure 6 and 7 except that here $\alpha = \beta = 45^\circ$).

At lower latitude sites (below 40°) the rectenna inclination angle α is less than 45° and the 45° cone of protection intersection becomes an ellipse; in Figure 6 the vertical projection illustrates the intersection in the plane through the lightning rod. The elliptic solutions leave regions along the base of the rectenna unprotected. Hence, the parabolic solutions of Figure 8 and the table (Fig. 9) represent maximum protection capabilities of the cone of protection with the panel scale protection configuration. The small ellipse in Figure 11 shows the cone of protection intersection for $\alpha = 40^\circ$, $\beta = 45^\circ$, and $L = 0.74$ m.

2.2 Lightning Rod Protection at the Bay or Billboard Scale

In this system a longer lightning rod is placed at the center (or end) of each bay or billboard making them 14.69m apart. The mathematical description here is identical to that for the panel scale system (2.1). Only sizes are different. Figure 10 illustrates the billboard scale system.

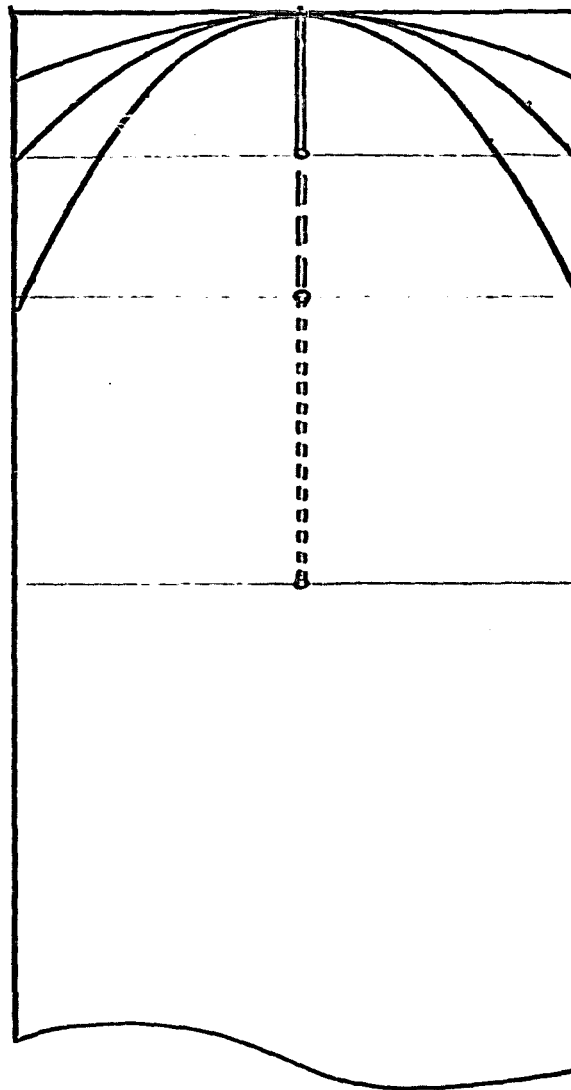


FIGURE 8

THE INTERSECTION OF THE CONE OF PROTECTION WITH A RECTENNA PANEL (THE CURVED LINES) SHOWN IN THE PLANE OF THE PANEL.
LIGHTNING ROD LENGTHS = $\frac{1}{4}$, $\frac{1}{2}$ AND 1 TIMES THE PANEL WIDTH ARE SHOWN PROJECTED VERTICALLY ONTO THE PANEL.

PARABOLIC TYPE SOLUTIONS

<u>ROD LENGTH IN METERS</u>	<u>UNPROTECTED AREA IN %</u>	<u>UNPROTECTED AREA X ENHANCEMENT FACTOR</u>
.185	1.1%	2.9%
.37	.55%	1.5%
.74	.28%	.74%

FIGURE 9

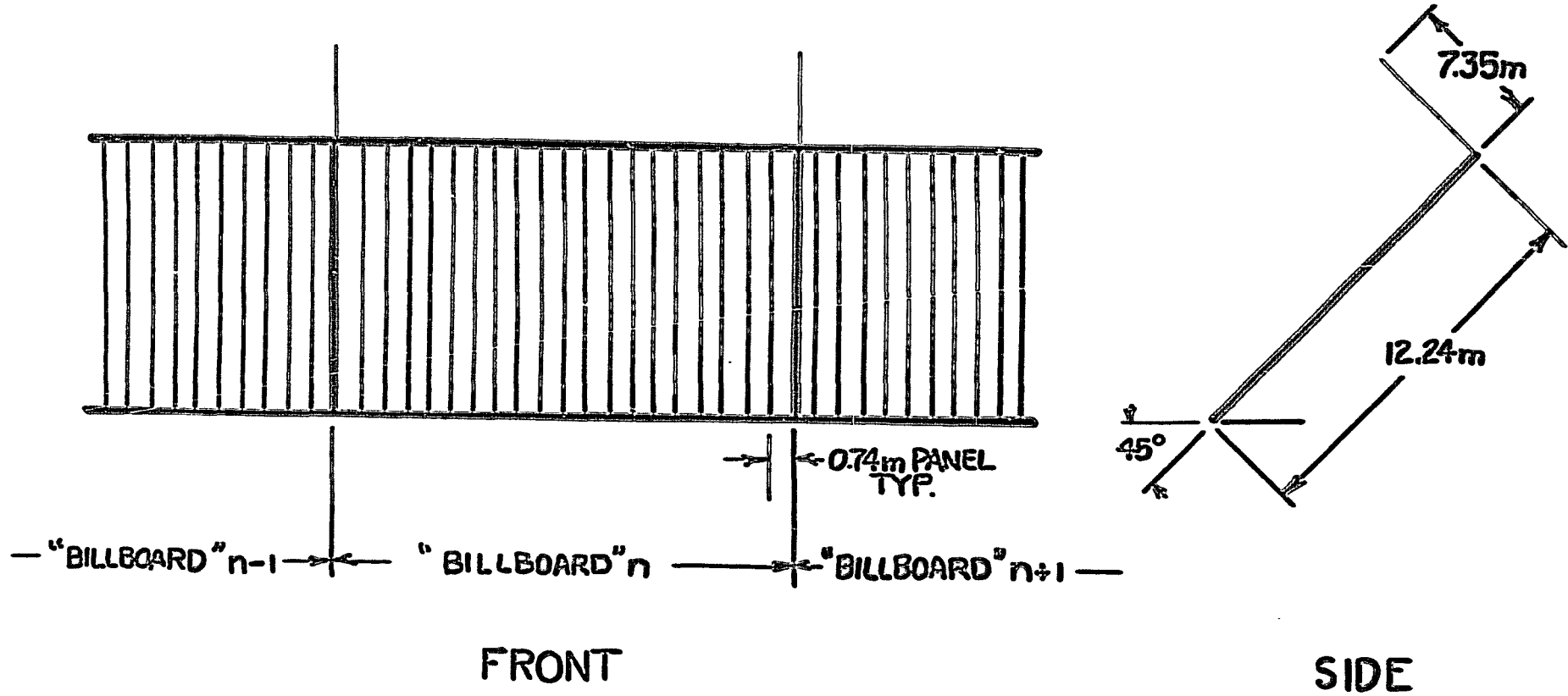


FIGURE 10
BILLBOARD SCALE LIGHTNING PROTECTION SYSTEM

To illustrate the cone of protection concept for this configuration we use as an example, $\alpha = 40^\circ$, $\beta = 45^\circ$, and $L = 7.35\text{m}$ ($= 1/2$ billboard width). The resulting intersection is a portion of an ellipse and is shown on Figure 12. Even if these long (7.35m) lightning rods were placed every 14.69m, a significant fraction of the rectenna (6.7% or when weighted by enhancement factor 18%) is unprotected (i.e. is not inside a cone of protection).

Furthermore, there are serious mechanical problems associated with supporting these long (i.e., over 22 feet) lightning rods. We think these examples are sufficient to demonstrate that configurations employing fewer lightning rods at longer spacing decreases protection and creates structural problems that ultimately will increase the total materials requirement.

For example, if we were to increase the length of the lightning rod in this configuration to the point that it could offer protection to the billboard in front of the one on which it is mounted (i.e. to the south), then with the appropriate phasing of rods between rows of billboards we could get total protection in the cone of protection context. The length of the rods would need to be 12m in order to provide this coverage.

2.3 The Distributed Lightning Protection System

The distributed lightning protection approach replaces the many lightning rods with a continuous horizontal conducting structure, as depicted in Figure 13. The region of protection now becomes the volume beneath two planes whose intersection is the horizontal protecting structure. This protection tactic is essentially the one employed by the power transmission companies. The angle between the protecting planes and vertical is variable; 45° is thought to be adequate but some designs use 30° for extra protection. This line is called the "static" by the power companies and this term is used here for convenience.

Figures 7 and 8 provide the correct geometric considerations for the distributed lightning protection if we interpret the end point of the lightning rod to be the location of the static. We note that the figures apply anywhere along the rectenna, not just in the specific locations required by the lightning rod analysis.

For consistent comparisons with the other lightning rod systems we will use $\alpha = 45^\circ$. Since $\alpha < 45^\circ$ for rectennas below 40° latitude, the top edge of the rectenna is protected by the static for any value of L , the displacement distance. If we try to use a smaller, more conservative value for α , we will run into problems in protecting the top edge of the rectenna with any system that does not cast a radio shadow on an active rectenna surface. The design constraint that we will use to specify L will be that the southward plane of protection intersect the rectenna surface at the base. Therefore,

$$L = 12.2\text{m} \tan(45^\circ - \alpha).$$

For α in the range 45° to 30° , L has the range of values 0m to 3.3m. This simple analysis ignores the protecting capability of the immediate southward row of the rectenna on the base of the row being considered. When these additional protective effects are considered we find that:

$$L = 6.1m (1 - \tan \alpha)$$

For α in the range 45° to 30° , L now has the range 0m to 2.6m.

Figure 13 gives the configuration of the distributed lightning protection system for $\alpha = 30^\circ$, which represents the most difficult situation to protect. In this situation the static is displaced by 2.6 meters from the top edge of the rectenna; note that the 45° planes of protection provide total coverage of the rectenna.

We wish to emphasize that the set of horizontal statics not only provide total protection in the sense that lightning flashes are expected to hit the statics instead of the active rectenna surfaces but that this system also reduces the induced voltages and currents in the rectenna. We estimate that induced charges, currents, and potentials are reduced by 1/2 by the static protection system.

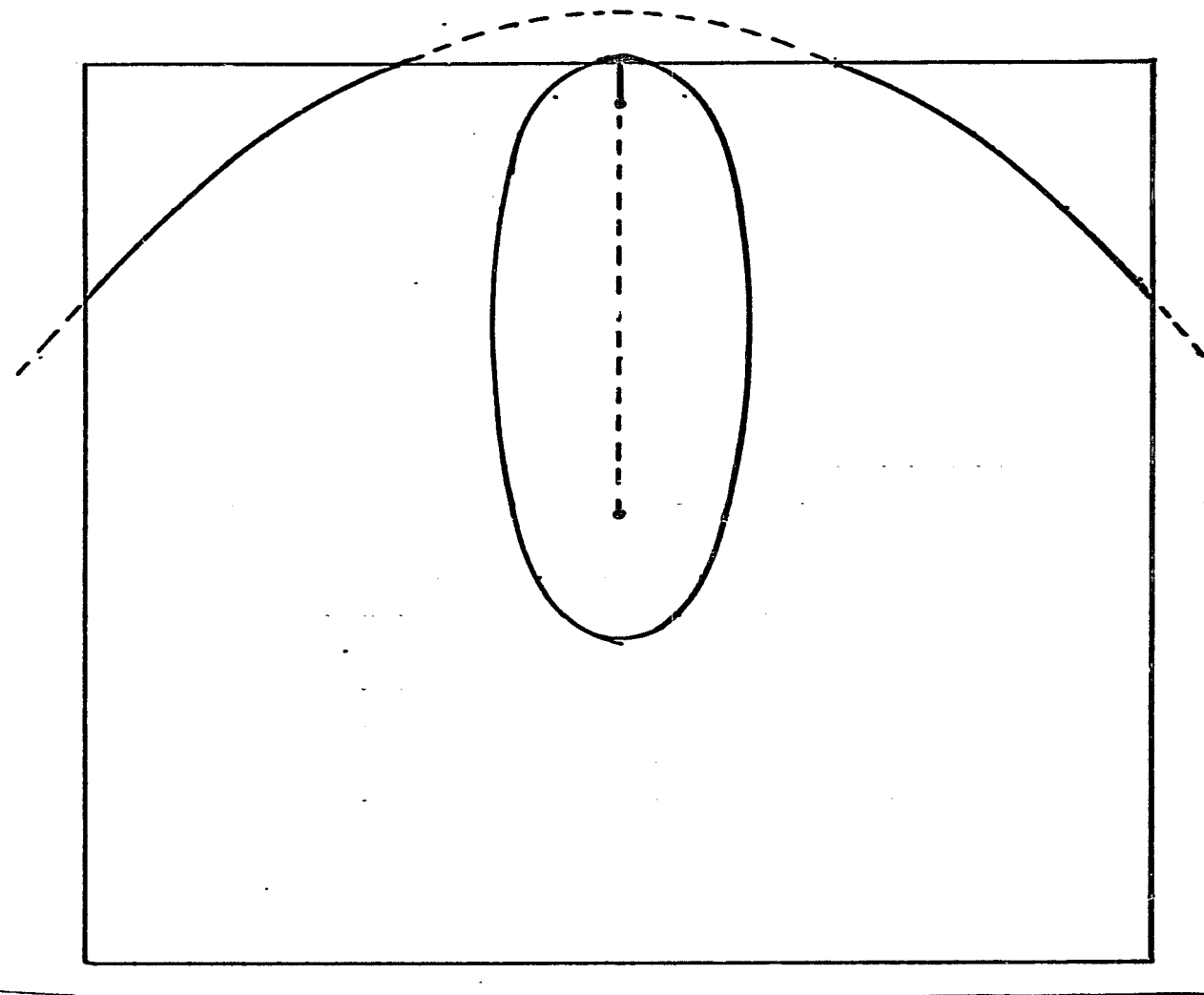
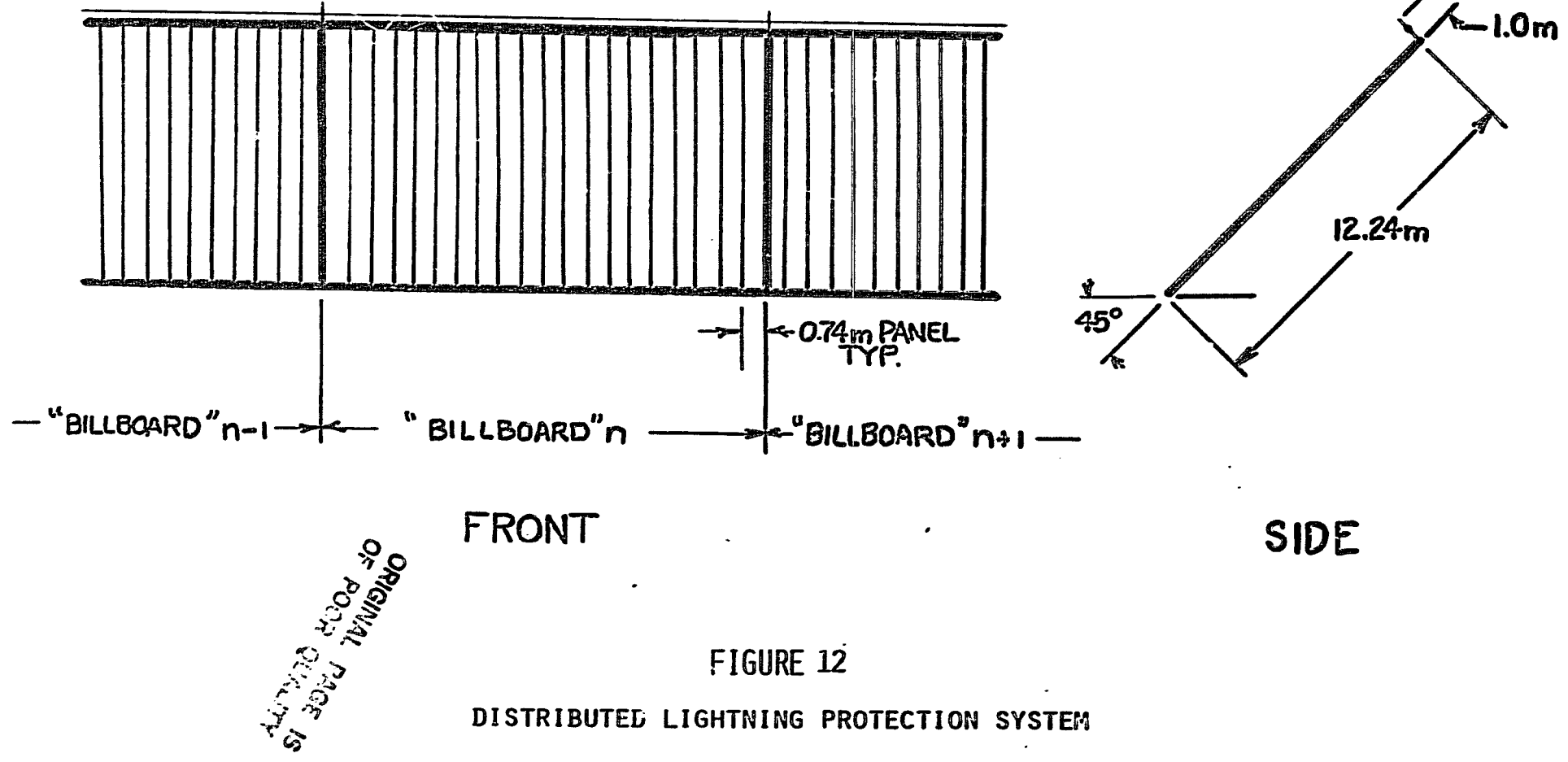


FIGURE 11

PANEL SCALE PROTECTION COMPARED TO BILLBOARD
SCALE PROTECTION SHOWN AS IN FIGURE 8 EXCEPT
HERE ON A BILLBOARD.



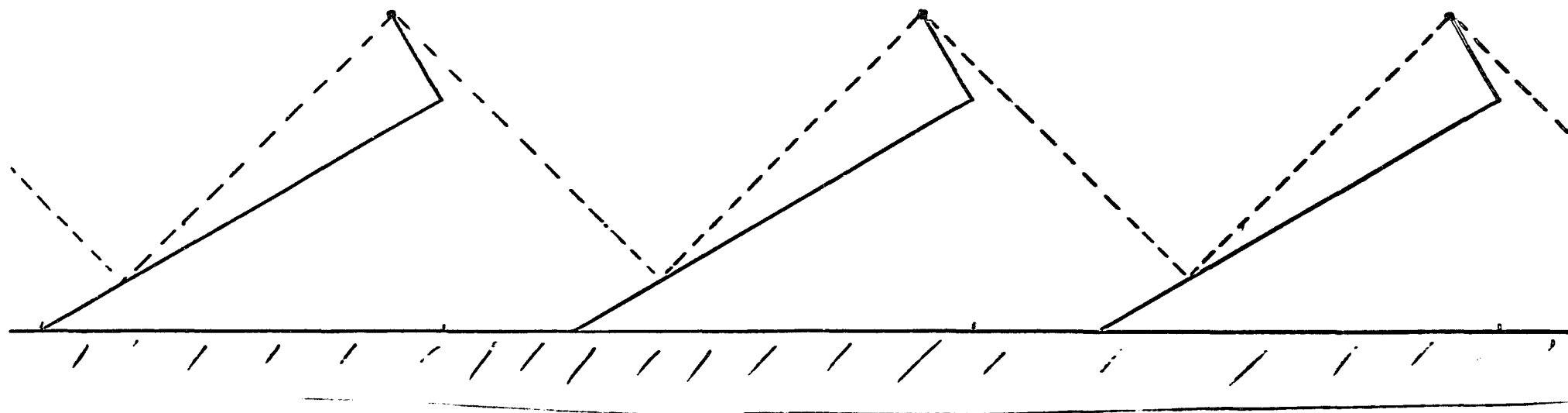


FIGURE 13

DISTRIBUTED LIGHTNING PROTECTION SYSTEM
ILLUSTRATING FORWARD AND BACKWARD PRO-
TECTION FOR SMALL INCLINATION ANGLES

II. SIMULATIONS OF LIGHTNING STRIKES TO THE SPS RECTENNA WITH AND WITHOUT PROTECTION

A series of experiments were performed in our electrostatic test chamber with a scale model of the SPS rectenna. The experiments consisted of exposing the model rectenna to a series of high voltage discharges produced with a Tesla coil.

The strikes to the rectenna were photographed using time exposures in a darkened room. A wire from the upper plate conducted the discharge to the vicinity of the model rectenna and provided us with a limited control over the area of the strike. This allowed us to keep the strikes near the volume in focus by the camera.

Different areas of the model rectenna were protected by different systems, and one area was unprotected. The following paragraphs describe samples of these experiments:

1. The Unprotected Rectenna

Most of the strikes were to the upper edge of the billboard because of the larger enhancement factor at that point. Several strikes to the billboard face occurred.

In Figure 14, we see two strikes to the unprotected billboard section, one of which is to the billboard face. Notice that these strikes are perpendicular to the face when near the face; we would anticipate this because the equipotential lines are nearly parallel to the face here.

In Figure 14, we also see for comparison the three lightning protection systems modeled. To the left is the billboard scale system; to the right is the panel scale system; and behind the flashes is the distributed lightning protection system.

2. The Panel-Scale Protection System

The next three figures are examples of strikes photographed on the section of the model rectenna that was protected by the panel-scale lightning protection system.

In Figure 15, we see two strikes on the same billboard, both of which terminate on the panel-scale lightning rods.

Figure 16 shows two strikes from a different view going to two different billboards. The panel-scale protection system here is seen to protect only the front billboard. Protection is probably greater for real lightning because in our experiments we artificially bring the "leader tip" very close to the billboard with the wire.

Multiple strikes to the panel-scale protection system are seen in Figure 18. One of the strikes goes directly to the billboard face. This type of failure will occur in nature, but with lower probability than illustrated here.

3. The Billboard-Scale Lightning Protection System.

Two sets of experiments were made with the billboard-scale lightning protection system. The one illustrated in Figure 19 corresponds to rods of length 7.35m. (A second series of strikes were made with rods cut to one-half of this length, but these were photographed in color and are not suitable for this report.) Figure 19 illustrates the capability of these long rods to direct lightning to the desired point.

In Figure 20, we have a side view of a billboard-scale protector taking a strike and protecting the billboard-face. Figure 21 illustrates the "hole in the armor" of the billboard-scale lightning protection system. Two flashes strike the protection system, but a third strikes the billboards between two protectors, as predicted in Figure 12. With real lightning this is less likely to happen, but it can and will occur.

4. The Distributed Lightning Protection System.

The displacement distance of the static from the billboard was scaled from 0.74m to make it correspond to the height of the panel-scale protection system. Fewer failures-to-protect were observed with this system but they did occur. With real lightning, they would be even less likely to occur.

In Figure 22, we see two strikes to two different billboards from the side view. Figure 23 shows two strikes to the same billboards, which were provided with a distributed lightning protection system. One strike is to the terminal support rod at the billboard edge, which is the preferred point of strike. The other strike goes to the horizontal static line between the terminal support rods.

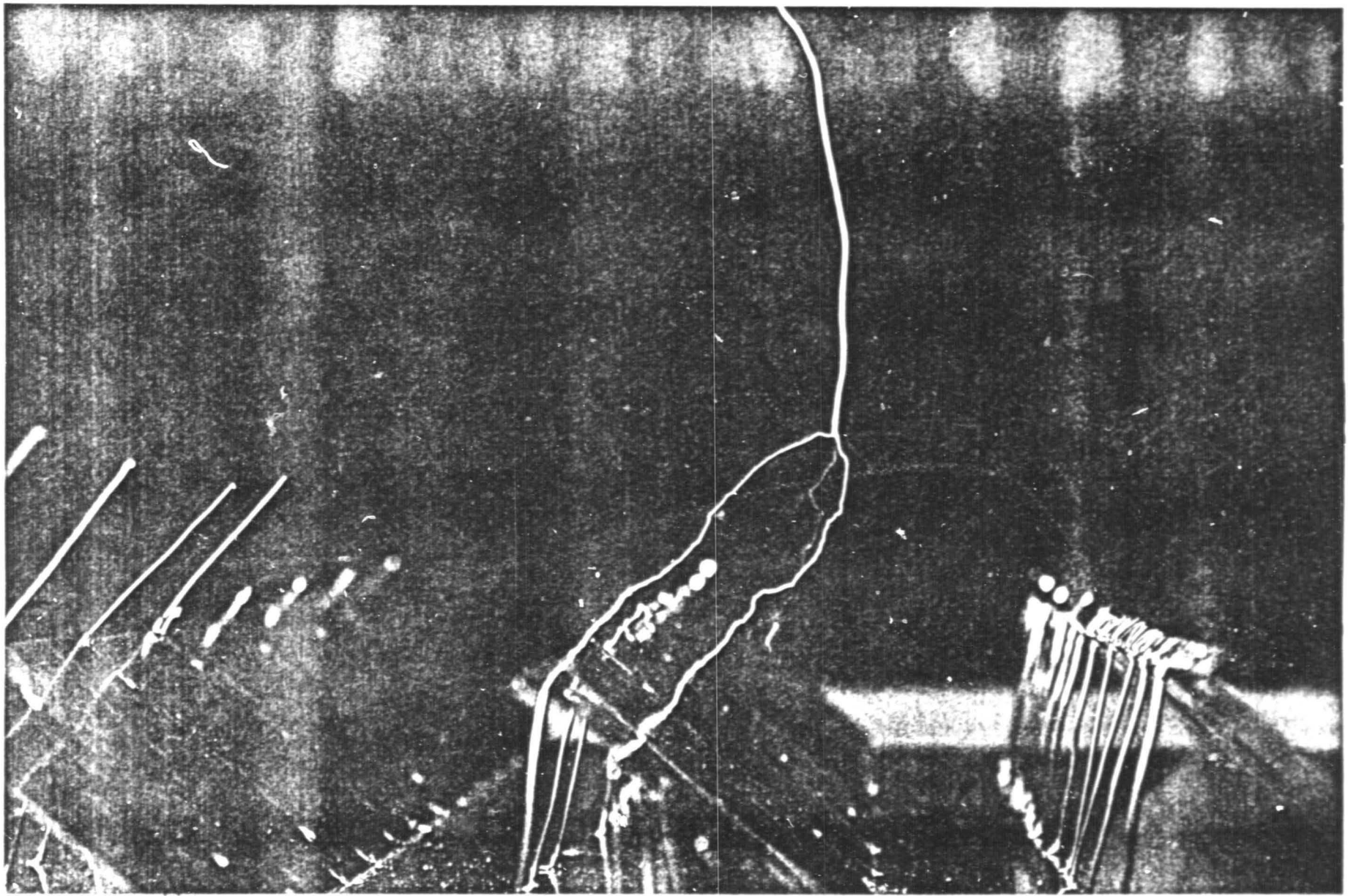


FIGURE 14

FIGURE 14

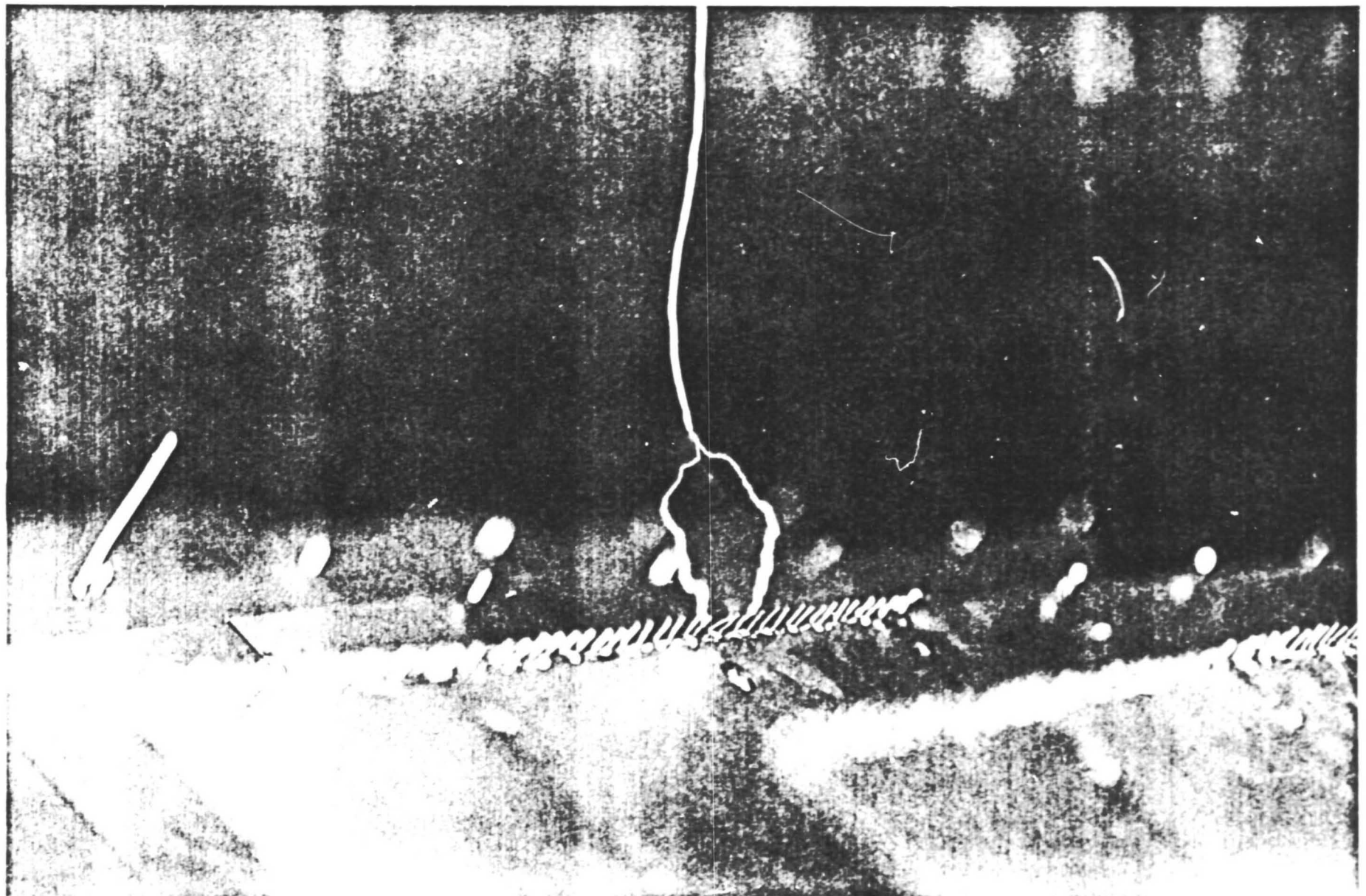


FIGURE 15

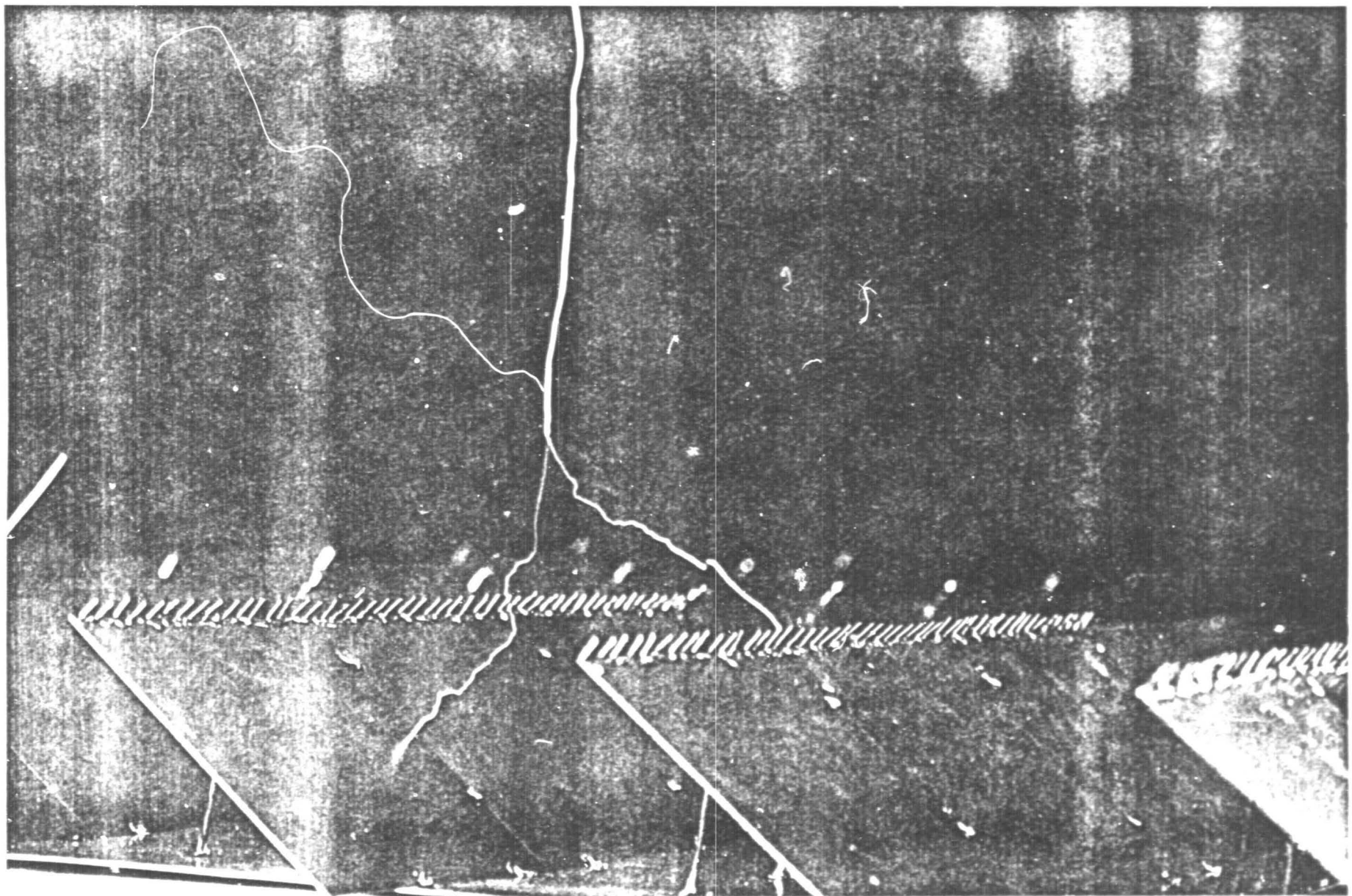
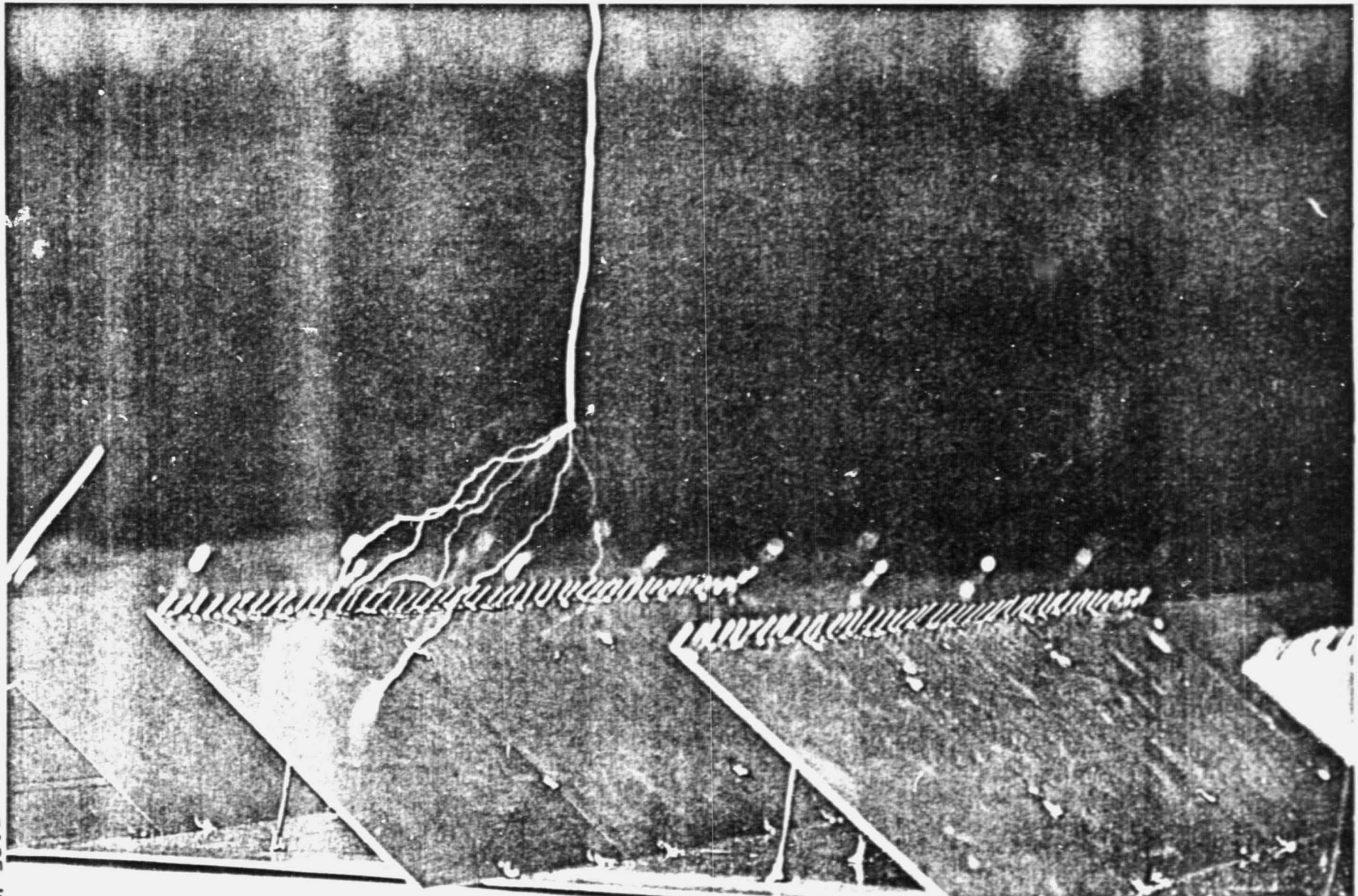
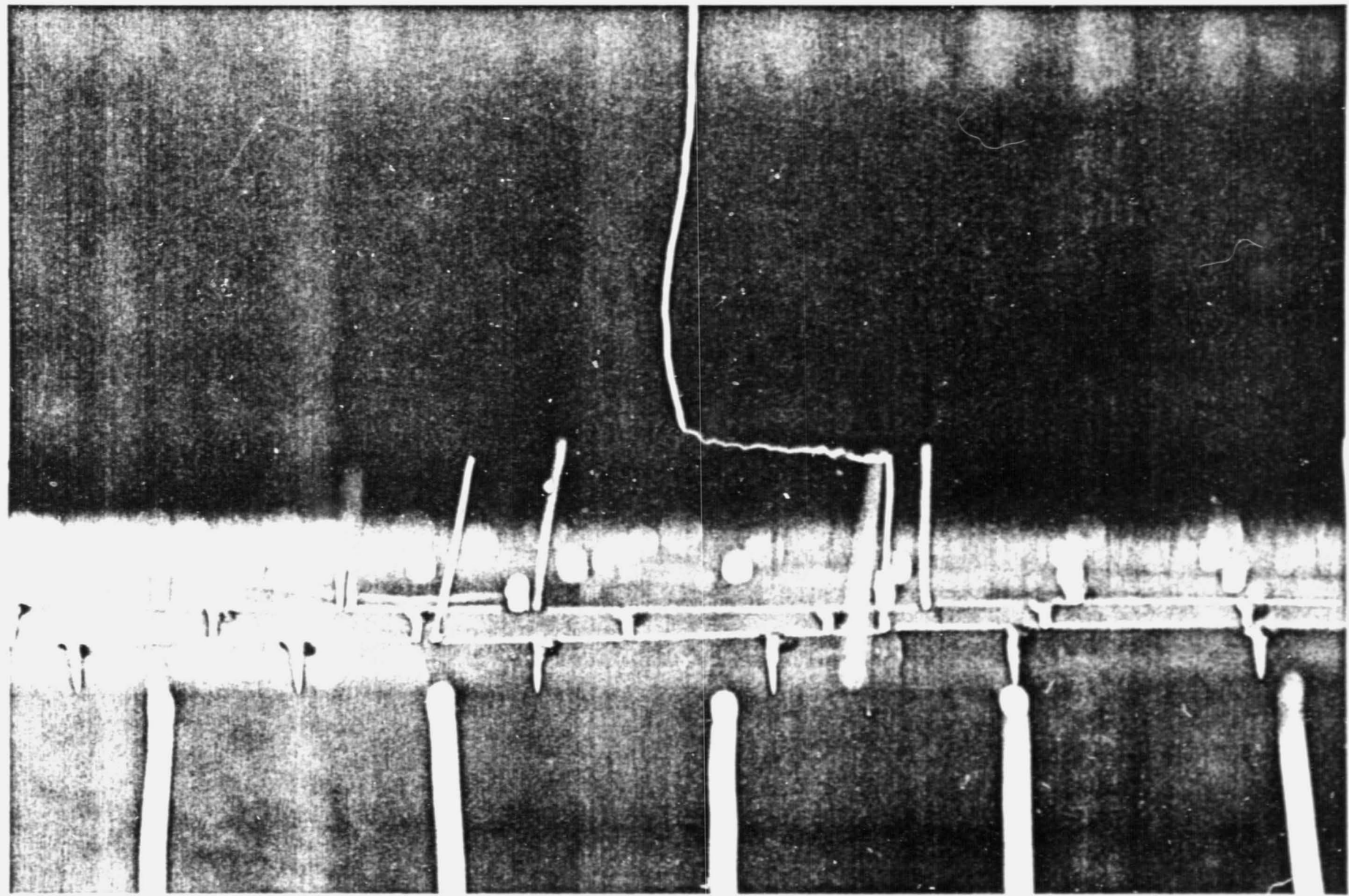


FIGURE 16



ORIGINAL PAGE IS
OF POOR QUALITY

FIGURE 17



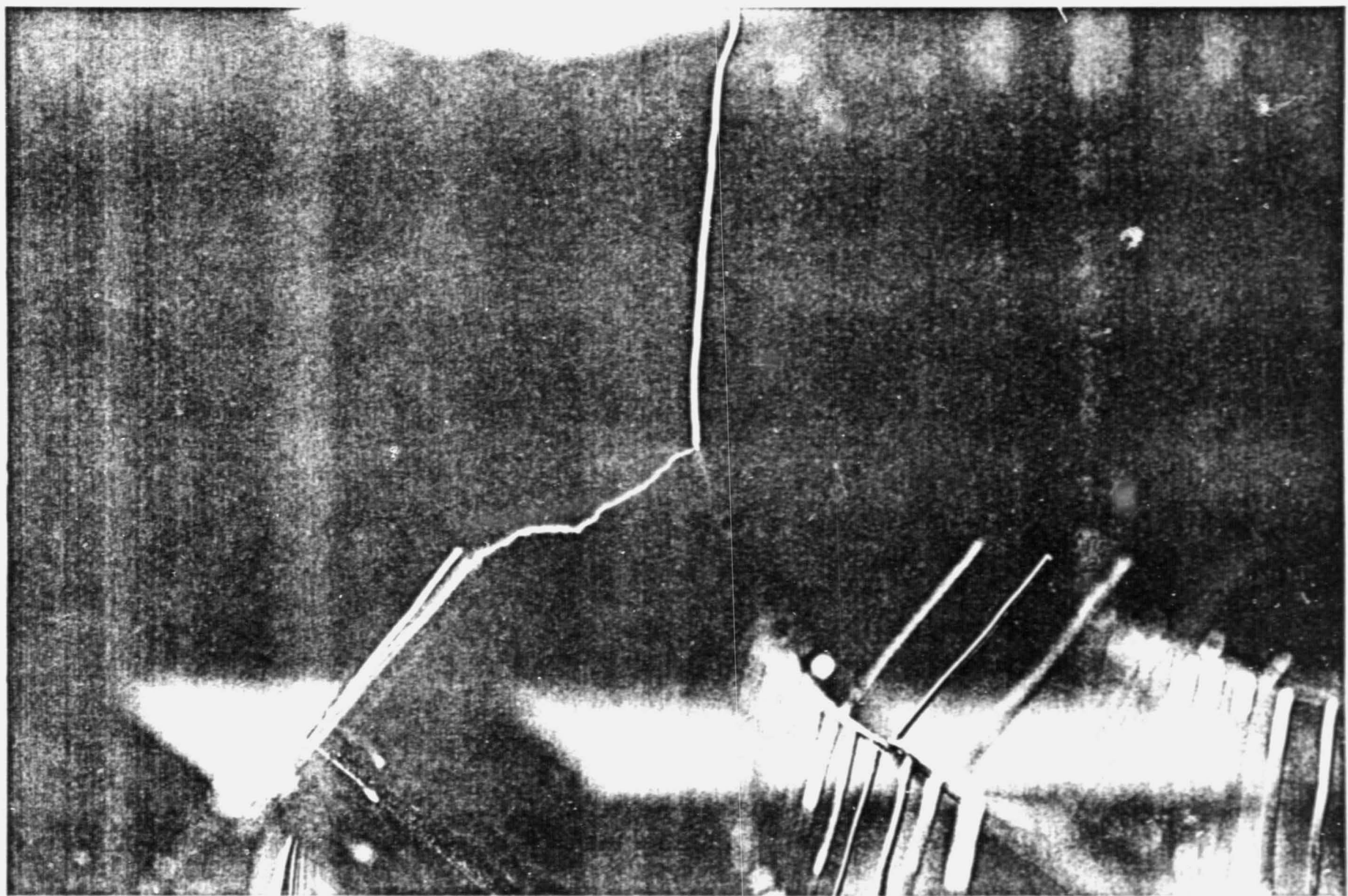


FIGURE 10

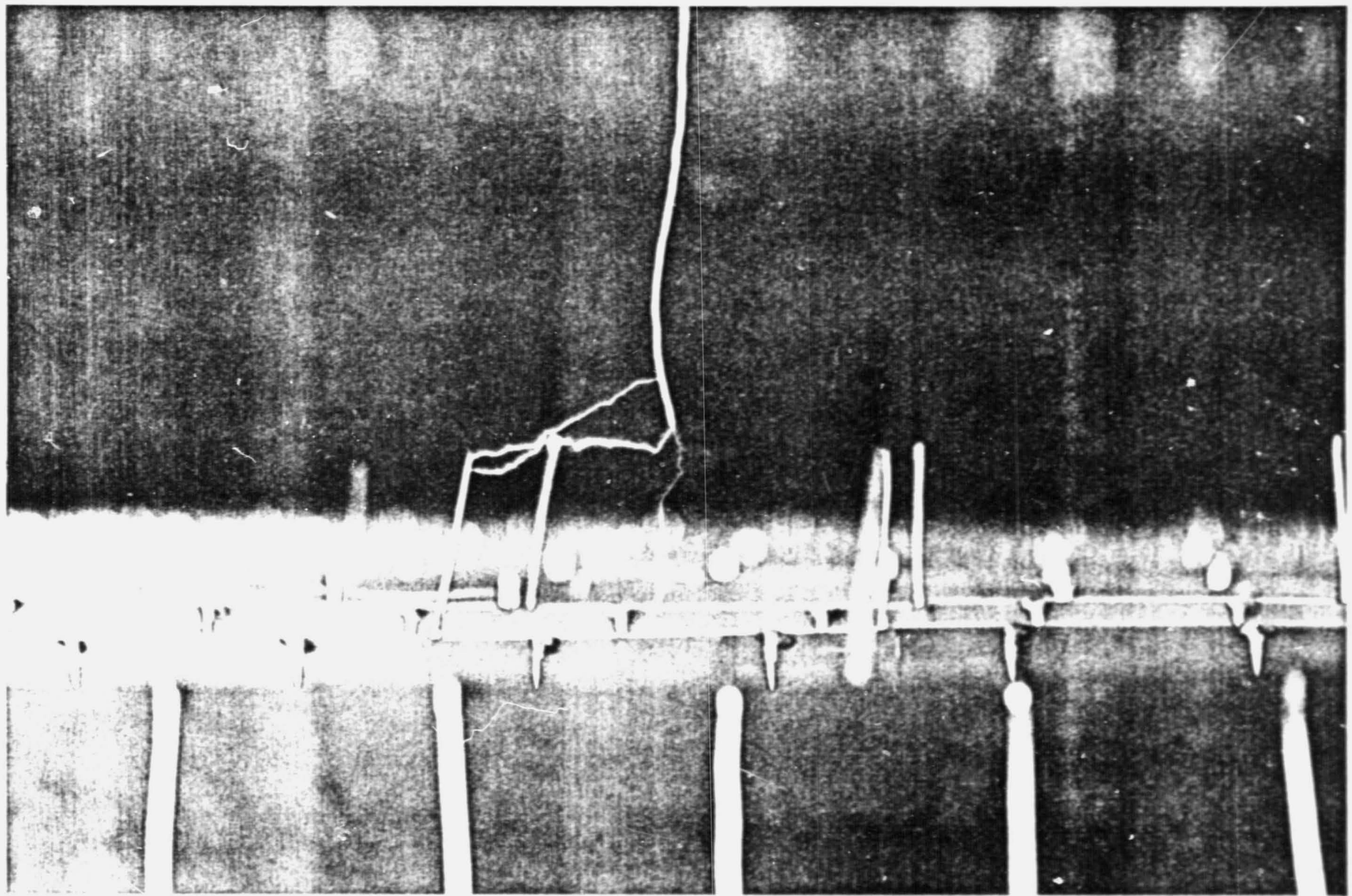
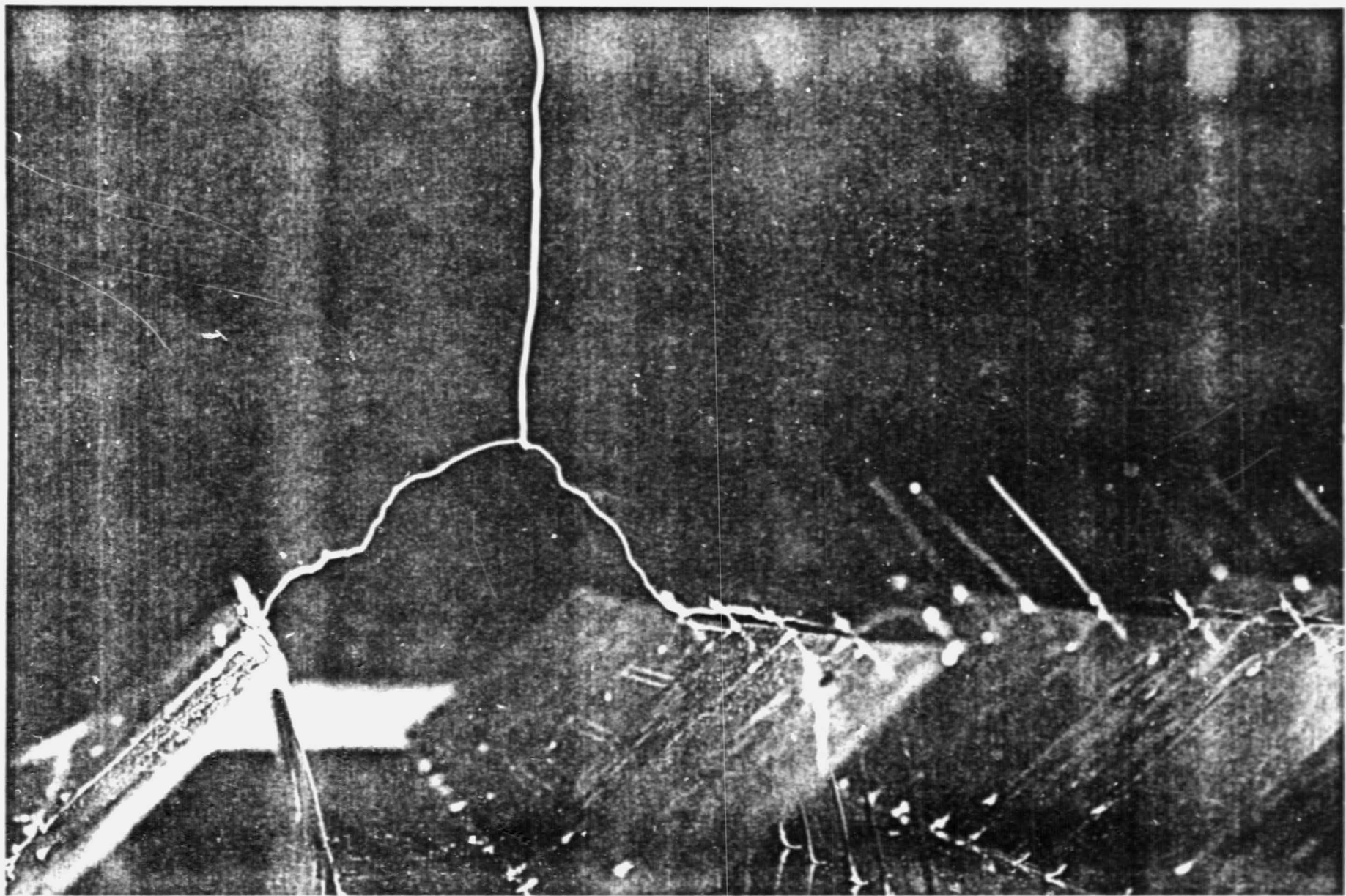
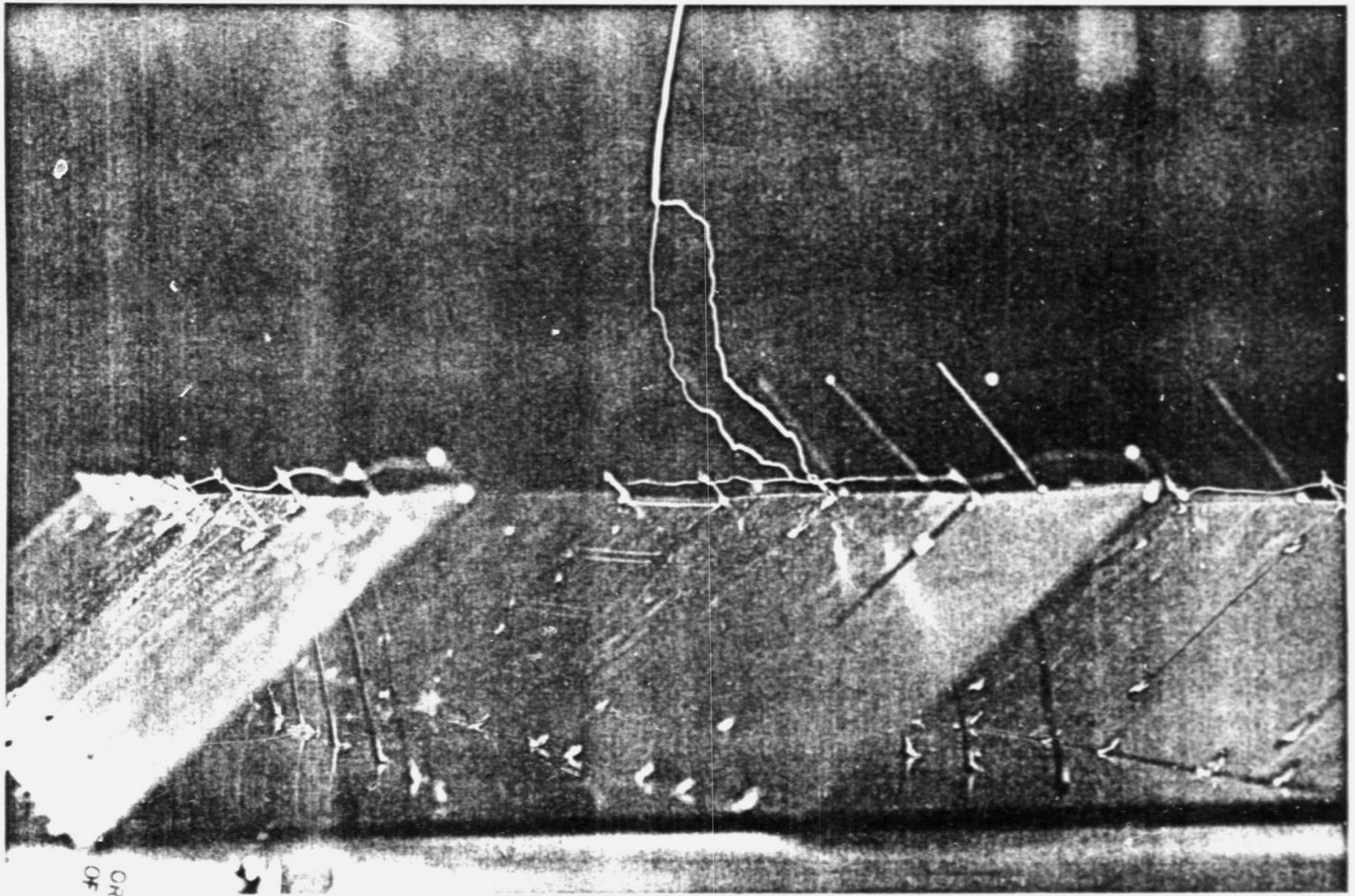


FIGURE 20





ORIGINAL PAGE IS
OF POOR QUALITY

FIGURE 22

III. GROUNDING CONSIDERATIONS FOR THE PROPOSED LIGHTNING PROTECTION SYSTEM

The thundercloud charges induce a large surface charge on the rectenna below the cloud; during the stepped leader period even larger surface charges are induced on the region below the leader tip. Most of the current flowing during the return strokes of the lightning flash must be distributed by the grounding system to connect with the induced surface charges. If adequate paths for these currents are not planned and provided, the lightning will make its own paths. Most of the induced surface charge will reside on the horizontal statics of the recommended distributed lightning protection system. The primary grounding system described here is to provide low impedance paths for the redistribution of the induced surface charges and the part of the lightning charge that resides on the rectenna surface.

1. Primary East-West Grounding

It is absolutely necessary that the horizontal statics have a good low impedance connection at billboard edges. The static should appear to be a continuous very low impedance conductor in the east-west direction, as illustrated in Figure 24.

2. Primary North-South Grounding

It is also necessary that the statics are mutually grounded in the north-south directions; there are two methods of achieving this:

2.1 Periodic connections north-south at the level of the statics. If these north-south statics are aligned along the billboard edges, then there will be little power loss due to microwave shadows (See Figure 24.)

2.2 Interconnect grounding in the north-south direction at the surface or sub-surface level (see figure 25) can also be used, but this approach creates a higher impedance to north-south currents on the static system.

2.3 A surface level grounding network is required in addition to the primary static grounding network. The surface network must handle the redistribution of induced charges on the rectenna surfaces and power distribution systems and it provides a safe working environment at the surface level. East-west continuity with low impedance connections must be provided at the base of the rectenna support structures, and north-south continuity with low impedance connections as discussed in 2.2 and illustrated in Figure 25 must be provided. Figure 26 highlights the surface level grounding network.

2.4. Interconnections between the primary and surface grounding networks should be provided by the vertical conductors located at every billboard upper corner; these are the same structures on which are mounted the terminals and supports for the statics. The vertical interconnections are highlighted in Figure 27.

2.5 The ultimate or final component of the grounding system is the tie-in to Earth ground. At regular intervals in the rectenna a deep earth grounding rod must be driven into the soil to make good contact with a conducting soil for earth ground²⁸

The organization of the earth grounding system should be along diagonals, as illustrated in Figure 28. Here we see that the placement of earth ground at every fourth billboard but on a diagonal produces a grid such that lightning striking the primary grounding network will never have to travel more than 30 meters along the east-west conductors before finding a ground, or 32 meters along the north-south conductors (for a rectenna with a 40° inclination angle).

THE PRIMARY GROUNDING SYSTEM AT THE STATIC LEVEL

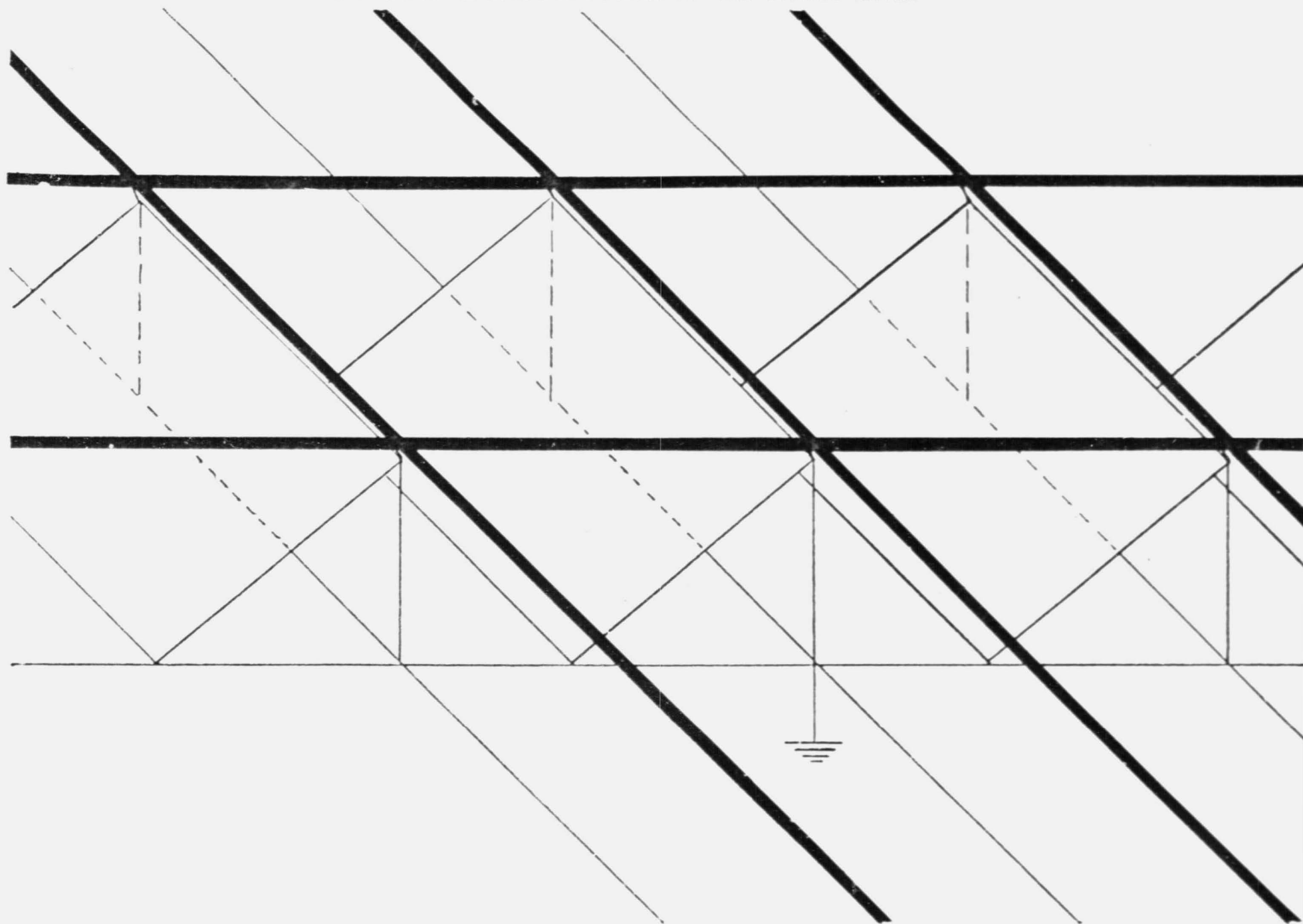


FIGURE 24

GROUNDING
RECTENNA LIGHTNING ROD SYSTEM

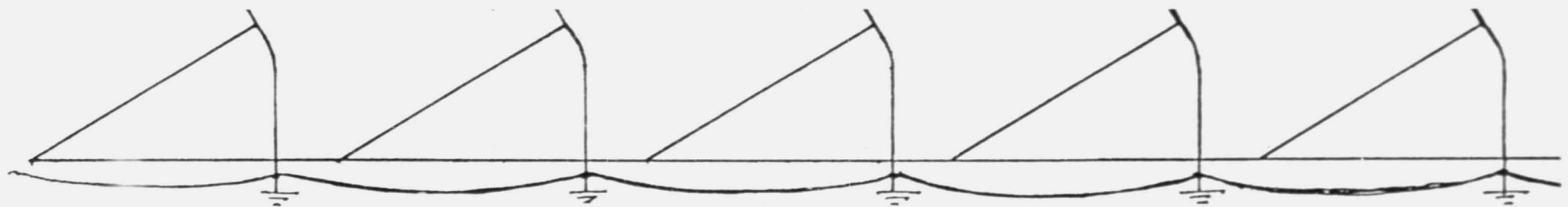


FIGURE 25

THE SURFACE-LEVEL GROUNDING NETWORK

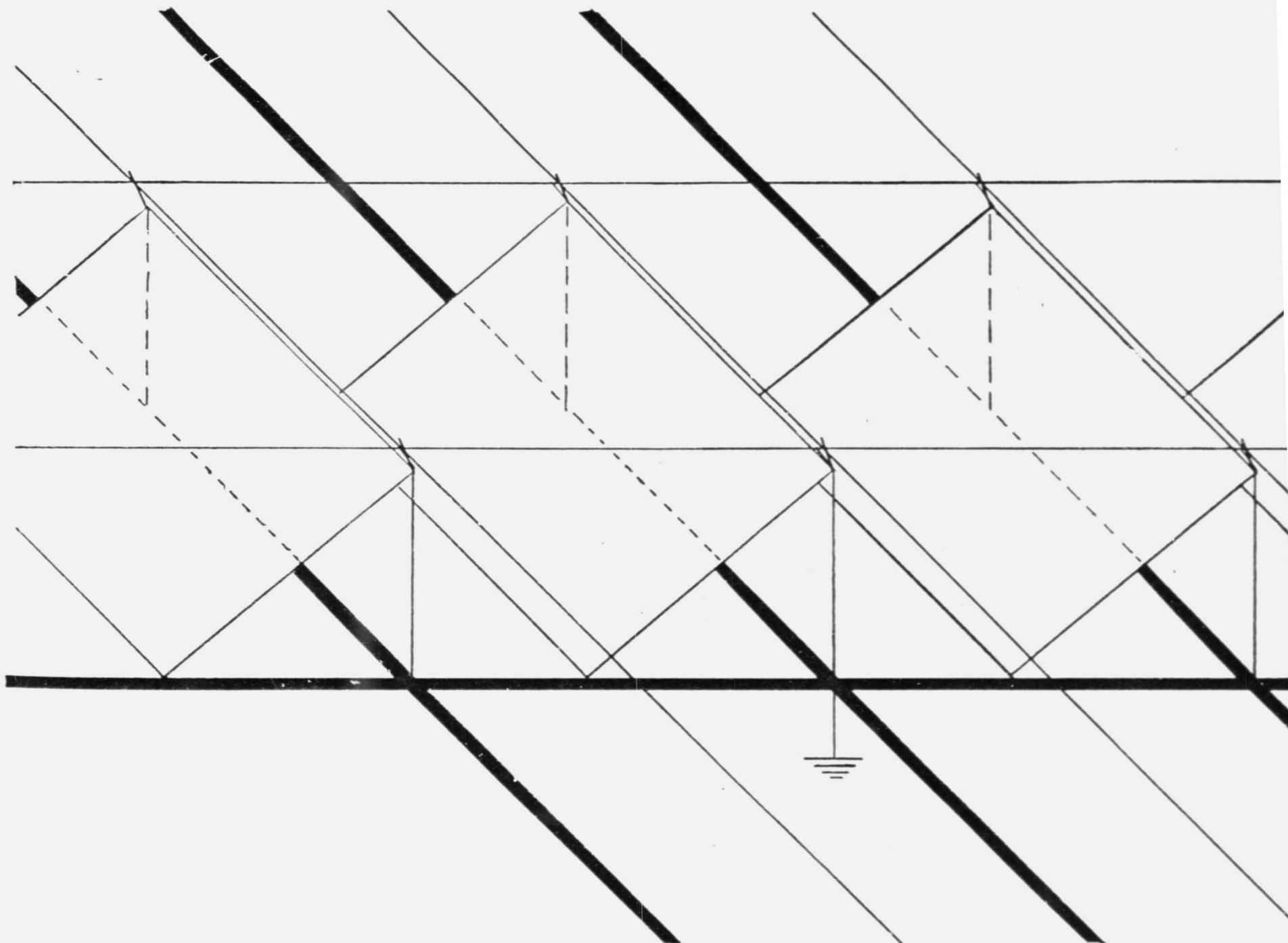
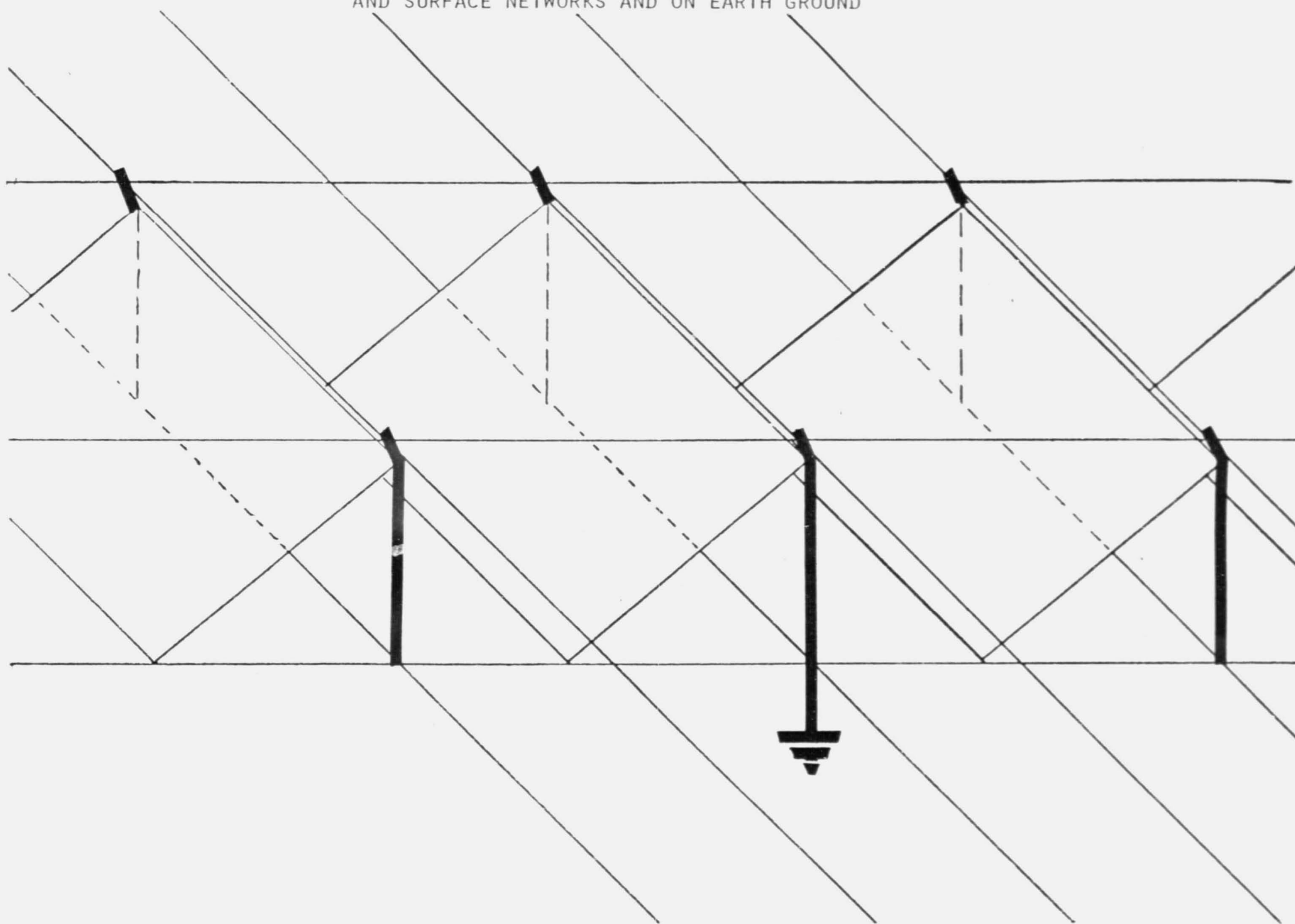


FIGURE 26

VERTICAL INTERCONNECTIONS BETWEEN PRIMARY
AND SURFACE NETWORKS AND ON EARTH GROUND



PLACEMENT OF EARTH GROUNDS

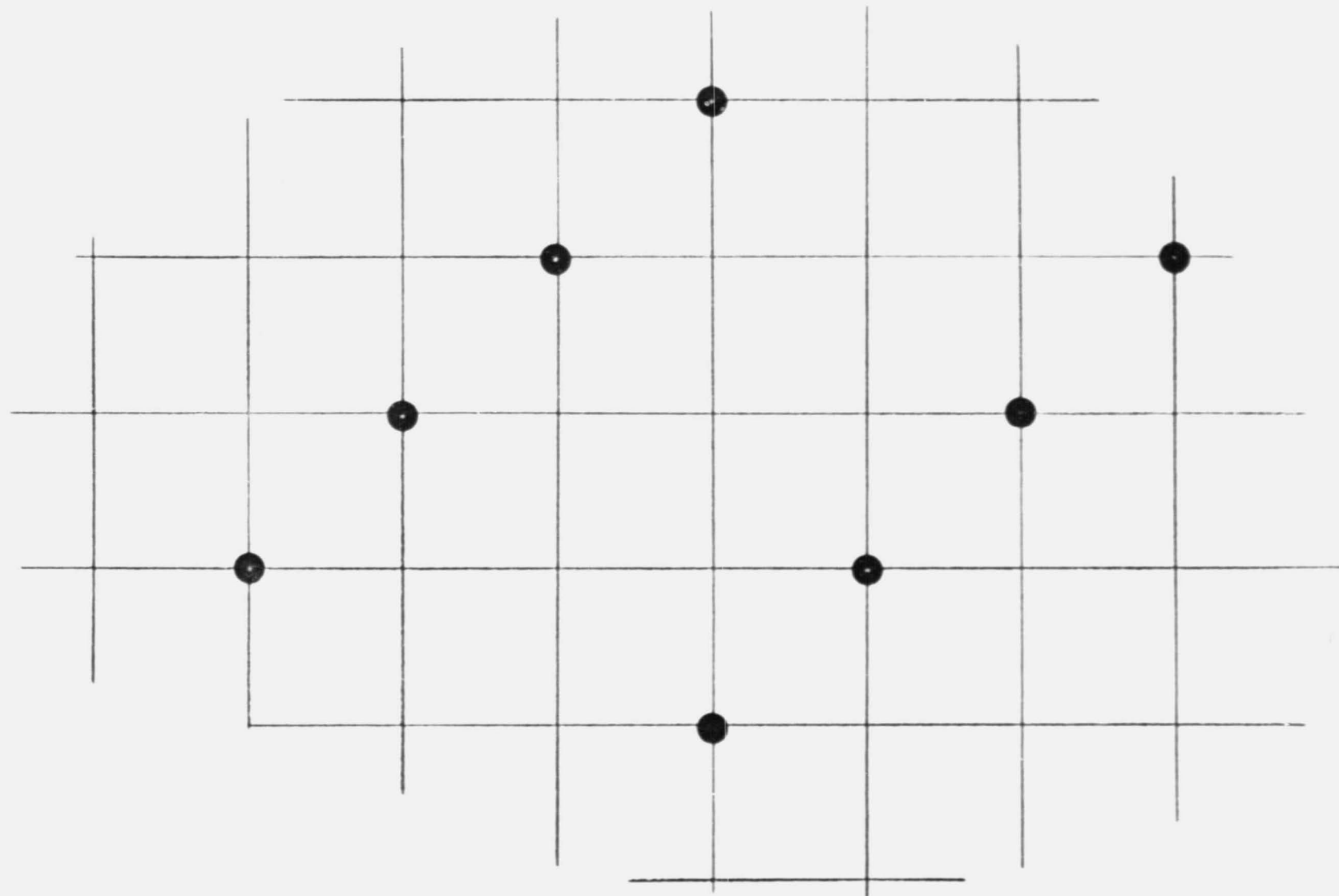


FIGURE 28

IV. MATERIALS AND SPECIFICATIONS FOR LIGHTNING PROTECTION

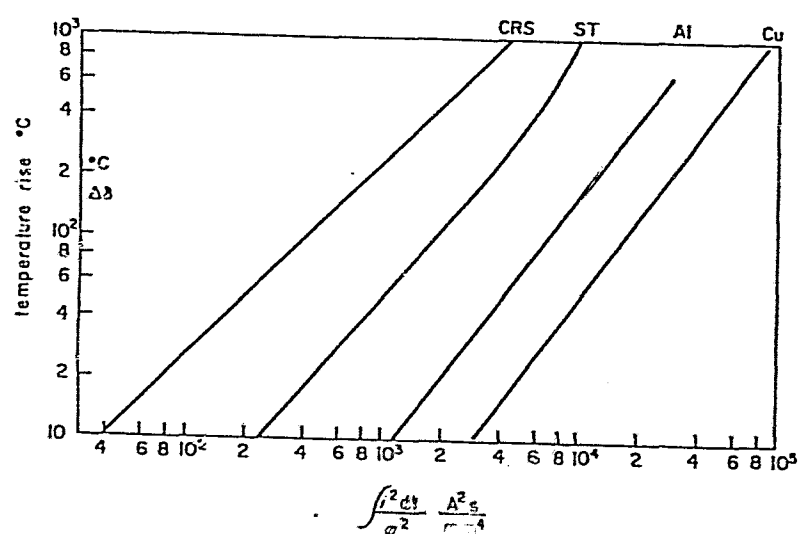
It is premature to specify the final form for the materials for the lightning protection system. We think that the system should be integrated into the structural design of the rectenna itself; in this case many other considerations are necessary in addition to the capability to conduct lightning currents. The data displayed in Figure 2.9 (H. Baatz, Protection of Structures, in Lightning Vol. 2, ed. by R.H. Golde) is useful for order-of-magnitude estimates of the lightning current requirements.

Example: If the design permits a 100° C temperature rise in an aluminum member carrying 10^5 Amps for 10^5 seconds, we need approximately 3 mm^2 cross-sectional area of aluminum material in the conductor. Note that the recommended crosssections for building codes are larger ($\sim 80 \text{ mm}^2$) indicating designs for lower temperature operation plus safety margins.

The lightning conductor need not be solid. From a structural point of view a tubular or other extruded shape would be preferable. Such configurations are compatible also with the lightning protection recommendations.

Specific values of materials for wire

Material	Steel	Copper	Aluminium
Density (g/cm^{-3})	7.7	8.92	2.7
Electrical resistance ($\Omega \text{ mm}^{-2} \text{ m}^{-1}$)	0.17	0.0178	0.029
Heat ($\text{cal } ^\circ\text{C}^{-1} \text{ g}^{-1}$)	0.115	0.093	0.023
Melting point ($^\circ\text{C}$)	1,350	1,083	658



Temperature rise of conductors as function of current square impulse per cross-section square; Cu = copper, Al = aluminium, ST = steel, CRS = corrosion-resistant steel.

Cross-section for lightning conductors

Installation components	Material	Cross-section (mm^2)	Dimension	
			Rod (mm, radius)	Strip ($\text{mm} \times \text{mm}$)
Air termination rods up to 0.5 m long	Steel, galvanized	50 (25) ^a	8	20 × 2.5
	Steel, stainless	110	12	30 × 3.5
Down conductors	Copper	50 (16) ^a	8	20 × 2.5
Conductors in ground	Aluminium ^b	80 (25) ^a	10	20 × 4
Sheet metal	{ Steel, galvanized Copper Aluminium, Zinc Lead			0.5 mm 0.3 mm 0.7 mm 2.0 mm

^a Lowest cross-sections used in some countries.

^b Not for use below ground.

FIGURE 29

V. ESTIMATE OF POWER LOSS FROM THE BEAM

A rough maximum estimate of the power loss from the microwave beam due to the lightning protection devices can be obtained by assuming that the microwave shadow cast by the static lightning protection system is twice the crossectional area of the devices. We assume that the conductors are 2 cm wide of 1 mm thickness tubular material, providing 60 mm² of crossectional area for conducting. The assumed shadow of these structures is approximately 0.6% of the rectenna area (see Figure 30.). This is a maximum estimate of the loss.

ORIGINAL PAGE IS
OF POOR QUALITY

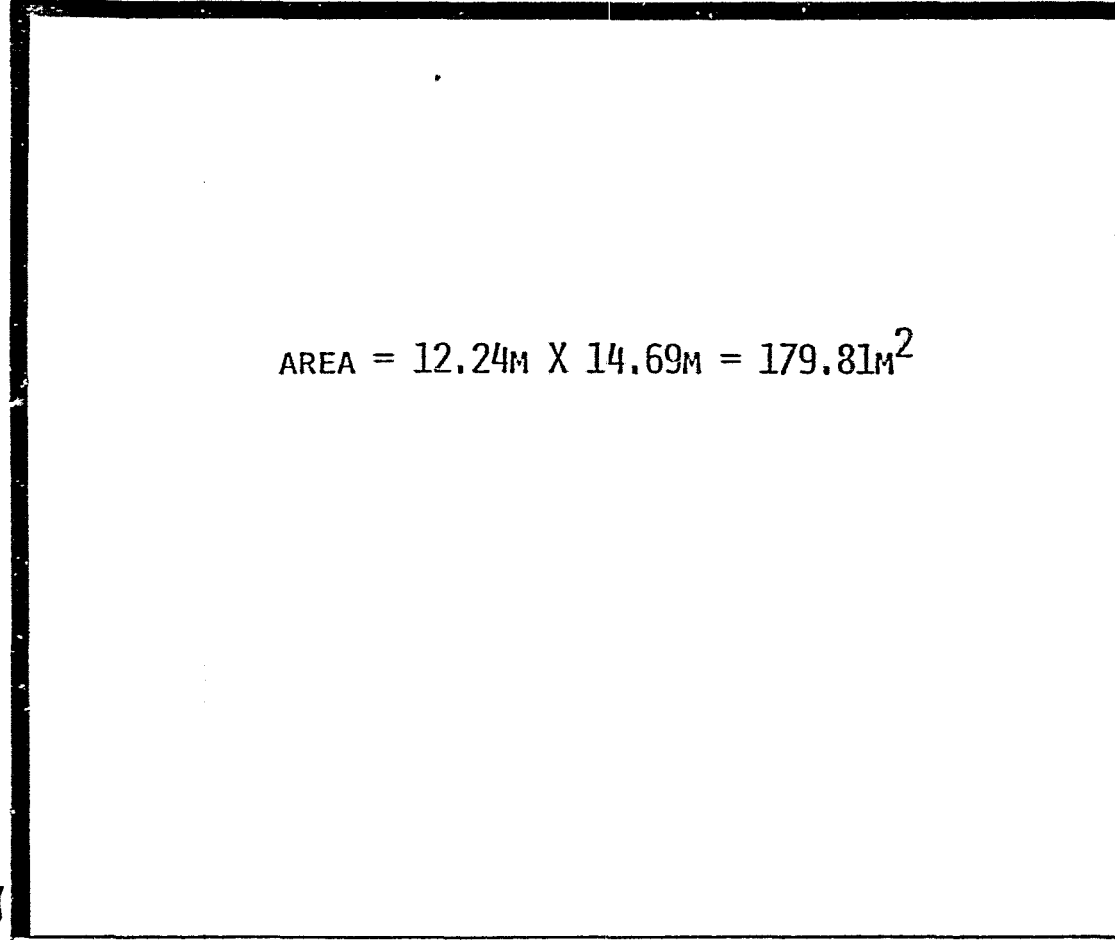


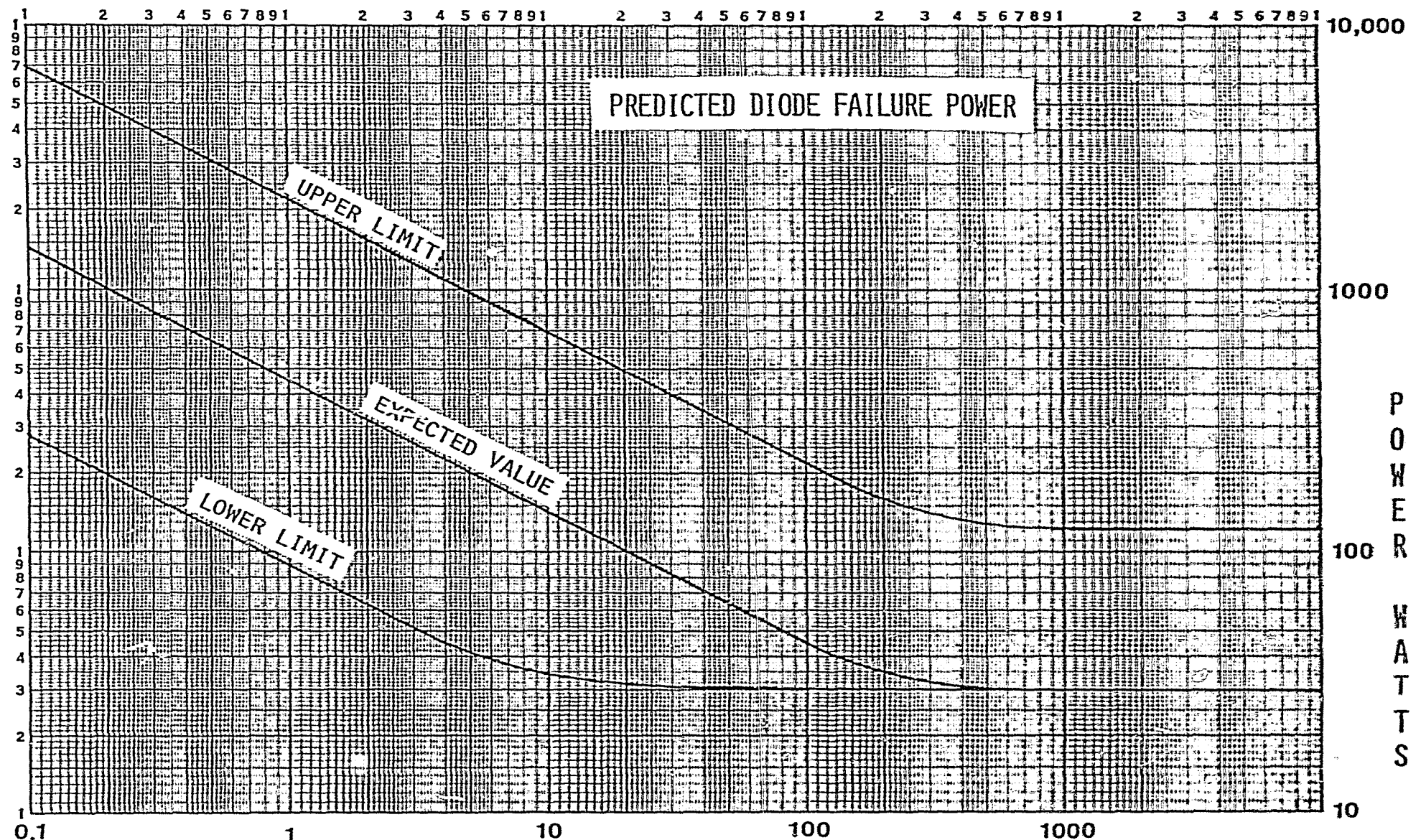
FIGURE 30

VI. MICROWAVE DIODE FAILURES DUE TO INDUCED CURRENT TRANSIENTS

The 25 W S GaAs diodes used in the design of the SPS rectenna have not been produced and no failure data is available for these devices. In order to obtain estimates of failure power of the diodes in the design, we used the specification data for the HP5082-2824 microwave diode and scaled the characteristics to 25 W using the "Wunsch relationship" described in the references below. We also obtained advice directly from Dr. D.C. Wunsch regarding the extrapolated power failure current.

1. Defense Department Report D224-13042-1 EMP, Susceptibility of Semiconductor Components, dated September, 1974.
2. Defense Department Report D224-10022-1 EMP, Electronic Analysis Handbook, dated May, 1973.
3. Defense Department Report D224-10019-1 EMP, Electronic Design Handbook, dated April, 1973.

Figure 31 shows the predicted failure power for 25 watt diodes, as a function of pulse width.



PULSE WIDTH - MICROSECONDS

FIGURE 31

VII. COMPUTER SIMULATION OF ELECTROSTATIC FIELD AROUND AN SPS RECTENNA

The electrostatic fields produced by the charges on the lightning channel induce charges on the rectenna and on the lightning protection conductors. Changes in this electrostatic field require a redistribution of charge on the rectenna system; the resulting currents can cause diode failure even with a lightning grounding system in place. One output of the computer simulation of the electrostatic field around the SPS rectenna is an evaluation of the induced current on the rectenna with and without the recommended lightning protection equipment.

An additional output from the computer simulation is the potential around the rectenna billboard enabling us to estimate the enhancement factors of the electric field due to the billboard shape.

The algorithm used in the simulation computes an array of values for the potential around the middle of five infinitely long billboards. We assume here that the contribution to the local potential from billboards further away is ignorably small. The surface charge distribution on the billboards is simulated with ten infinitely long line charges evenly spaced along the billboard. The value for the line charges is determined interactively with the computer to produce a zero potential contour that has the same shape as the billboard. Figure 32 illustrates this simulation.

In order to compute the potential, we will need $U(x,y)$, the electrostatic potential at a point (x,y) in free space, where the coordinate system is such that the line of electrical charges giving rise to the potential is located at the origin. If we call the y -coordinate the height h , then $U(x,H)$ is the electrostatic potential at x and h of a line charge λ (coulomb/meter) at a height d directly above the point $x = 0$. There is also a contribution to U from the image charge. Thus,

$$U(x,h) = -\frac{\lambda}{2\pi\epsilon_0} \ln \left[\frac{x^2 + (h-d)^2}{x^2 + (h+d)^2} \right]^{1/2}.$$

From this, the potential distribution around the rectenna may be calculated. Let $U(1,h)$ be the potential at $x = 1$ and $y = h$ due to a periodic system of line charges simulating the rectenna (see Figure 31.) We then have that

$$U(1,h) = \sum_{i=1}^N \sum_{j=1}^M \left(-\frac{\lambda j}{2\pi\epsilon_0} \right) \ln \left[\frac{(1-L[i-1]-x_j)^2 + (h-sx_d)^2}{(1-L[i-1]-x_j)^2 + (h+sx_j)^2} \right]^{1/2},$$

where the free-space value for the dielectric constant is assumed and where

- i = Billboard number,
- j = Line charge number on billboard i,
- s = Slope of billboard ($= \tan \alpha$),
- M = Number of line charges ($= 10$),
- N = Number of billboards ($= 5$).

SIMULATION OF SPS RECTENNA WITH LINE CHARGES

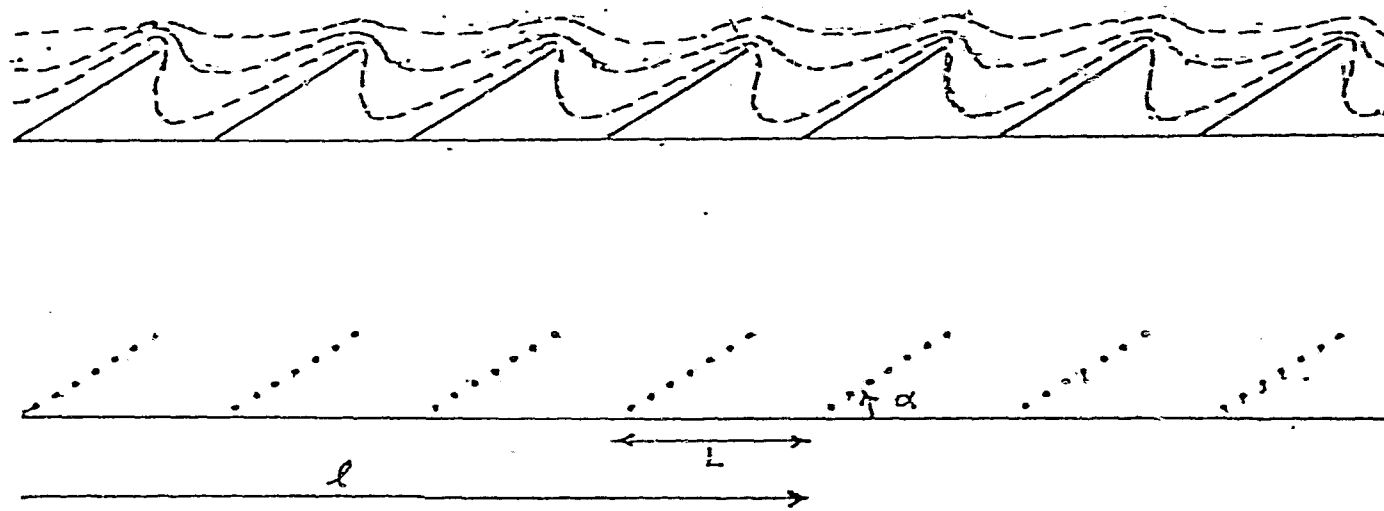


FIGURE 32

In the presence of a uniform electric field of 100,000 volts/meter (directed upward), ten line charges have been selected to produce the array of values shown in Figure 33. Three potential contours have been sketched (zero, 10,000 V, and 100,000 V) around the ten line charges on the billboard. The zero contour follows closely the position of the billboard surface, as required by the simulation algorithm. Note how closely spaced the contours are at the top edge of the billboard. Electric field enhancement factors of at least 6.5 exist in this region based upon our simulations. Higher resolution simulations would be required to refine the enhancement factor estimates.

The values obtained for the 10 individual line charges found for the solution shown in Figure 33 are (in $\mu\text{Coul./m}$):

0.36, 0.465, 0.572, 0.679, 0.924, 1.02, 1.14, 1.78, 2.91, 4.14.

We can convert these to a surface charge density by dividing each value by the billboard distance represented by the line charge. The first line charge serves approximately $3/2 (\frac{12.24 \text{ m}}{10})$; the last line charge serves $1/2 (\frac{12.24 \text{ m}}{10})$; and all others are associated with a length $(\frac{12.24 \text{ m}}{10})$.

Figure 34 is a plot of charge/unit area ($\mu\text{Coul./m}^2$) on the billboard as a function of length (northward) along the billboard surface.

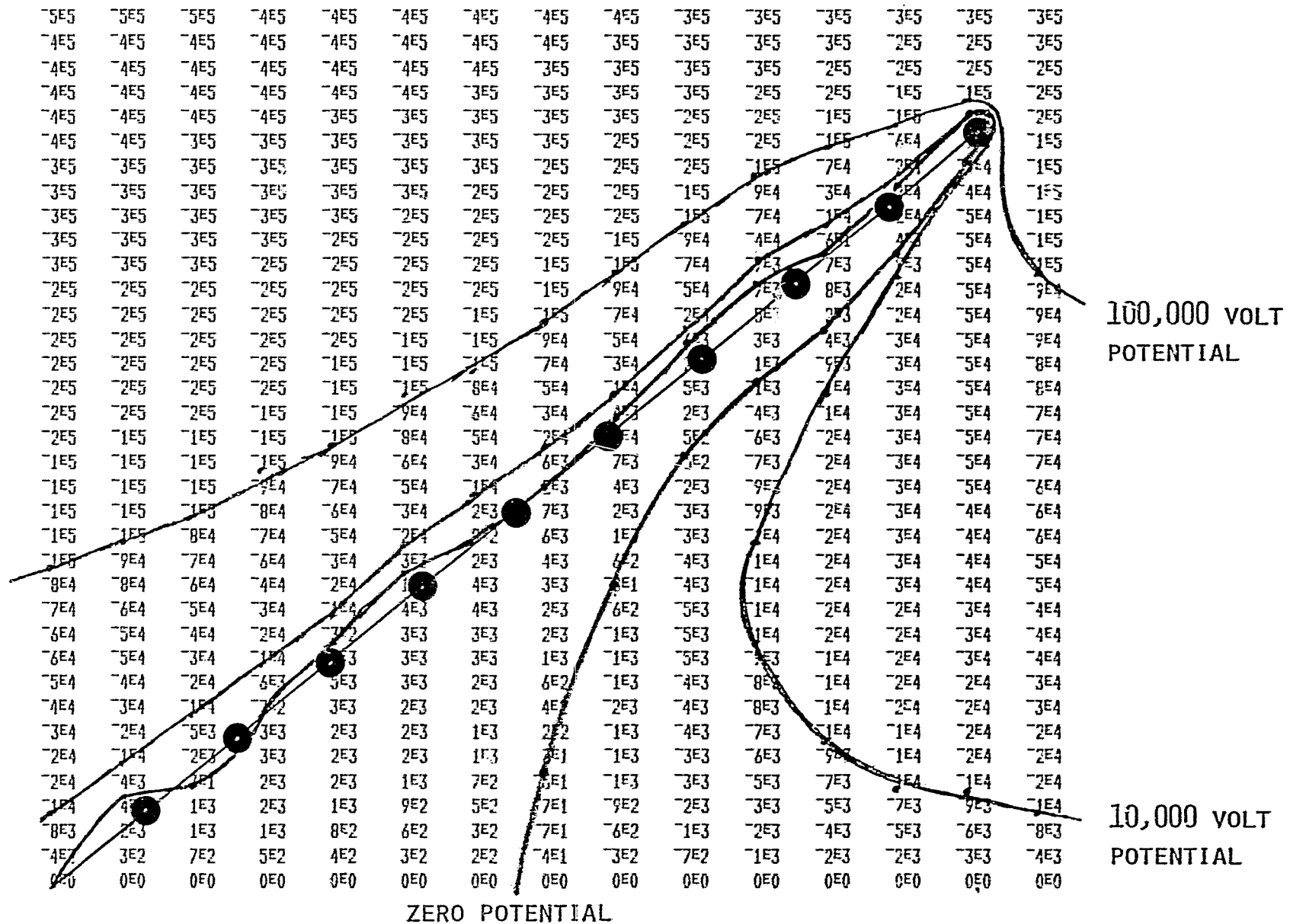
When an additional line charge is placed at the position of the lightning static, and all of line charge values are adjusted to the new configuration, we find the simulated potential function around a protected billboard - Figure 35. The placement of the static in this example is based upon the discussion in Section I.2.3., with $L = 0.98\text{m}$, corresponding to $\alpha = 40^\circ$. The charge/unit length for the static is $4.6 \mu\text{Coul./m}$. The charge/unit lengths for the ten billboard line charges in ($\mu\text{Coul./m}$) are:

0.315, 0.47, 0.51, 0.57, 0.87, 0.89, 0.90, 1.35, 1.78, 2.1.

These line charges may be compared with the unprotected billboard charges corresponding to the solutions of Figure 35. The protected billboard charges approach approximately one-half of the corresponding unprotected charges.

The line charges used to simulate the rectenna are normalized to a charge/unit area through division by the associated lengths, as previously described, to obtain the induced charge distribution on the protected rectenna billboard.

Figure 36 is a plot of charge/unit area in $\mu\text{Coul./m}^2$ as a function of the distance (northward) along the billboard face.



● LOCATION OF LINE CHARGES SIMULATING BILLBOARD

FIGURE 33

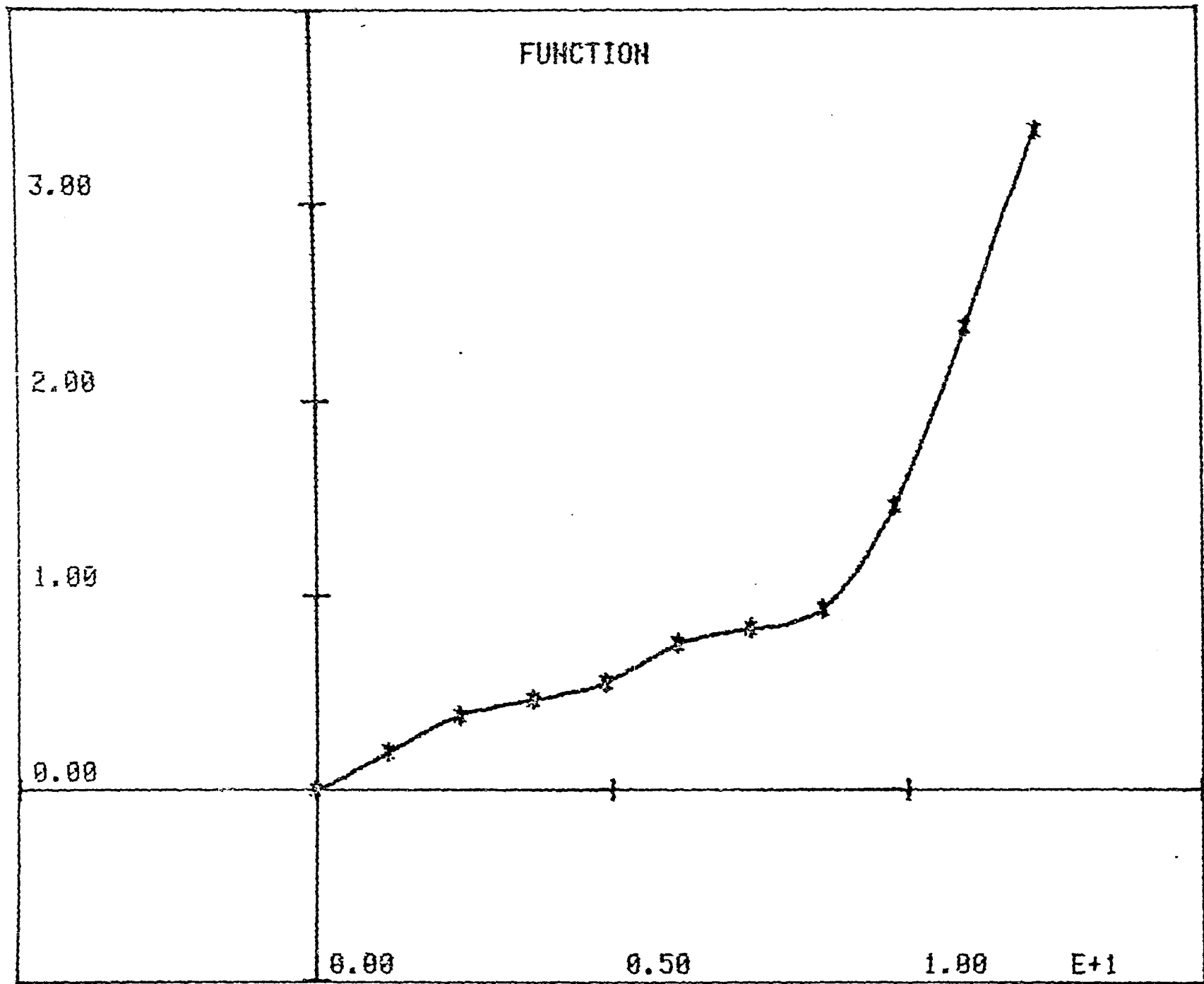
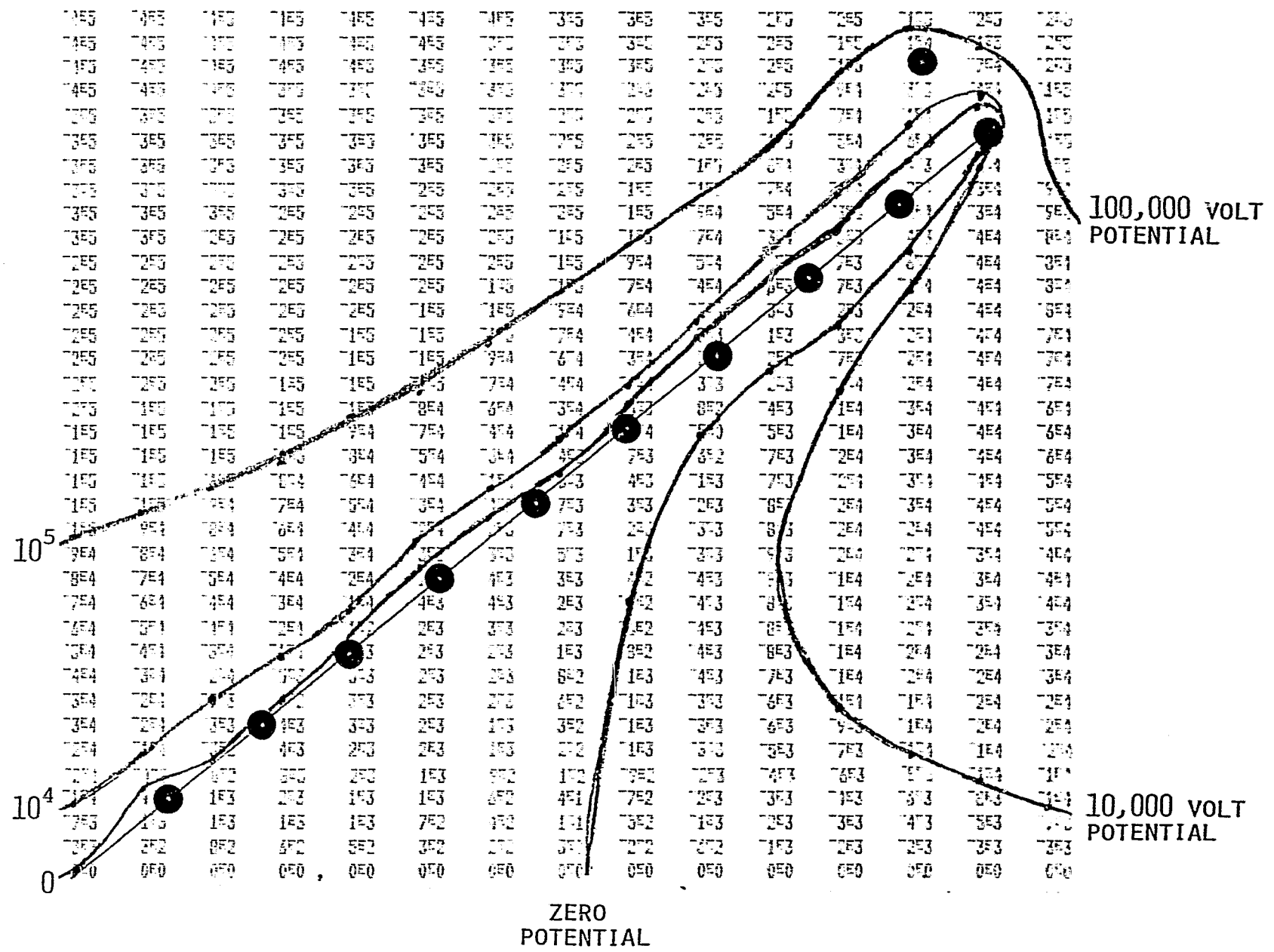


FIGURE 34



● LOCATION OF LINE CHARGES SIMULATING BILLBOARD

FIGURE 35

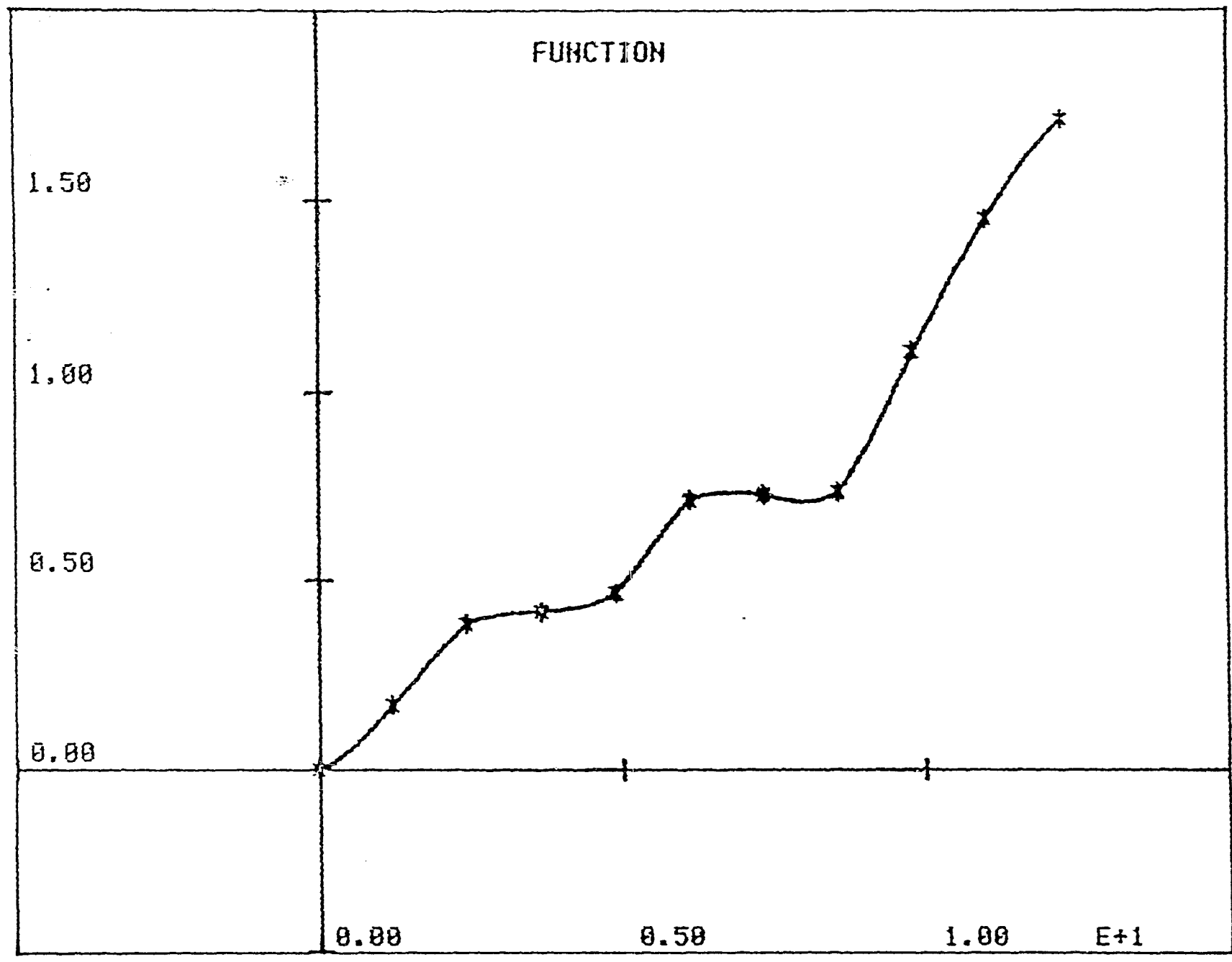


FIGURE 36

36

17

47

VIII. COMPUTATION OF LIGHTNING ELECTRIC FIELDS

In section VII, a rectenna was simulated in the presence of a uniform electric field of 100,000 Volts. The induced surface charges derived from the simulation are directly proportioned to the imposed electric field strength.

In this section we describe a computer program that was written to derive values for the lightning-produced electric fields as a function of time and of distance from "ground zero" - the point of strike. We have run the program for a range of lightning parameters obtained from actual measurements reported in the literature.

The program computes the contribution to the electric field from the thundercloud charge center participating in the cloud-to-ground flash, the charge on the lightning channel, and the images of these charges. All charges are allowed to vary with time in a manner consistent with observations [Terrestrial Environment (Climatic) Criteria Guidelines for Use in Aerospace Vehicle Development, 1977 Revision; Edited by John W. Kaufman, NASA Technical Memorandum 78118].

Figure 37 displays the relevant equations and configurations covering the leader phases of the computation.

In Figure 38 the equations and conditions during the return stroke portion are shown. The program used in computing the fields is provided in the appendix.

The material following Figure 38 provides the tabular and graphic data used in these computations for the return stroke phase. These data are contained in Figures (39-44) inclusive.

The output of the computer program is a "blow-by-blow" history of the electrical field at a specified distance from ground zero as a function of time. Figure 45 displays one section of the output from one of the computer runs. This corresponds to a worst-case situation, 10 meters away from the very-severe-model. The units of time are seconds(along the abscissa), and the units of the ordinate are kilovolts per meter.

Table 8.4 in figure 46 provides a summary of the output for the various computer runs. Listed are the peak negative fields, the peak positive fields (when positive fields occur), and the ΔE and ΔT for the portion of the flash with the peak rate of change of electric field.

These values are our input data to the computation of diode failure when used in conjunction with the induced surface charge results of the rectenna electrostatic simulations.

STEPPED OR DART LEADER PROCESSES:

INITIAL SPECIFICATIONS

$$\left\{ \begin{array}{l} Y_0 (\sim 5 \text{ KM}) \\ Q_0 (\sim -10 \text{ Coul}) \\ V_L (\sim 10^5 \text{ m/s}) \\ T = 0, Y = Y_0 \\ Q_L (\sim -5 \text{ Coul}) \\ P = P_L = Q_L/Y_0 \end{array} \right.$$

TEMPORAL FUNCTIONS:

$$X = Y_0 - V_L T$$

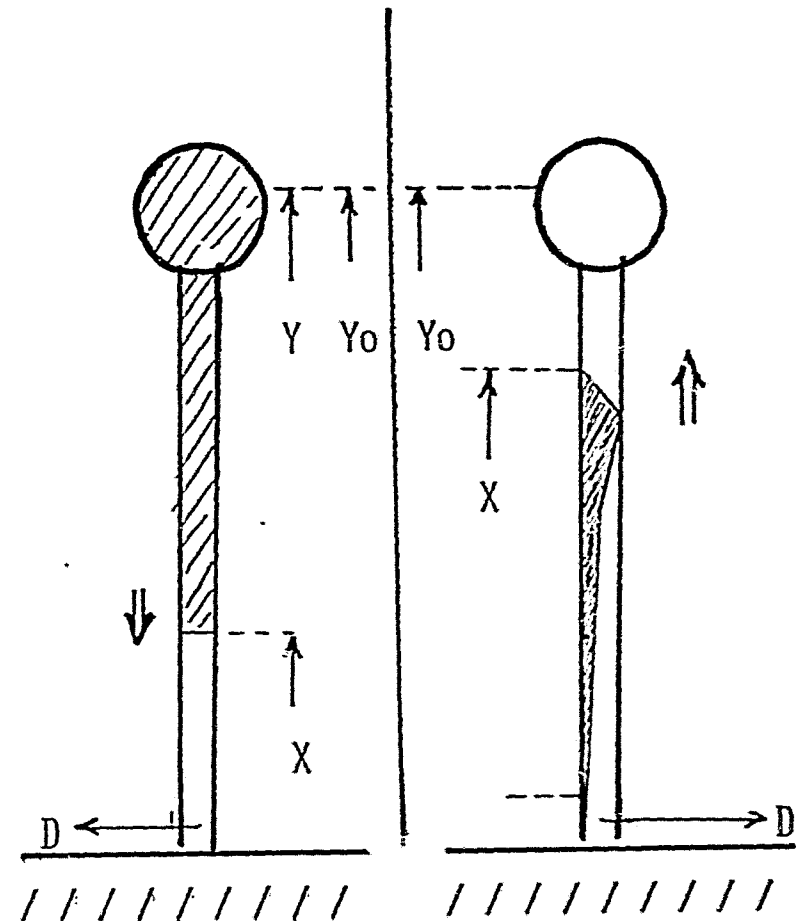
$$Q = Q_0 - P_L (Y - X)$$

SOLVE FOR $E_L(T, D)$ FOR $T \leq T_L$ WHERE

$$T_L = (Y_0 - X_L)/V_L$$

$$X_L (\sim 50 \text{ METERS})$$

FOR $T > T_L$, $E_L(T, D) = E_L(T_L, D)$



$$E = \frac{2P}{4\pi\epsilon_0} \left\{ \frac{1}{(D^2 + X^2)^{1/2}} - \frac{1}{(D^2 + Y^2)^{1/2}} \right\} +$$

$$\frac{2QY_0}{4\pi\epsilon_0 (D^2 + Y_0^2)^{3/2}}$$

FIGURE 37

RETURN STROKE PROCESS:

INITIAL SPECIFICATIONS

TEMPORAL FUNCTIONS:

$$Y = V_B T'$$

$$P = \{ I_{dT/Y} \} \quad \text{FOR } Y < Y_0$$

$$P = \left\{ I_d T / Y_0 \right\} \text{ FOR } Y > Y_0 \quad \text{AND} \quad P \leq -P_L$$

$$\theta = 0$$

$$\left. \begin{array}{l} P = -P_L \\ Q = \int I dT + Q_L \end{array} \right\} \text{FOR } Y > Y_0 \text{ AND } P > -P_L$$

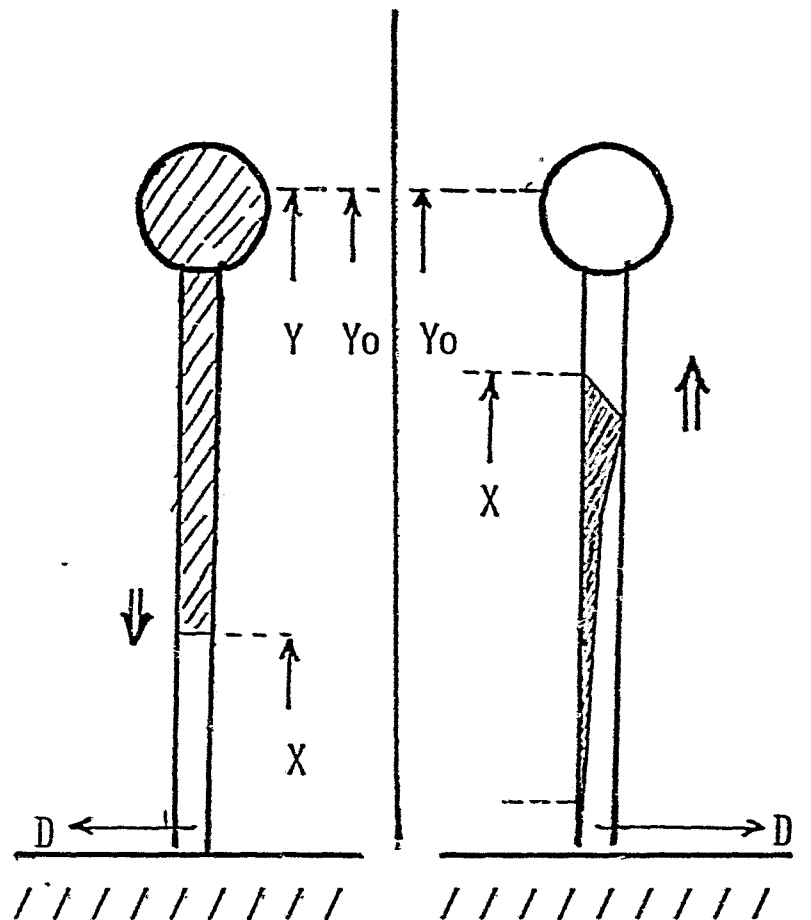
AND $Q \leq -(Q_{L_0} - Q_1)$

SOLVE FOR $E_R(\tau', \omega)$ FOR $\tau > \tau_1$ OR $\tau' > 0$

$$\text{TOTAL FIELD } E_T(\tau, d) = E_L(\tau_L, d) + E_R(\tau, d)$$

TERMINATE COMPUTATION WHEN $Q \geq -(Q_0 - Q_{10})$

卷之三



$$E = \frac{2P}{4\pi\epsilon_0} \left\{ \frac{1}{(\Omega^2 + \chi^2)^{1/2}} - \frac{1}{(\Omega^2 + \gamma^2)^{1/2}} \right\} +$$

$$\frac{2QY_0}{4\pi\epsilon_0 (\Omega^2 + \gamma_0^2)^{3/2}}$$

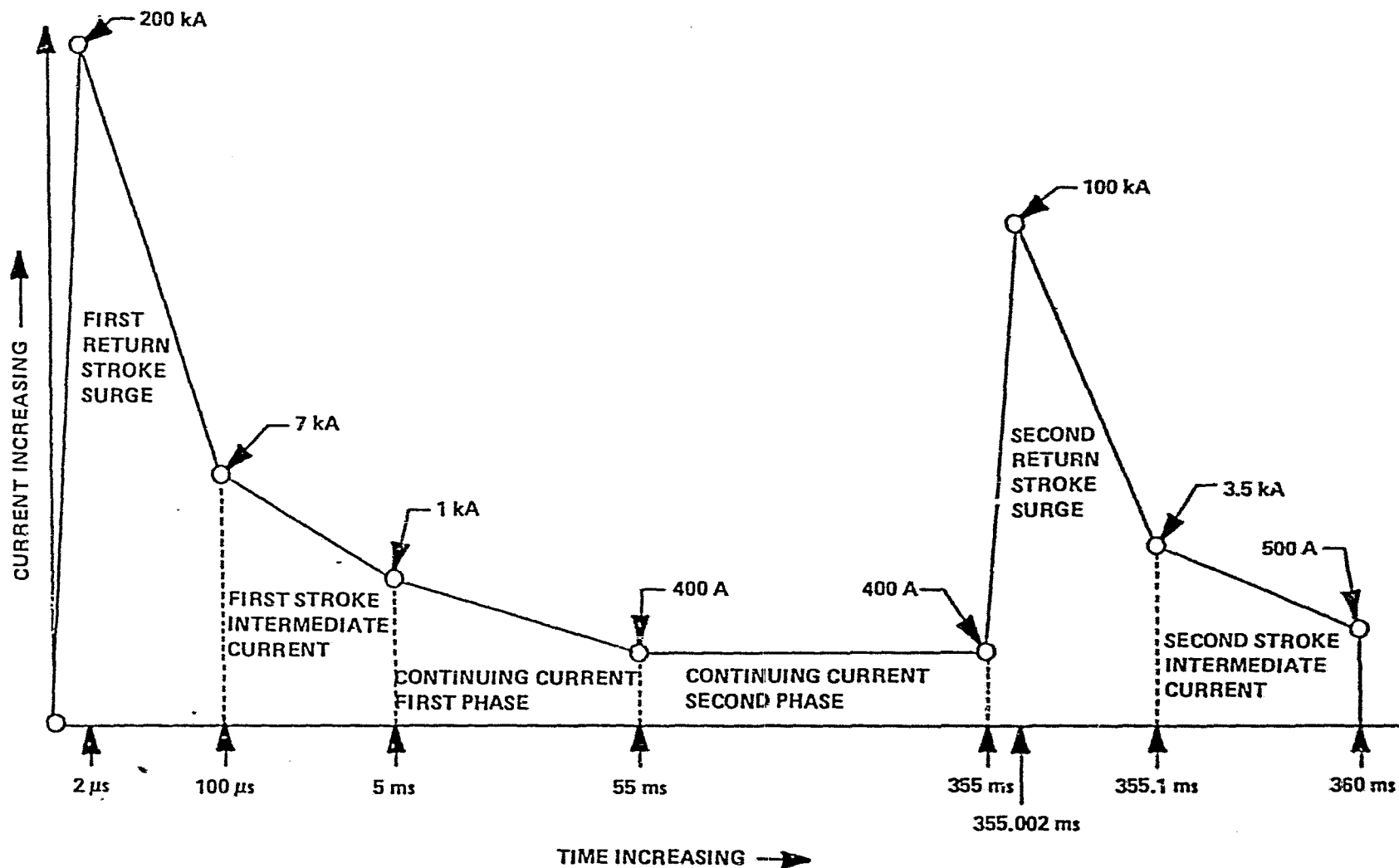
- FIGURE 38

DETAILS OF A VERY SEVERE LIGHTNING MODEL (MODEL 1)

Stage	Key Points		Rate of Current Change	Charge Passing
1. First Return Stroke Surge	$t = 0$	$i = 0$	Linear Rise - 100 kA/ μ s Linear Fall - 193 kA in 98 μ s	0.2 C*
	$t = 2 \mu$ s	$i = 200$ kA		
	$t = 100 \mu$ s	$i = 7$ kA		
2. First Stroke Intermediate Current	$t = 100 \mu$ s	$i = 7$ kA	Linear Fall - 6 kA in 4.9 ms	19.6 C
	$t = 5$ ms	$i = 1$ kA		
3. Continuing Current--First Phase	$t = 5$ ms	$i = 1$ kA	Linear Fall - 600 A in 50 ms	35.0 C
	$t = 55$ ms	$i = 400$ A		
4. Continuing Current--Second Phase	$t = 55$ ms	$i = 400$ A	Steady Current	120.0 C
	$t = 355$ ms	$i = 400$ A		
5. Second Return Stroke Surge	$t = 355$ ms	$i = 400$ A	Linear Rise ~ 50 kA/ μ s Linear Fall - 96.5 kA in 98 μ s	~ 0.1 C ~ 5.1 C
	$t = 355.002$ ms	$i = 100$ kA		
	$t = 355.1$ ms	$i = 3.5$ kA		
6. Second Stroke Intermediate Current	$t = 355.1$ ms	$i = 3.5$ kA	Linear Fall - 3 kA in 4.9 ms	9.8 C
	$t = 360$ ms	$i = 500$ A		

* Coulomb (C) is the quantity of electricity transported in one second by a current of one ampere.

FIGURE 39

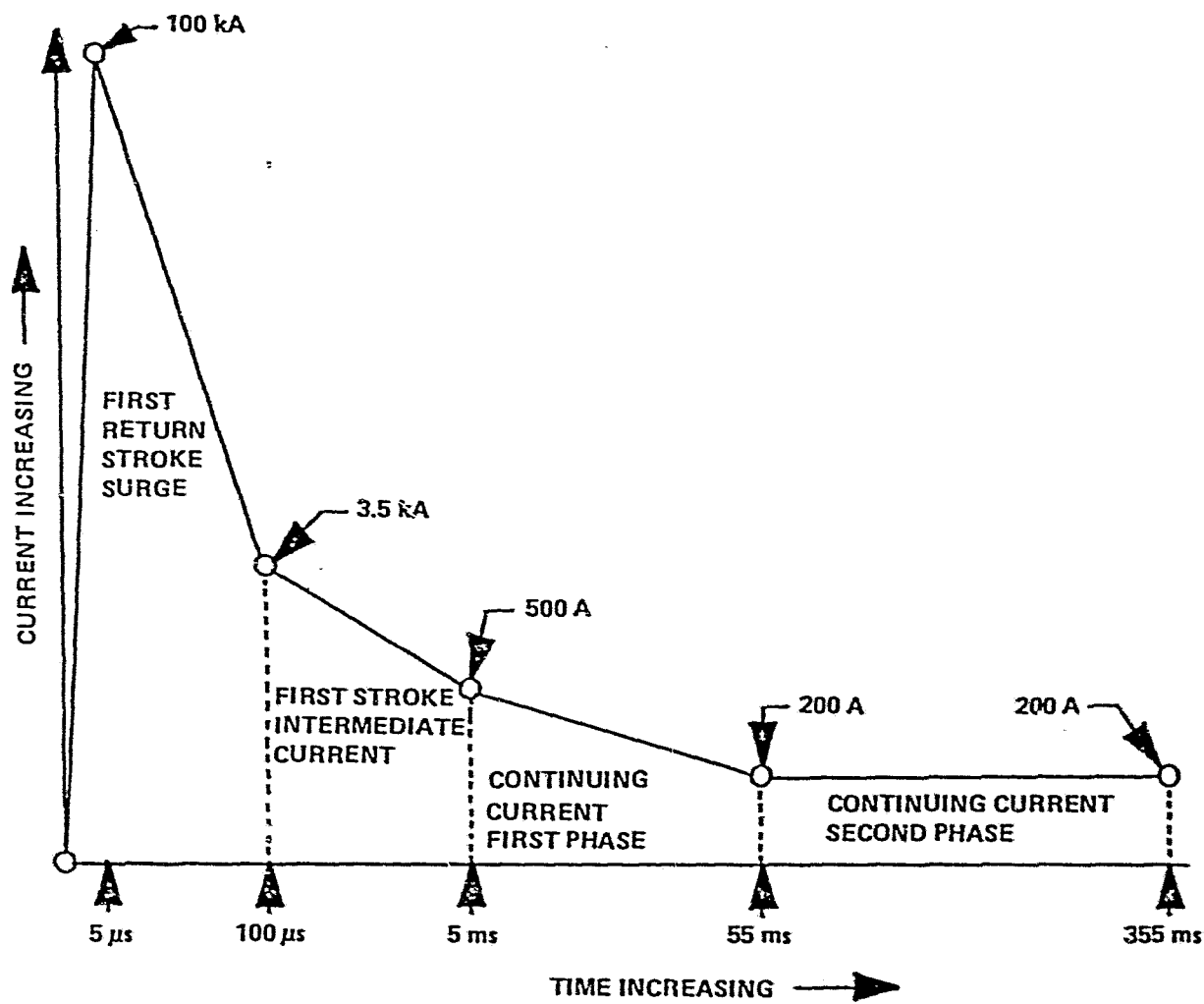


DIAGRAMMATIC REPRESENTATION OF A VERY SEVERE LIGHTNING MODEL
(MODEL 1) (Note that the diagram is not to scale)

DETAILS OF A 98 PERCENTILE PEAK CURRENT LIGHTNING MODEL (MODEL 2)

Stage	Key Points		Rate of Current Change	Charge Passing
1. First Return Stroke Surge	$t = 0$	$i = 0$	Linear Rise - $20 \text{ kA}/\mu\text{s}$ Linear Fall - 96.5 kA in $95 \mu\text{s}$	0.3 C $\sim 4.9 \text{ C}$
	$t = 5 \mu\text{s}$	$i = 100 \text{ kA}$		
	$t = 100 \mu\text{s}$	$i = 3.5 \text{ kA}$		
2. First Stroke Intermediate Current	$t = 100 \mu\text{s}$	$i = 3.5 \text{ kA}$	Linear Fall - 3 kA in 4.9 ms	9.8 C
	$t = 5 \text{ ms}$	$i = 500 \text{ A}$		
3. Continuing Current--First Phase	$t = 5 \text{ ms}$	$i = 500 \text{ A}$	Linear Fall - 300 A in 50 ms	17.5 C
	$t = 55 \text{ ms}$	$i = 200 \text{ A}$		
4. Continuing Current--Second Phase	$t = 55 \text{ ms}$	$i = 200 \text{ A}$	Steady Current	60 C
	$t = 355 \text{ ms}$	$i = 200 \text{ A}$		

FIGURE 41



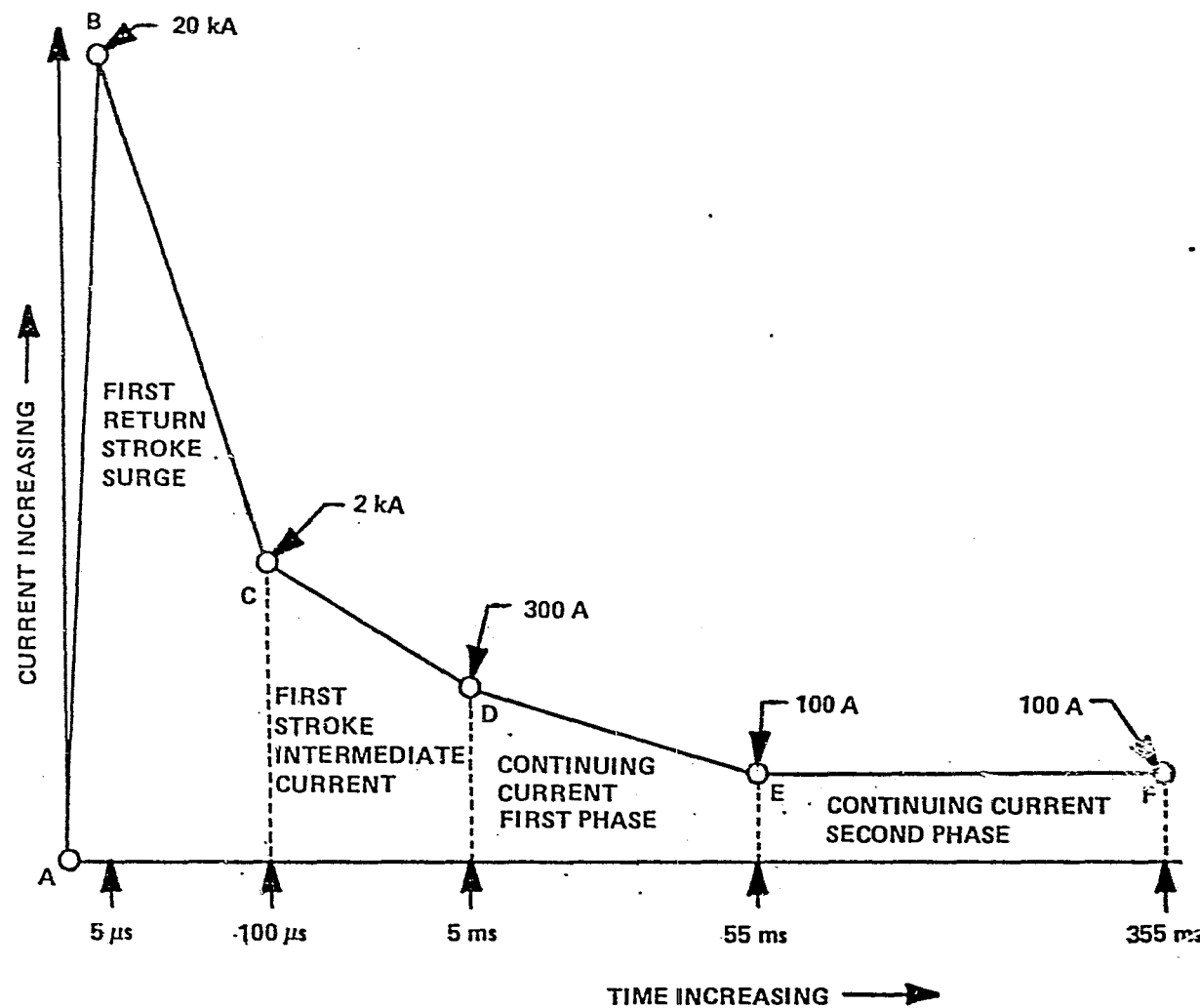
DIAGRAMMATIC REPRESENTATION OF A 98 PERCENTILE PEAK CURRENT LIGHTNING MODEL (MODEL 2) (Note that the diagram is not to scale.)

DETAILS OF AN AVERAGE LIGHTNING MODEL (MODEL 3)

Stage	Key Points		Rate of Current Change	Charge Passing
1. First Return Stroke Surge	$t = 0$	$i = 0$	Linear Rise - $4 \text{ kA}/\mu\text{s}$ Linear Fall - 18 kA in $95 \mu\text{s}$	0.1 C
	$t = 5 \mu\text{s}$	$i = 20 \text{ kA}$		$\sim 1.0 \text{ C}$
	$t = 100 \mu\text{s}$	$i = 2 \text{ kA}$		
2. First Stroke Intermediate Current	$t = 100 \mu\text{s}$	$i = 2 \text{ kA}$	Linear Fall - 1.7 kA in 4.9 ms	5.6 C
	$t = 5 \text{ ms}$	$i = 300 \text{ A}$		
3. Continuing Current -- First Phase	$t = 5 \text{ ms}$	$i = 300 \text{ A}$	Linear Fall - 200 A in 50 ms	10.6 C
	$t = 55 \text{ ms}$	$i = 100 \text{ A}$		
4. Continuing Current -- Second Phase	$t = 55 \text{ ms}$	$i = 100 \text{ A}$	Steady Current	30.0 C
	$t = 355 \text{ ms}$	$i = 100 \text{ A}$		

FIGURE 43

C-2



DIAGRAMMATIC REPRESENTATION OF AN AVERAGE LIGHTNING MODEL
(MODEL 3) (Note that the diagram is not to scale.)

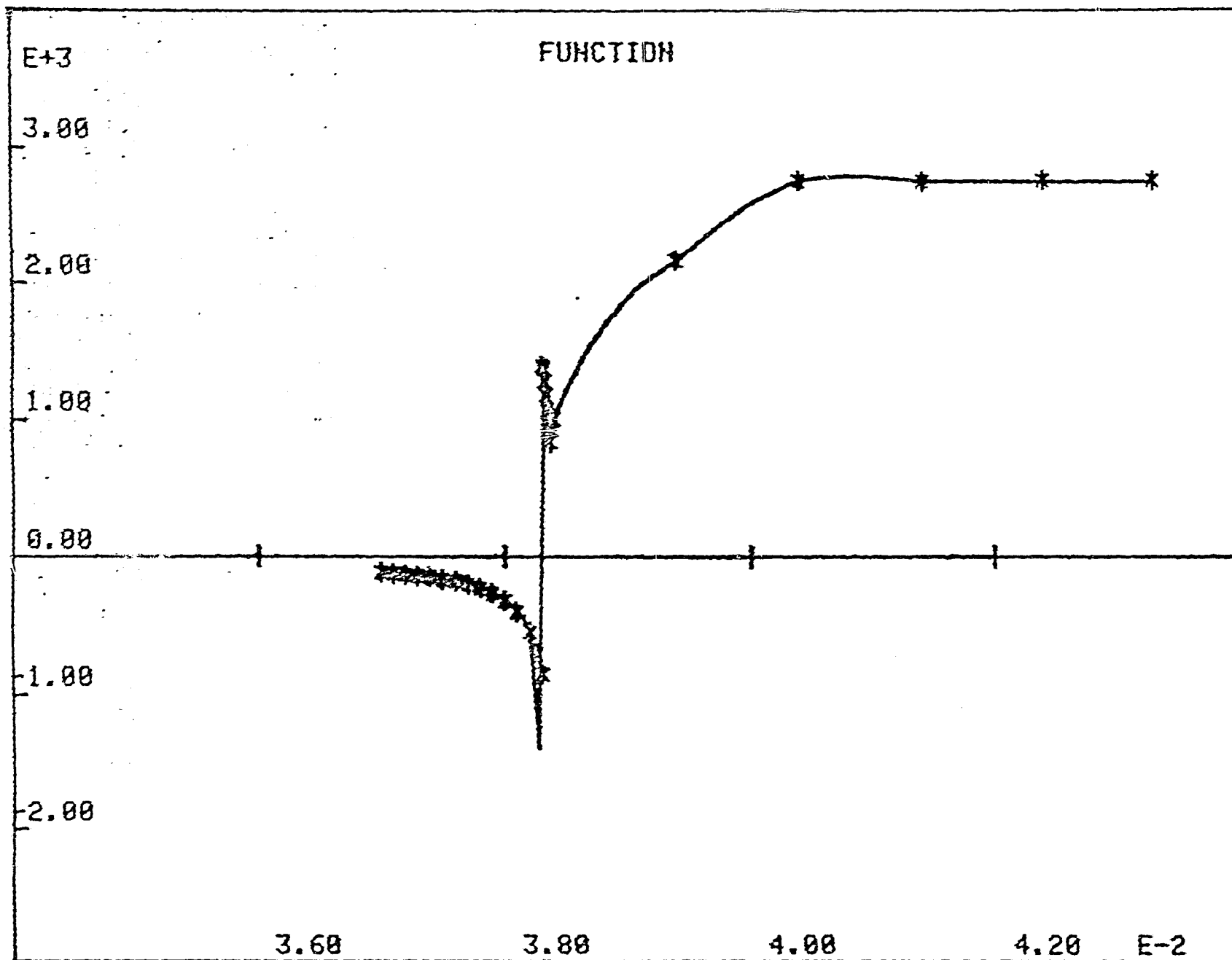


FIGURE 45

TABLE 8.4

	VERY SEVERE MODEL			98 PERCENTILE MODEL			AVERAGE MODEL		
Distance	Peak Negative	Peak Positive	$\Delta E/\Delta T$ Peak	Peak Negative	Peak Positive	$\Delta E/\Delta T$ Peak	Peak Negative	Peak Positive	$\Delta E/\Delta T$ Peak
10 m	-8.5X10 ⁵	2.8X10 ⁶	2.2X10 ⁶	-5.95X10 ⁵	1.81X10 ⁶	6.46X10 ⁵	-5.09X10 ⁵	1.30X10 ⁶	5.68X10 ⁵
			1.2X10 ⁻⁵			3.00X10 ⁻⁶			2.59X10 ⁻⁵
50 m	-5.7X10 ⁵	1.7X10 ⁵	4.37X10 ⁵	-3.88X10 ⁵	1.04X10 ⁵	3.59X10 ⁵	-3.10X10 ⁵	6.1X10 ⁴	1.14X10 ⁵
			2.2X10 ⁻⁵			2.5X10 ⁻⁵			2.50X10 ⁻⁵
100 m	-3.49X10 ⁵	2.49X10 ⁴	2.15X10 ⁵	-2.36X10 ⁵	N/A	1.75X10 ⁵	-1.85X10 ⁵	N/A	5.47X10 ⁴
			2.2X10 ⁻⁵			2.5 X10 ⁻⁵			3.5 X 10 ⁻⁵
500 m	-8.94X10 ⁴	N/A	3.79X10 ⁴	-6.15X10 ⁴	N/A	2.96X10 ⁴	-5.12X10 ⁴	N/A	N/A
			3.2 X10 ⁻⁵			4.5 X 10 ⁻⁵			
1000 M	-5.35X10 ⁴	N/A	1.69X10 ⁴	-2.61X10 ⁴	N/A	N/A	-3.29X10 ⁴	N/A	N/A
			4.2X10 ⁻⁵						

FIGURE 46

IX. COMPUTATIONS OF DIODE FAILURE

We are now to the point of having generated all of the data that are required to evaluate the conditions under which the microwave rectifier diodes will fail due to induced currents from nearby lightning flashes. For a given ΔE and ΔT (from Table 8.4) we obtain from Figure 31 the power required for diode failure and from Figure 32 the induced charge/unit area on the rectenna surface. We assume that a diode designed to operate at 67 V will have a breakdown voltage of about 100 Volts.

The surface area of the rectenna that has an induced surface charge of the size sufficient to cause diode failure is then computed from comparison with areas of the rectenna served by individual diodes and by series strings of diodes. Sample computations follow.

SAMPLE COMPUTATION OF DIODE FAILURE (98TH PERCENTILE - 10 METER - NO PROTECTION)

1. 98 percentile model - 10 meters: $\Delta T = 3 \times 10^{-6}$ and $\Delta E = 6.46 \times 10^5$.
2. Expected diode failure power from Figure 30: 250 Watts.
3. Energy dissipated in the diode: $250 \text{ Watts} \times 3 \times 10^{-6} \text{ s} = 7.5 \times 10^{-4} \text{ Joules}$.
4. Charge transferred across 100 Volts diode breakdown voltage = $7.5 \times 10^{-6} \text{ Coulombs}$.
5. From ΔE in step 1 and figure 37, the induced charge/unit area = $3 \times 10^{-6} \text{ C/m}^2 \times 6.46 = 19.38 \times 10^{-6} \text{ C/m}^2$.
6. From steps 4 and 5, the rectenna area with surface charge equivalent to the charge required to cause diode failure is: 0.39 m^2 .
7. Area served by diodes: rectenna center,

$$\frac{25 \text{ watts}}{230 \text{ w/m}^2} = 0.11 \text{ m}^2; \text{ rectenna edge}, \frac{25 \text{ watts}}{10 \text{ w/m}^2} = 2.5 \text{ m}^2.$$

8. Compare 6 with 7: single diode configuration near rectenna center is safe. Single diode configuration near rectenna edge is vulnerable.
9. However, the diodes are to be put in series (597 to a string) hence the diodes near the bottom must carry all of the induced current to the entire string. For these bottom-string diodes the area served with respect to the induced charge is: rectenna center, 60 m^2 ; rectenna edge, 1400 m^2 .
10. To protect against the 98 percentile flash within 10 meters of ground zero would require fast surge protection diodes (back to back zeners) on all diodes in the rectenna. This extent of protection may not be cost effective; however the considerations in Section X indicate that simpler protection arrangements will probably be effective near the rectenna center.

FAILURES PRODUCED BY THE AVERAGE LIGHTNING FLASH

The situation considered here is the extent of the protection required for an "average" lightning flash if we are willing to accept losses from the extreme cases.

The computation sequence follows the same procedure described immediately above. Here we use data for the average flash from Table 8.4 at a 10 m distance from ground zero.

SAMPLE COMPUTATION OF DIODE FAILURE
(AVERAGE FLASH, 10 M, WITH "STATIC" PROTECTION)

1. From Table 8.4: $\Delta E = 3.68 \times 10^5$ v/m; $\Delta T = 2.59 \times 10^{-5}$ s.
2. From Figure 6.1: 80 watts.
3. $80 \text{ w} \times 2.59 \times 10^{-5} \text{ s} \approx 2 \times 10^{-3}$ Joules.
4. 2×10^{-5} coulombs.
5. From 1 and Figure 38: $1.5 \times 10^{-6} \times 5.68 \approx 8.52 \times 10^{-6}$ coul/m².
6. From 4 and 5: Area = 2.35 m².
7. Since the rectenna area served by individual diodes even on the edge < 2.5 m, the individual diodes are self-protecting and able to take an "average" lightning flash.
8. However, when arranged in a series stack of 597, the diodes at the bottom of the stack must conduct the induced currents for the whole stack. The diodes cannot safely carry these currents.

X. LIGHTNING PROTECTION FOR SERIES DIODE STRINGS

As demonstrated in Section IX, the connection of microwave rectifier diodes in series requires special lightning protection considerations. We cannot make specific recommendations for these protection devices at this time because the rectenna current design is not advanced to the point that allows such detailed analysis. Rockwell International has provided us with an equivalent circuit for the rectenna; a slightly modified form of that circuit is shown in Figure 46. We have assumed that the series connections are to be made at the points indicated by the large spots and that the output filter operates around 30 Hz. A series string of rectenna elements of this design can be protected with a variety of methods. One cost-effective means is a spark gap arrangement incorporated in the diode feedthroughs, or the output filter inductors, or on the billboard configuration itself.

RECTENNA EQUIVALENT CIRCUIT AT 2.45 GHz

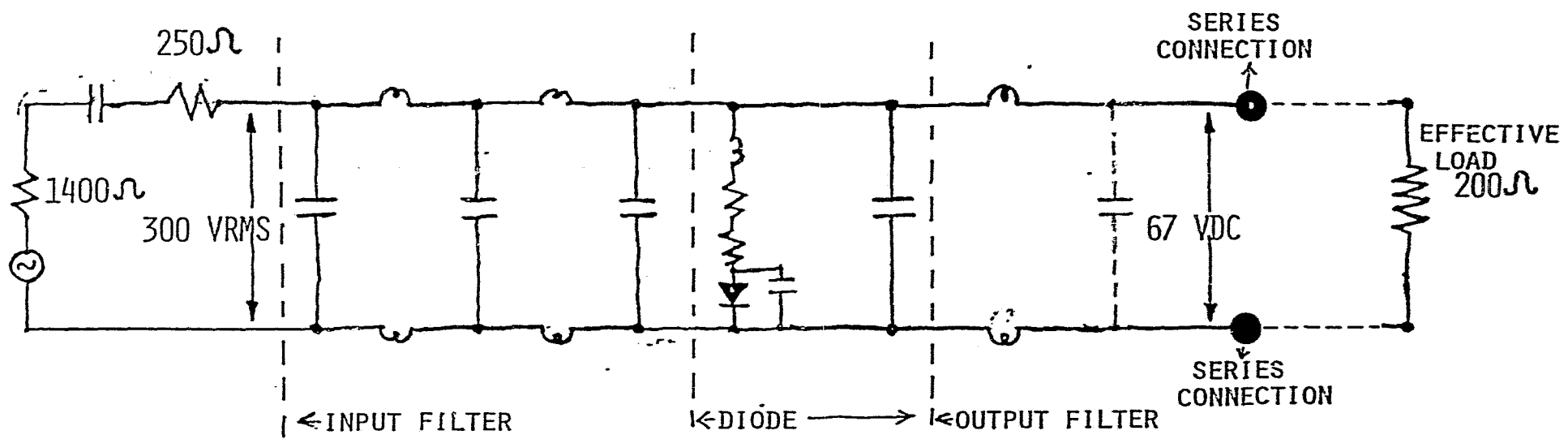


FIGURE 46

XI. CLOUD-TO-GROUND LIGHTNING DISTRIBUTION IN THE UNITED STATES

In order to have a working estimate of the hazard presented by lightning to rectennas, we need to know the cloud-to-ground lightning flash density for various possible rectenna sites in the United States. The cloud-to-ground lightning flash density (in #/km² for example) is not a parameter that is measured as a climatological variable. We have found it necessary to use the number-of-thunderstorm days as a proxy variable because it is available as a climatological variable. Figure 47 gives contours of annual number-of-thunderstorm days.

XI.1. Pierce Conversion Formula

Several attempts have been made to derive a conversion formula to convert thunderstorm days into the flash density by using lightning flash counters in research areas for correlation with the count of thunderstorm days. The best of the various conversion formulas is that due to E.T. Pierce ("A Relationship Between Thunderstorm Days and Lightning Flash Density," *Trans. AGU*, 49, 686, 1967.) The Pierce formula (as does most others) has a quadratic term, which reflects the relationship between frequencies of local storms and storm intensity. In addition, the formula utilizes the monthly thunderstorm days as opposed to the annual average in order to incorporate seasonal effects in the conversion formula.

This formula is

$$q_M^2 = aT_M + a^2 T_M^4,$$

where: T_M = monthly number of thunderstorm days and q_M is the monthly ground flash density (#km⁻²/Mt.). The parameter a is,

$$a = 3 \times 10^{-2}$$

If σ is the annual ground flash density (# km⁻²/yr.), then

$$\sigma = \frac{1}{M=1}^{12} \sigma_M.$$

XI.2. Climatological Data -- Number of Thunderstorm Days

The inputs needed to compute the U.S. Distribution of ground lightning flash density are: (1) The monthly number of thunderstorm days for all U.S. stations recording these observations, (2) the coordinates of the observing sites, and (3) the computer software to compute the density and display the results geographically.

Items 1 and 2 were obtained from "Local Climatological Data - Annual Summaries for 1977" published by The National Oceanic and Atmospheric Administration on magnetic tape. The geographic plotting software of Item 3 was obtained from The National Technical Information Service, and the computer programming was done by J.L. Bohannon at Rice.

A detailed list of flash density for all of the stations used is provided in the Appendix.

Note the hot spots on the contours in Figure 48 that result when stations are located near geographic features that promote local thunderstorms. There are probably other similar hot spots in the U.S. that do not show up on this display because of the absence of an observing station nearby.

UNITED STATES DISTRIBUTION OF THE NUMBER OF THUNDERSTORM DAYS

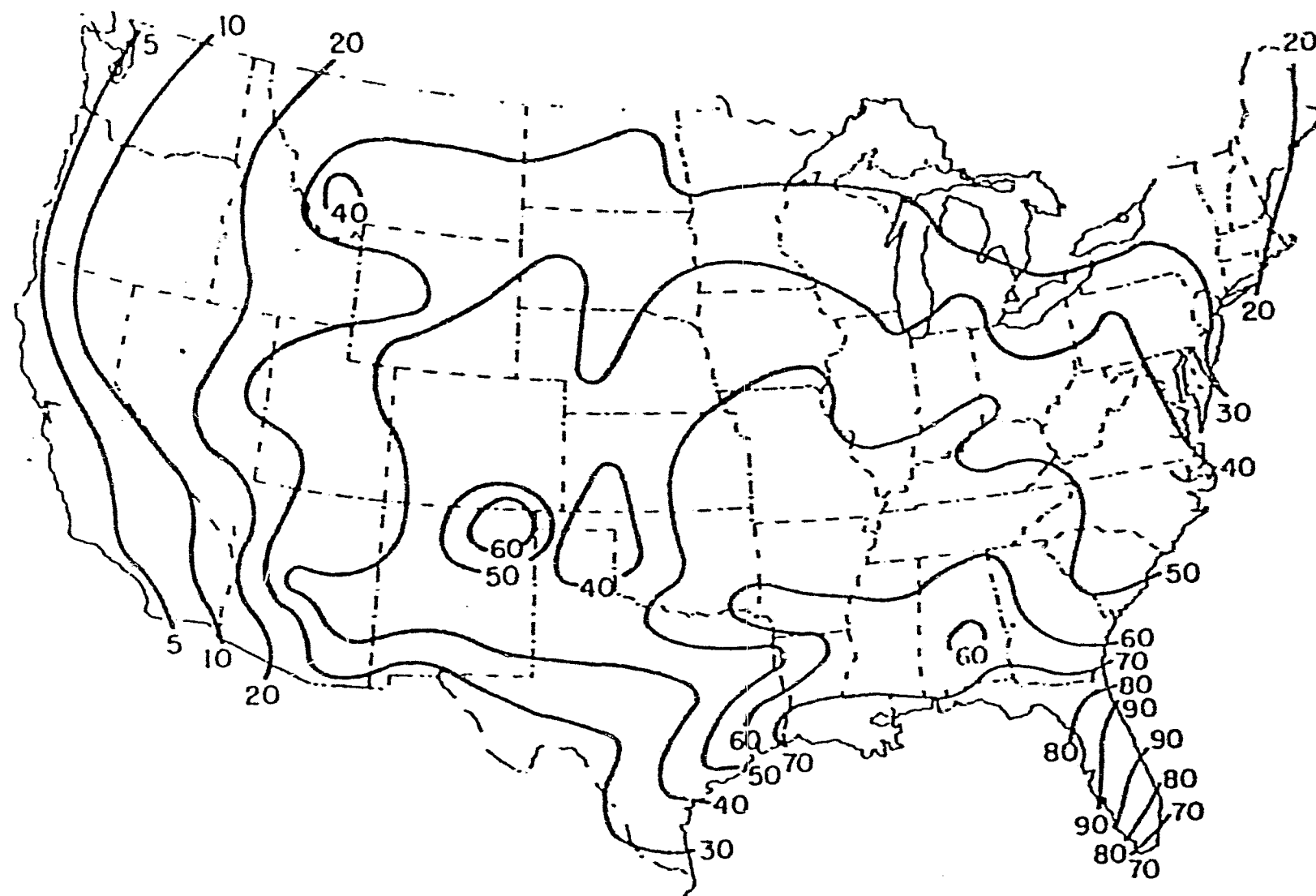


FIGURE 47

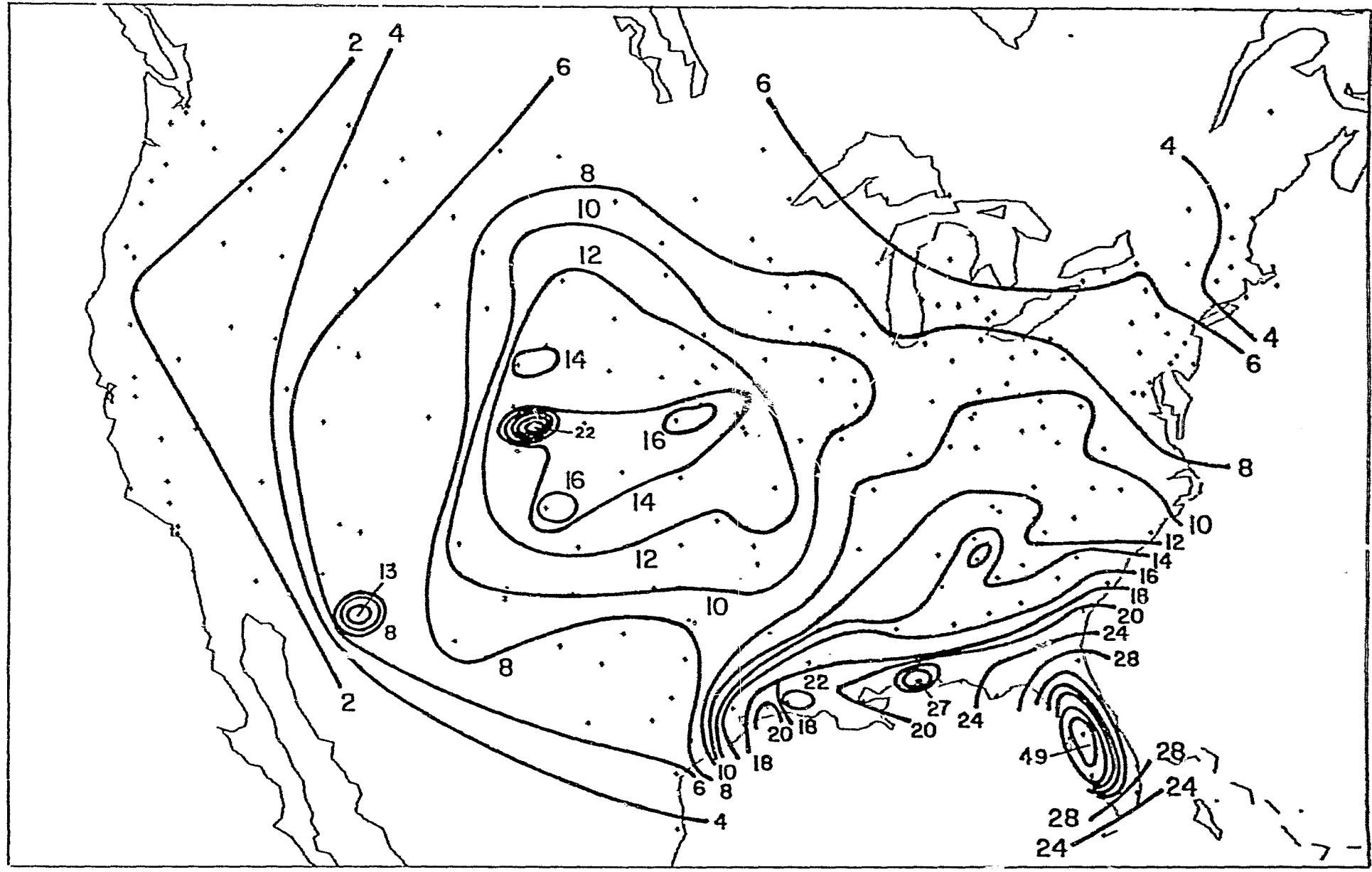


FIGURE 48

APPENDICES

Computer programs developed under this contract.

All programs are in FORTRAN H, unless otherwise specified. All of the programs were run on an IBM 370/155 and/or an ITEL AS/6 computer.

Appendix A

Computer Program PANEL: A Computer Model of the SPS Plasma Interaction

The following pages are the listing of the program "PANEL," written to model the interaction of a high voltage solar array with an ambient Maxwellian plasma. The program was originally written by Dr. Lee W. Parker and was modified for application to the SPS problem by David L. Cooke.

A grid of 'X' characters arranged in a pattern that forms an arrow pointing from the top-left towards the bottom-right. The arrow's path is defined by a series of diagonal steps, with the tip pointing towards the bottom-right corner of the grid.

COMPILER OPTIONS - NAME= MAIN,OPT=02,LINECNT=60,SIZE=00000K,
 SOURCE,EBCDIC,NOLIST,NODECK,LOAD,MAP,NOEDIT,NOID,NOXREF

```

      C      SOLAR PANEL PROBLEM
TSN 0002      COMMON/CP/NPRINT,NPTS,MA,MB,ME,KMAX,XPT,YPT,AL1,BE1,EV,SMACH,
      I TVOLTS,CUR,XMETER
ISN 0003      COMMON/BK/IIM,IIP,JJH,JJP,NTOT,IV,JV,II,JJ,M,N,VPC(30),
      1 XYZ(2080,3),YVC(30,20,10),XPC(30),XMC(10),YP(20),YM(10),ZZ(10),
      2 XX(400),YY(300),ILX,IUX,KUK,KBC,KBD,VRF,NFPS,SKPRFL,SKPLST
ISN 0004      COMMON/FD/XC(2080,2),COEF(2080,7),INDX(2080,6),SKPCO
ISN 0005      COMMON/CD/PVOLTS,XMACH,DENST,NN,PARTCL(2),PART1(2),PART2(2)
ISN 0006      COMMON/INTER/INT,IIA,JJA,KKA,IGOUT,JGOUT,KGOUT,XA,YA,ZA,
      1 XI(30),YJC(20),ZK(10)
      DIMENSION DATE(20)
ISN 0008      DIMENSION VFC(4),IFC(4),JFC(4),KFC(4)
ISN 0009      INTEGER SKPRFL,SKPLST,SKPCO
ISN 0010      NFC(IJX,JX,KX)=IJX+II*(JX-1)+JJ*(KX-1)
ISN 0011      L=5
ISN 0012      M=6
ISN 0013      100 READCL,9999,END=990 DATE
ISN 0014      9999 FORMAT(20A4)
ISN 0015      2 WRITE(M,9998) DATE
ISN 0016      9998 FORMAT(42H1SOLAR PANEL ELECTRIC FIELD AND CURRENTS. ,20A4)
      C      READ GEOMETRIC PARAMETERS
ISN 0017      READCL,111) IIP,IIM,JJP,JJM,KK,IV,JV
ISN 0018      II=IIM+IIP-1
ISN 0019      JJ=JJM+JJP-1
ISN 0020      NTOT=II*JJ*KK
ISN 0021      READCL,222) (XP(I),I=1,IIP)
ISN 0022      READCL,222) (XM(I),I=1,IIM)
ISN 0023      READCL,222) (YP(J),J=1,JJP)
ISN 0024      READCL,222) (YM(J),J=1,JJM)
ISN 0025      READCL,222) (ZZ(K),K=1,KK)
      C      READ PANEL POTENTIALS
ISN 0026      READCL,116) (VPC(I),I=1,IV),VRF
ISN 0027      READCL,111) SKPRFL,SKPLST,ILX,IUX,KLK,KUK,KBC,KBD,NFPS,SKPCO
ISN 0028      DO 140 NPC=1,NTOT
ISN 0029      X(NPC,1)=0
ISN 0030      140 X(NPC,2)=0
ISN 0031      IIM1= IIM+IV-1
ISN 0032      JJM1 = JJM+JV-1
ISN 0033      DO 150 I = IIM,IIM1
ISN 0034      DO 150 J = JJM,JJM1
ISN 0035      III = I+I-IIM
ISN 0036      N = NFC(I,J,1)
ISN 0037      X(N,1) = VPC(III)
ISN 0038      X(N,2) = I
ISN 0039      150 CONTINUE
      C      CONSTRUCT REFLECTORS
ISN 0040      IF(SKPRFL.EQ.1)GO TO 163
ISN 0042      DO 160 I = ILX,IUX
ISN 0043      DO 160 K = KLK,KUK
ISN 0044      JW = KBC-K
ISN 0045      NW = NFC(I,JW,K)
ISN 0046      X(NW,1) = VRF
ISN 0047      X(NW,2) = 1

```

ISN 0048 JW = K+MBD
 ISN 0049 NW = NFC(I,JW,K)
 ISN 0050 X(NW,2) = 1
 ISN 0051 X(NW,1) = VRF
 ISN 0052 CONTINUE
 ISN 0053 WRITE(M,231) VRF
 ISN 0054 FORMAT(//IX,'REFLECTOR POTENTIAL = ',1PE15.5)
 C
 ISN 0055 READ ADDITIONAL FIXED POTENTIALS
 ISN 0057 163 IF(NFPS.LE.3)GO TO 220
 ISN 0058 WRITE(M,118)
 118 FORMAT(//,'ADDITIONAL FIXED POTENTIALS'/
 14(6X,'POT',7X,'I',3X,'J',3X,'K'))
 DO 170 NOC = 1,NFPS,4
 READ(L,119)(VFC(I),IFC(I),JFC(I),KFC(I),I=1,4)
 119 FORMAT(4(E8.0,3I4))
 WRITE(M,117)(VFC(I),IFC(I),JFC(I),KFC(I), I=1,4)
 117 FORMAT(4(3X,1PE10.2,3I4))
 DO 170 I=1,4
 NN = NFC(IFC(I),JFC(I),KFC(I))
 X(NN,1)=VFC(I)
 X(NN,2)=1
 170 CONTINUE
 ISN 0068 220 CONTINUE
 ISN 0069 IVP=IV+1
 ISN 0070 JV=P+1
 TSN 0071 WRITE(M,113)IIP,IIM,JJP,JJM,KK,IV,JV
 ISN 0072 WRITE(M,223)(I,XP(I),I=1,IV)
 ISN 0073 WRITE(M,224)(I,XP(I),I=IVP,IIP)
 ISN 0074 WRITE(M,225)(I,XM(I),I=1,IIM)
 ISN 0075 WRITE(M,226)(J,YP(J),J=1,JV)
 ISN 0076 WRITE(M,227)(J,YP(J),J=JV,JJP)
 ISN 0077 WRITE(M,228)(J,YM(J),J=1,JJM)
 ISN 0078 WRITE(M,229)(K,ZZ(K),K=1,KK)
 ISN 0079 WRITE(M,230)(XP(I),I=1,IV)
 ISN 0080 WRITE(M,241)(VP(I),I=1,IV)
 C
 ISN 0082 111 FORMAT(16I5)
 ISN 0083 113 FORMAT(//IX,I3,18H POSITIVE X-VALUES/
 1 1X,I3,18H NEGATIVE X-VALUES/
 2 1X,I3,18H POSITIVE Y-VALUES/
 3 1X,I3,18H NEGATIVE Y-VALUES/
 4 1X,I3,25H Z-VALUES (POSITIVE ONLY)/
 5 1X,I3,33H POSITIVE X-VALUES DEFINING PANEL/
 6 1X,I3,33H POSITIVE Y-VALUES DEFINING PANEL)
 ISN 0084 116 FORMAT(8E10.0)
 ISN 0085 222 FORMAT(16E5.0)
 ISN 0086 223 FORMAT(//IX,27HX-VALUES POSITIVE ON PANEL=(I3,1PE15.4))
 ISN 0087 224 FORMAT(//IX,35HX-VALUES POSITIVE OUTSIDE OF PANEL=(I3,1PE15.4))
 ISN 0088 225 FORMAT(//IX,18HX-VALUES NEGATIVE=(I3,1PE15.4))
 ISN 0089 226 FORMAT(//IX,27HY-VALUES POSITIVE ON PANEL=(I3,1PE15.4))
 ISN 0090 227 FORMAT(//IX,35HY-VALUES POSITIVE OUTSIDE OF PANEL=(I3,1PE15.4))
 ISN 0091 228 FORMAT(//IX,18HY-VALUES NEGATIVE=(I3,1PE15.4))
 ISN 0092 229 FORMAT(//IX,37HZ-VALUES (POSITIVE ONLY) ABOVE PANEL=(I3,1PE15.4))
 ISN 0093 230 FORMAT(///IX,25HARRAY OF PANEL POTENTIALS//
 1 15X,3HX = ,3X,(8(F8.4,4X)/20X))
 ISN 0094 240 FORMAT(//IX,2HY(,I2,2H)=,F8.4,6X,(8(1PE12.4)/20X))
 ISN 0095 241 FORMAT(8X,1LL Y,,5X,(8(1PE12.4)/20X))

ORIGINAL PAGE
OF POOR
QUALITY

```

I1,1515)
7IX,34HNPRINT,NPTS,MA,MB,ME,KMAX,PROBNO =,6I6,I10/
NUMBER =, F9.1, 9X,13H TEMPERATURE =, F9.1, 6H VOLTS,9X,
        F9.1, 7H PER CC, 9X, 6H MASS =, F9.0,11H ELECTRONS /
J1 SCALE =,F9.1,30H METERS = X-DIMENSION OF PANEL)
23HSINGLE SPACE POINT. X =,F10.5,5X, 3HY =,F10.5)
34HSINGLE ENERGY (MONOENERGETIC). E =,F10.5, 6H VOLTS)
27HSINGLE TRAJECTORY. X =,F10.5,5X, 3HY =,F10.5/
L1 ALPHA =,F20.8 , 8H DEGREES/
L1 BETA =,F20.8 , 8H DEGREES/
RGY =,F20.5 , 6H VOLTS)
J2HRANDOM THERMAL CURRENT DENSITY =,1PE13.4,
FI SQUARE METER, FOR,2A5)
I1 .INTERFACE X-VALUES/(I3,1PE15.4))
18HINTERFACE Y-VALUES/(I3,1PE15.4))
18HINTERFACE Z-VALUES/(I3,1PE15.4))
5^22H -- CURRENTS AND POWER))

```

II

C GO TO 420

C I

C)

I.

6

$$\gamma_1(1) = \gamma_M(b) = -5$$

$$\approx \gamma_1(11) = 5$$

$$\gamma_1(c) = 0$$

I
 I-1)+XX(I))

J
 J-1)+YY(J))

```

ISN 0141      ZK(1)=ZZ(1)
ISN 0142      ZK(KKA)=ZZ(KK)
ISN 0143      DO 560 K=2,KK
ISN 0144      ZK(K)=.5*(ZZ(K-1)+ZZ(K))
ISN 0145      WRITE(M,561) (I,XI(I),I=1,IIA)
ISN 0146      WRITE(M,562) (J,YJ(J),J=1,JJA)
ISN 0147      WRITE(M,563) (K,ZK(K),K=1,KKA)

ISN 0148      C
ISN 0149      DO 600 N=1,NTOT
ISN 0150      CALL FIND(IFIND,JFIND,KFIND)
ISN 0151      XYZ(N,1)=XX(IFIND)
ISN 0152      XYZ(N,2)=YY(JFIND)
ISN 0153      XYZ(N,3)=ZZ(KFIND)
ISN 0154      C
ISN 0156      IF(SKPLST.EQ.1) GO TO 660
ISN 0157      NFPP=(NTOT/300)+1
ISN 0158      DO 650 IP=1,NFPP
ISN 0159      WRITE(M,9000) FORMAT(1H1/6X,1HN,3X,4HX(N),2X,4HY(N),2X,4HZ(N)//)
ISN 0160      CALL LIST(2,IP)
ISN 0161      650  CONTINUE
ISN 0162      660  CONTINUE
ISN 0163      C
ISN 0164      DO 700 J=1,JJ
ISN 0165      DO 700 I=1,II
ISN 0166      N = NF(I,J,1)
ISN 0167      VV(I,J,1) = X(N,1)
ISN 0168      C
ISN 0169      WRITE(M,8000) K,ZZ(K),(XX(I),I=1,II)
ISN 0170      DO 750 J=1,JJ
ISN 0171      WRITE(M,240) J,YY(J),(VV(I,J,K),I=1,II)
ISN 0172      750  CONTINUE
ISN 0173      C
ISN 0174      CALL FIELD
ISN 0175      C
ISN 0176      DO 800 K=1,KK
ISN 0177      DO 800 J=1,JJ
ISN 0178      DO 800 I=1,II
ISN 0179      N=NF(I,J,K)
ISN 0180      VV(I,J,K) = X(N,1)
ISN 0181      C
ISN 0182      800  CONTINUE
ISN 0183      DO 900 K=1,KK
ISN 0184      WRITE(M,8000) K,ZZ(K),(XX(I),I=1,II)
ISN 0185      FORMAT(1H1ARRAY OF POTENTIALS AT ZC,I2,2HD=,F8.4//,
ISN 0186      1 15X,3HX =,3X,(8(F8.4,4X)/20X))
ISN 0187      DO 850 J=1,JJ
ISN 0188      WRITE(M,240) J,YY(J),(VV(I,J,K),I=1,II)
ISN 0189      850  CONTINUE
ISN 0190      900  CONTINUE
ISN 0187      C
ISN 0188      1000 READ(L,333,END=99) NPRINT,NPTS,MA,MB,ME,KMAX,MORE
ISN 0189      1001 READ(L,116) SMACH,TVOLTS,DENCC,XHASS,XMETER
ISN 0190      NPROB=NPROB+1

```

ISN 0191 WRITECH,999
ISN 0192 WRITECM,4440 NPRINT,NPTS,MA,MB,ME,KMAX,NPROB ,SHACH,TVOLTS,DENCC,
1 XMASS,XMETER
ISN 0193 IF(NPTS.EQ.0.OR.ME.EQ.0.OR.MA.EQ.0) READCL,222)XPT,YPT,AL1,BE1,EV
ISN 0195 IF(NPTS.EQ.0) WRITECM,445) XP1,YPT
ISN 0197 IF(ME.EQ.0) WRITECM,446) EV
ISN 0199 IF(MA.EQ.0) WRITECM,447) XPT,YPT,AL1,BE1,EV
ISN 0201 IF(PA.GT.0.AND.XMASS.LE.0.) STOP
ISN 0203 IF(MA.GT.0) CUR=2.68E-8*DENC*SORT(ABS(TVOLTS)/XMASS)
ISN 0205 IF(TVOLTS.GT.0.) PARTCL(1)=PART1(1)
ISN 0207 IF(TVOLTS.GT.0.) PARTCL(2)=PART1(2)
ISN 0209 IF(TVOLTS.LT.0.) PARTCL(1)=PART2(1)
ISN 0211 IF(TVOLTS.LT.0.) PARTCL(2)=PART2(2)
ISN 0213 WRITECM,448) CUR,PARTCL
ISN 0214 CALL POWER
ISN 0215 IF (MORE.GT.0) GO TO 1000
ISN 0217 GO TO 100
ISN 0218 STOP
ISN 0219 END

99

COMPILER OPTIONS - NAME= MAIN,OPT=02,LINECNT=60,SIZE=0000K,
SOURCE,EBCDIC,NOLIST,NODECK,LOAD,MAP,NOEDIT,NOID,NOXREF

ISN 0002 C SUBROUTINE ORBIT
ISN 0003 C STEP ACROSS 3-D BOX ASSUMING CONSTANT POTENTIAL WITHIN BOX
ISN 0004 COMMON/BK/IIM,IIP,JJM,JJP,KK,NTOT,IV,JV,II,JJ,M,N,VPC(30),
ISN 0005 1XYZ(2080,3),VV(30,20,10),XP(30),XM(10),YP(20),YM(10),ZZ(10),
2XX(40),YY(30),ILX,IUX,KUK,MBC,MBD,VRF,NFPS,SKPRFL,SKPLST
COMMON/ORB/XDOT,YDOT,ZDOT,X1,X2,Y1,Y2,Z1,Z2,X,Y,Z,PHI,NTIME,SAVE
ISN 0006 DIMENSION TIME(6),U(3),UDOT(3),B(2,3)
ISN 0007 TOOM=3.3333E+33.
ISN 0008 ROUND = 1.E-11.
ISN 0009 TROUND = 1.E-6 (5 x 10^-5) .
ISN 0011 IF(XDOT.EQ.0..AND.YDOT.EQ.0..AND.ZDOT.EQ.0..) WRITE(6,999)
ISN 0013 999 IF(XDOT.EQ.0..AND.YDOT.EQ.0..AND.ZDOT.EQ.0..) RETURN
FORMAT(IX,3BHSPEED=0 - HENCE PARTICLE DOES NOT MOVE)

ISN 0014 C U(1)=X
ISN 0015 C U(2)=Y
ISN 0016 C U(3)=Z
ISN 0017 C UDOT(1)=XDOT
ISN 0018 C UDOT(2)=YDOT
ISN 0019 C UDOT(3)=ZDOT
ISN 0020 C B(1,1)=X1
ISN 0021 C B(2,1)=X2
ISN 0022 C B(1,2)=Y1
ISN 0023 C B(2,2)=Y2
ISN 0024 C B(1,3)=Z1
ISN 0025 C B(2,3)=Z2
ISN 0026 C DO 101 N2=1,3
ISN 0027 C IF(UDOT(N2).EQ.0..) GO TO 101
ISN 0029 C DO 100 N1=1,2
ISN 0030 C NR=N1 + 2*(N2-1)
ISN 0031 C TIME(NR)=TOOM
ISN 0032 C TT=(B(N1,N2))- U(N2))/UDOT(N2)
ISN 0033 C SS=U(N2)+UDOT(N2)*TT
ISN 0034 C IF(SS.GE.B(1,N2).AND.SS.LE.B(2,N2)) TIME(NR)=TT
100 C CONTINUE
101 C CONTINUE
C FIND SHORTEST SIGNIFICANT TIME
ISN 0038 C TIMIN=TOOM
ISN 0039 C DD 200 NR=1,6
ISN 0040 C IF(TIME(NR).EQ.TOOM) GO TO 200
ISN 0042 C IF(TIME(NR).GT.ROUND.AND.TIME(NR).LT.TIMIN) NTIME=NR
ISN 0044 C IF(TIME(NR).GT.ROUND.AND.TIME(NR).LT.TIMIN) (TIMIN=TIME(NR))
200 C CONTINUE
C ADVANCE TO APPROPRIATE END-POINT

ORIGINAL PAGE IS
OF POOR QUALITY

*x2 > x1
etc.*



*what or smallest n
if you run the short
you'll take the next*

SS = U(N2) +

SS = b

?

ISN 0047 X=X + XDOT*TIMIN
 TSN 0048 Y=Y + YDOT*TIMIN
 ISN 0049 Z=Z + ZDOT*TIMIN
 C
 ISN 0050 XSAV=X
 ISN 0051 YSAV=Y
 ISN 0052 ZSAV=Z
 C
 ISN 0053 IF(NTIME.EQ.1) X=X1
 ISN 0055 IF(NTIME.EQ.2) X=X2
 ISN 0057 IF(NTIME.EQ.3) Y=Y1
 ISN 0059 IF(NTIME.EQ.4) Y=Y2
 ISN 0061 IF(NTIME.EQ.5) Z=Z1
 ISN 0063 IF(NTIME.EQ.6) Z=Z2
 C
 ISN 0065 DX=X-XSAV
 ISN 0066 DY=Y-YSAV
 ISN 0067 DZ=Z-ZSAV
 C
 ISN 0068 IF((NTIME.EQ.1.OR.NTIME.EQ.2).AND.ABS(DX).GT.TROUND), NTIME=-1
 ISN 0070 IF((NTIME.EQ.3.OR.NTIME.EQ.4).AND.ABS(DY).GT.TROUND), NTIME=-2
 ISN 0072 IF((NTIME.EQ.5.OR.NTIME.EQ.6).AND.ABS(DZ).GT.TROUND), NTIME=-3
 ISN 0074 IF(NTIME.EQ.-1) SAVE=XSAV
 ISN 0076 IF(NTIME.EQ.-2) SAVE=YSAV
 ISN 0078 IF(NTIME.EQ.-3) SAVE=ZSAV
 C
 ISN 0080 RETURN
 ISN 0081 END

$$X = X + XDOT * (X)$$

COMPILER OPTIONS - NAME= MAIN,OPT=02,LINECNT=60,SIZE=0000K,
 SOURCE,EBCDIC,NOLIST,NOECK,LOAD,HAP,NOEDIT,NOID,NOXREF

ISN 0002 C SUBROUTINE DEN

C ROUTINE FOR EVALUATING CURRENT-DENSITY INTEGRALS OVER VELOCITY SPACE

ISN 0003 COMMON/BK/IIM,IIP,JJM,JJP,KK,NTOT,IV,JV,II,JJ,M,N,VP(30),
 1XYZ(2080,3),VV(30,20,10),XP(30),XM(10),YP(20),YM(10),ZZ(10),
 2XX(40),YY(30),ILX,IUX,KUK,MBC,MDD,VRF,NIPS,SKPRFL,SKPLST

ISN 0004 COMMON/CP/NPRINT,NPTS,MA,MB,ME,KMAX,XPT,YP,ALI,BE1,EV,SHACH,

ISN 0005 1 TVOLT, CUR, XHETER

COMMON/CD/PVOLTS,XHACH,DENST,NN,PARTCL(2),PART1(2),PART2(2)

ISN 0006 COMMON/ORB/XDOT,YDOT,ZDOT,X1,X2,Y1,Y2,Z1,Z2,X,Y,Z,PHI,NTIME,SAVE,

ISN 0007 COMMON/INTER/INT,IIA,JJA,KKA,IGOUT,JGOUT,KGOUT,XA,YA,ZA,
 1XI(30),YJ(20),ZK(10)

DIMENSION A(2),END1(2),END2(2),FATE(2)

DATA END1/4HABSO,4HRBED/,END2/4HESCA,4HPES /

ISN 0009 XSAVE=XPT

ISN 0010 YSAVE=YPT

ISN 0011 TEMP= ABS(TVOLTS)

ISN 0012 IF(TEMP.LE.0.) WRITE(6,999) TEMP

ISN 0013 999 FORMAT(//1X, 38H TROUBLE - NEGATIVE OR ZERO TEMPERATURE)

ISN 0015 IF(TEMP.LE.0.) RETURN

ISN 0016 IF(MA.EQ.0.OR.ME.EQ.0) EE=EV/TEMP.

ISN 0018 PI=3.1415926536

ISN 0020 AC(1)=-1./SQRT(3.)

ISN 0021 AC(2)=-AC(1)

ISN 0022 MOSTPS=0

ISN 0023 MSTEP=1000

C SET UP SUMS OVER TRAJECTORIES

ISN 0025 C IF(MA.EQ.0) GO TO 250

ISN 0027 JAMAX=2

ISN 0028 JBMAX=2

ISN 0029 KAMAX=MA

ISN 0030 KBMAX=MB

ISN 0031 NUMBER=MA*MB*4

ISN 0032 IF(NN.EQ.1) WRITE(6,990) MA,MB,NUMBER

ISN 0034 990 FORMAT(1X,I4,16H ALPHA-INTERVALS,3X,I4,15H BETA-INTERVALS,6X,
 1 5HHENCE,I4,35H TRAJECTORIES FOR EACH ENERGY-VALUE)

ISN 0035 C IF(ME.EQ.0) GO TO 200

ISN 0037 ME2=2*ME

ISN 0038 JEMAX=2

ISN 0039 KEMAX=ME

ISN 0040 IF(NN.EQ.1) WRITE(6,988) ME,ME2

ISN 0042 988 FORMAT(1X,I4,27H ENERGY INTERVALS AND HENCE,I4,14H ENERGY VALUES)

ISN 0043 C GO TO 300

C SINGLE VALUE OF ENERGY

ISN 0044 200 JEMAX=1

ISN 0045 KEMAX=1

ISN 0046 IF(NN.EQ.1) WRITE(6,986) EV,EE

ISN 0048 986 FORMAT(1X,31H MONOENERGETIC CASE WITH ENERGY,1PE16.4,30H VOLTS, 23
 1 DIMENSIONLESS VALUE,E16.4)

ORIGINAL PAGE IS
OF POOR QUALITY

```

ISN 0049      C      GO TO 300
ISN 0049      C      SINGLE TRAJECTORY ONLY
ISN 0050      250    JAMAX=1
ISN 0051      JBMAX=1
ISN 0052      JEMAX=1
ISN 0053      KAmax=1
ISN 0054      KBMAX=1
ISN 0055      KEMAX=1
ISN 0056      AL=AL1*PI/180.
ISN 0057      BE=BE1*PI/180.
ISN 0058      WRITE(M,904) AL,AL,BE1,BE,EV,EE
ISN 0059      984    FORMAT(1X,17HSINGLE; TRAJECTORY
ISN 0060      1/1X, 7HALPHA =,F20.8 ,12H DEGREES, OR,F20.8 , 8H RADIANS
ISN 0061      2/1X, 7HBETA =,F20.8 ,12H DEGREES, OR,F20.8 , 8H RADIANS
ISN 0062      3/1X, 8HENERGY =,1PE16.4,30H VOLTS, OR DIMENSIONLESS VALUE,E16.4)
ISN 0063      SINA=SIN(AL)
ISN 0064      COSA=COS(AL)
ISN 0065      C      SUM OVER ENERGY, BETA, AND ALPHA
ISN 0066      C      300 CONTINUE
ISN 0067      DENS=0.
ISN 0068      DO 1001 KE=1,KEMAX
ISN 0069      DO 1001 JE=1,JEMAX
ISN 0070      DENS=0.
ISN 0071      NOESC=0.
ISN 0072      DO 1000 KB=1,KBMAX
ISN 0073      DO 1000 JB=1,JBMAX
ISN 0074      DO 1000 KA=1,KAmax
ISN 0075      DO 1000 JA=1,JAMAX
ISN 0076      C      INITIAL POSITION
ISN 0077      C      Z=0.
ISN 0078      X=XSAVE
ISN 0079      Y=YSAVE
ISN 0080      IFCMA.EQ.0) GO TO 320
ISN 0081      CA=(A(JA) + FLOAT(2*KA - 1 - MA))/FLOAT(MA)
ISN 0082      SINA=SQRT(.5*(1.+CA))
ISN 0083      COSA=SQRT(1. - SINA**2)
ISN 0084      CBETA=(A(JB) + FLOAT(2*KB - 1 - MB))/FLOAT(MB)
ISN 0085      BE=PI*(1. + CBETA)
ISN 0086      C      XDOT=SINA*COS(BE)
ISN 0087      YDOT=SINA*SIN(BE)
ISN 0088      ZDOT=COSA
ISN 0089      INT=0
ISN 0090      CALL INTERP
ISN 0091      C      IFCIGOUT.GE.1.AND.IGOUT.LE.IIA.AND.JGOUT.GE.-1.AND.JGOUT.LE.JJA.
ISN 0092      1 AND.KGOUT.GE.-1.AND.KGOUT.LE.KKA) GO TO 340
ISN 0093      330    WRITE (M,9999)

```

```

:ISN 0090      9999 FORMAT(////1X,43)NONE OF THE IG-JG-KG INDICES IS OUT OF RANGE)
ISN 0091      WRITE (H,800) KSTEP,X,Y,Z,XDOT,YDOT,ZDOT,IGOUT,JGOUT,KGOUT,PHI
ISN 0092      WRITE(M,982)KE,JE,KB,JB,KA,JA,BE1,AL1,EV,PVOLTS
ISN 0093      STOP

C
ISN 0094      340   INT=1
ISN 0095      PHISAV=PHI
ISN 0096      SPEED=0.
ISN 0097      PHIOLD=PHI
ISN 0098      IF(ME.GT.0) GO TO 350

C
ISN 0100      E=EE
ISN 0101      GO TO 400

C
ISN 0102      350   CE=(AC(JE) + FLOAT(2*KE-1-ME))/FLOAT(ME)
ISN 0103      E=(1.+CE)/(1.-CE)
ISN 0104      IF(XMACH.GT.1.) E=XMACH**2*(1.+CE)/(1.-CE)
ISN 0106      E=E + AMAX1(PHI, 0.)

C
ISN 0107      400   IF(CE.LT.PHI) GO TO 1001
ISN 0109      SPEED=SQRT(CE-PHI)

C
ISN 0110      XDOT=SPEED*SINA*COS(BE)
ISN 0111      YDOT=SPEED*SINA*SIN(BE)
ISN 0112      ZDOT=SPEED*COSA
ISN 0113      AL=ARCOS(COSA)
ISN 0114      AL1=AL*180./PI
ISN 0115      BE1=BE*180./PI
ISN 0116      EV=E*TEMP
ISN 0117      PVOLTS=PHISAV*TVOLETS
ISN 0118      ZOLD=Z
ISN 0119      KSTEP=0
ISN 0120      IF(NPRINT.NE.2.AND.NPRINT.NE.3) GO TO 490

C
C PRINT INITIAL CONDITIONS OF TRAJECTORY
C
ISN 0122      WRITE(H,982) KE,JE,KB,JB,KA,JA,BE1,AL1,EV,PVOLTS
ISN 0123      982   FORMAT(/1X,52HKE,JE, KB,JB, KA,JA, BETA,ALPHA,ENERGY,POTENTIAL=
1,/1X,3(I3,12),1PE22.8 ,4H DEG,4X,E22.8 ,4H DEG,8X,E16.4,2H V,4X,
2 E16.4,2H V)

C
ISN 0124      WRITE(M,980)
ISN 0125      980   FORMAT( 9X, 95HSTEPS X Y Z XDOT
1 YDOT ZDOT IG JG KG PHI)
C
ISN 0126      WRITE(M,888) KSTEP,X,Y,Z,XDOT,YDOT,ZDOT,IGOUT,JGOUT,KGOUT,PHI
ISN 0127      888   FORMAT( 9X,I5,1P6E11.3,3I6,E11.3)
C
C TAKE A STEP
C
ISN 0128      490   IF (KSTEP.EQ.0) GO TO 550
ISN 0130      500   CALL DROUT
ISN 0131      KSTEP=KSTEP + 1
ISN 0132      IF(NPRINT.EQ.3) WRITE(H,888) KSTEP,X,Y,Z,XDOT,YDOT,ZDOT,IGOUT,
1 JGOUT,KGOUT,PHI
ISN 0134      IF(KSTEP.LE.HSTEP) GO TO 550
ISN 0136      WRITE(M,998) HSTEP
ISN 0137      998   FORMAT(////1X, 9HMORE THAN,16,19H STEPS - HENCE STOP)

```

ISN 0138 STOP
 C
 ISN 0139 550 IF(Z.EQ.0..AND.ZDOT.LT.0.
 1.AND.Y.GE.YP(1).AND.Y.LE.YP(JV)) GO TO 600
 C
 ISN 0141 IF((X.LE.XX(1).AND.ZDOT.LT.0.).OR.
 1(X.GE.XX(II)).AND.ZDOT.LT.0.)GO TO 600
 C
 ISN 0143 IF((X.LE.XX(1).AND.XDOT.LT.0..AND.ZDOT.GT.0.).OR.
 1(Y.LE.YY(1).AND.YDOT.LT.0.).OR.
 2(X.GE.XX(II).AND.XDOT.GE.0..AND.ZDOT.GT.0.).OR.
 3(Y.GE.YY(JJ).AND.YDOT.GT.0.).OR.
 4(Z.GE.ZZ(KK).AND.ZDOT.GT.0.))GO TO 700

$y < 0 \times S(2)$

ISN 0145
 ISN 0147 IF(SKPRFL.EQ.1) GO TO 538
 IF(((Y.LE.(YY(MBC)-.5*Z)).AND.(Y.GT.(YY(MBC)-.5*ZZ(KUK))))).OR.
 1((Y.GE.(YY(MBD)+.5*Z)).AND.(Y.LT.(YY(MBD)+.5*ZZ(KUK))))
 2.AND.X.GE.XX(ILX).AND.X.LE.XX(IUX)) GO TO 600

ISN 0149 538 CONTINUE
 ISN 0150 IF(Z.NE.0..OR.ZDOT.GE.0.) GO TO 540
 ZDOT=-ZDOT
 ISN 0152 IF(NPRINT.EQ.3) WRITE(6,888) KSTEP,X,Y,Z,XDOT,YDOT,ZDOT,IGCUT,
 1 JGOUT,KGOUT,PHI
 ISN 0153 GO TO 590

ISN 0155 540 CONTINUE
 ISN 0156 C
 ISN 0157 IF(CKSTEP.EQ.0) GO TO 500
 PHIOLD=PHI
 ISN 0159 CALL INTERP
 ISN 0160 IF(IGOUT.LT.1.OR.IGOUT.GT.IIA.OR.JGOUT.LT.1.OR.JGOUT.GT.JJA.OR.
 1KGOUT.LT.1.OR.KGOUT.GT.KKA) GO TO 330
 ISN 0161 IF(NTIME.LT.1.OR.NTIME.GT.6) GO TO 580

ISN 0163 C
 ISN 0165 IF(NTIME.NE.1.AND.NTIME.NE.2) GO TO 560
 XDOTS=XDOT**2 + PHIOLD-PHI
 ISN 0167 IF(XDOTS.EQ.0.) XDOT=0.
 ISN 0168 IF(XDOTS.GT.0..AND.XDOT.NE.0.) XDOT=SORT(XDOTS)*SIGN(1.,XDOT)
 ISN 0170 IF(XDOTS.LT.0..AND.XDOT.NE.0.) XDOT=-XDOT
 ISN 0172 IF(NPRINT.EQ.3.AND.XDOTS.LT.0) WRITE(6,888) KSTEP,X,Y,Z,XDOT,YDOT,
 1 ZDOT,IGOUT,JGOUT,KGOUT,PHI

ISN 0174 C
 ISN 0176 560 IF(NTIME.NE.3.AND.NTIME.NE.4) GO TO 570
 YDOTS=YDOT**2 + PHIOLD-PHI
 ISN 0178 IF(YDOTS.EQ.0.) YDOT=0.
 ISN 0179 IF(YDOTS.GT.0..AND.YDOT.NE.0.) YDOT=SORT(YDOTS)*SIGN(1.,YDOT)
 ISN 0181 IF(YDOTS.LT.0..AND.YDOT.NE.0.) YDOT=-YDOT
 ISN 0183 IF(NPRINT.EQ.3.AND.YDOTS.LT.0) WRITE(6,888) KSTEP,X,Y,Z,XDOT,YDOT,
 1 ZDOT,IGOUT,JGOUT,KGOUT,PHI

ISN 0185 C
 ISN 0187 570 IF(NTIME.NE.5.AND.NTIME.NE.6) GO TO 590
 ZDOTS=ZDOT**2 + PHIOLD-PHI
 ISN 0189 IF(ZDOTS.EQ.0.) ZDOT=0.
 ISN 0190 IF(ZDOTS.GT.0..AND.ZDOT.NE.0.) ZDOT=SORT(ZDOTS)*SIGN(1.,ZDOT)
 ISN 0192 IF(ZDOTS.LT.0..AND.ZDOT.NE.0.) ZDOT=-ZDOT
 ISN 0194 IF(NPRINT.EQ.3.AND.ZDOTS.LT.0) WRITE(6,888) KSTEP,X,Y,Z,XDOT,YDOT,
 1 ZDOT,IGOUT,JGOUT,KGOUT,PHI

ISN 0196 ISN 0198 GO TO 590

```

ISN 0199      580  WRITECH,997) NTIME
ISN 0200      997  FORMAT(//1X,17H TROUBLE = NTIME =,I3,19H = OUT OF RANGE 1-6)
ISN 0201      887  WRITECH,887) KSTEP,X,Y,Z,XDOT,YDOT,ZDOT,IGOUT,JGOUT,KGOUT,PHI,SAVE
ISN 0202      887  FORMAT( 9X,I5,1P6E11.3,3I6,E11.3,'SAVE=',E18.10)
ISN 0203      C     STOP

ISN 0204      590  CALL INTERP
ISN 0205      590  IF(IGOUT.LT.1.OR.IGOUT.GT.IIA.OR.JGOUT.LT.1.OR.JGOUT.GT.JJA.OR.
ISN 0207      1KGOUT.LT.1.OR.KGOUT.GT.KKA) GO TO 330
ISN 0209      1IF(NPRINT.EQ.3) WRITECH,888) KSTEP,X,Y,Z,XDOT,YDOT,ZDOT,IGOUT,
ISN 0209      1JGOUT,KGOUT,PHI
ISN 0209      C     GO TO 500

ISN 0210      C     PARTICLE IS ABSORBED
ISN 0211      600  CONTINUE
ISN 0213      IF(NPRINT.NE.2.AND.NPRINT.NE.3) GO TO 1002
ISN 0214      FATE(1)=END1(1)
ISN 0215      FATE(2)=END1(2)
ISN 0215      GO TO 750

ISN 0216      C     PARTICLE ESCAPES
ISN 0217      C
ISN 0219      700  CONTINUE
ISN 0221      IF(NPRINT.NE.2.AND.VPRINT.NE.3) GO TO 740
ISN 0222      FATE(1)=END2(1)
ISN 0223      FATE(2)=END2(2)
ISN 0224      GO TO 740
ISN 0225      WRITECH,982) KE,JE,KB,JB,KA,JA,BE1,AL1,EV,PVOLTS
ISN 0226      740  NOESC=NOESC + 1
ISN 0226      IF(ME.EQ.0) GO TO 750

ISN 0228      C
ISN 0229      CSANGL=ZDOT/SORT(XDOT**2+YDOT**2+ZDOT**2)
ISN 0230      XPON=-2.*XHACH*SQRT(E)*CSANGL - E = XHACH**2
ISN 0231      COEFA=SPEED**2/FLOAT(NUMBER)
ISN 0233      IF(ABS(XPON).GT.36.) GO TO 1000
ISN 0233      ADD=COEFA*EXP(XPON)
ISN 0234      DENS=DENS + ADD

ISN 0235      C
ISN 0237      750  IF(NPRINT.NE.2.AND.NPRINT.NE.3) GO TO 1002
ISN 0238      WRITECH,889) FATE,KSTEP,X,Y,Z,XDOT,YDOT,ZDOT,IGOUT,JGOUT,XGOUT,PHI
ISN 0238      FORMAT(1X,2A4,I5,1P6E11.3,3I6,E11.3)

ISN 0239      C
ISN 0240      1002  CONTINUE
ISN 0242      IF(MOSTPS.GE.KSTEP) GO TO 1000
ISN 0243      KES=KE
ISN 0244      JES=JE
ISN 0245      KBS=KB
ISN 0246      JBS=JB
ISN 0247      KAS=KA
ISN 0248      JAS=JA
ISN 0249      MOSTPS=KSTEP

ISN 0249      1000  CONTINUE
ISN 0249      C     END OF SUM OVER ANGLES
ISN 0250      C     FRACT=FLOAT(NOESC)/FLOAT(NUMBER)

```

TSN 0251 C WRITECH,978) NOESC,NUMBER,FRACT,EV,DENS
TSN 0252 978 FORMAT(1X,16H RATIO ESCAPING =,15, 7H DUE. OF ,15.14H DR A FRACTION,
1 F13.8,14H AT ENERGY E =,F13.8, 6H VOLTS, X.6H(DENS=,1PE14.4,1H)
TSN 0253 C IFC(NPRINT.EQ.0) GO TO 800
TSN 0255 976 IF(CME.NE.0) WRITECH,976)
TSN 0257 FORMAT(1X,80H DENS IS THE SUM OF ADD=SPEED**2*EXP(XPON)/NUMBER OVER
1 A HEMISPHERE OF DIRECTIONS//)
TSN 0258 C 800 IF(CME.EQ.0) GO TO 1001
TSN 0260 COEFE=2.-(1.-CE)**2/FLOAT(CHE)
TSN 0261 IFC(XMACH.GT.1.) COEFE=COEFE*XMAHC**2
TSN 0263 DENST=DENST + COEFE*DENS
TSN 0264 1001 CONTINUE
TSN 0265 C IF(CME.EQ.0) DENST=SPEED**2*FRACT
C
C TRAJECTORY WITH HOST STEPS. PRINT K AND J INDICES.
C
TSN 0267 WRITECH,972) HOSTPS,KES,JES,KBS,JBS,KAS,JAS
TSN 0268 972 FORMAT(1//1X,15,3(I3,I2),29H =HOSTPS, KE,JE, KB,JB, KA,JA)
TSN 0269 WRITECH,974) XSAVE,YSAVE,PHISAV,DENST,PARTCL
TSN 0270 974 FORMAT(1X,26H AT DIMENSIONLESS X,Y,PHI =,3F12.6,1H,,5X,1PE16.4,
1 33H = NORMALIZED CURRENT DENSITY FOR,2A5//)
TSN 0271 RETURN
TSN 0272 END

COMPILE OPTIONS - NAME= MAIN,OPT=02,LINECNT=60,SIZE=0000K,
 SOURCE,EBCDIC,NOLIST,NOECK,LOAD,MAP,NOEDIT,NOID,NOXREF

ISN 0002	C	SUBROUTINE INTERP
	C	INTERPOLATION WITHIN GRID
TSN 0003	C	COMMON/BK/IIM,IIP,JJM,JJP,KK,NTOT,IV,JV,IT,JJ,M,N,VPC(30), 1XYZ(2080,3),VV(30,20,10),XPC(30),XMC(10),YP(20),YMC(10),ZZ(10), 2XXC(40),YYC(30),ILX,IUX,KUK,MBC,MBD,VRF,NFPS,SKPRFL,SKPLST
ISN 0004	C	COMMON/ORB/XDOT,YDOT,ZDOT,X1,X2,Y1,Y2,Z1,Z2,X,Y,Z,PHI,NTIME,SAVE
ISN 0005	C	COMMON/INTER/INT,IIA,JJA,KKA,IGOUT,JGOUT,KGOUT,XA,YA,ZA, 1XI(30),YJ(20),ZK(10)
ISN 0006	C	IGOUT=0
ISN 0007	C	JGOUT=0
ISN 0008	C	KGOUT=0
ISN 0009	C	NCH=0
ISN 0010	C	XA=X
ISN 0011	C	YA=Y
ISN 0012	C	ZA=Z
ISN 0013	C	LOCATE XA
ISN 0015	C	IF(XA.EQ.XI(IIA)) IG=IIA-1
ISN 0017	C	IF(XA.EQ.XI(IIA)) GO TO 103
	C	IF(INT.NE.0) GO TO 100
ISN 0019	C	DO 10 I=2,IIA
ISN 0020	C	IG=I-1
ISN 0021	C	IF(XA.LT.XI(I)) GO TO 103
ISN 0023	10	CONTINUE
ISN 0024	C	IF(XA.GE.XI(IG+1)) GO TO 102
ISN 0026	C	IF(XA.GE.XI(IG)) GO TO 104
ISN 0028	C	IG=IG-1
ISN 0029	C	IF(XA.LT.XI(IG)) GO TO 101
ISN 0031	C	GO TO 103
ISN 0032	C	IG=IG+1
ISN 0033	C	IF(XA.GE.XI(IG+1)) GO TO 102
ISN 0035	C	NCH=1
ISN 0036	C	CONTINUE
	C	ACCEPT IF XI(IG) LESS THAN OR EQUAL TO XA LESS THAN XI(IG+1).
	C	LOCATE YA
ISN 0037	C	IF(YA.EQ.YJ(JJA)) JG=JJA-1
ISN 0039	C	IF(YA.EQ.YJ(JJA)) GO TO 203
ISN 0041	C	IF(INT.NE.0) GO TO 200
ISN 0043	C	DO 20 J=2,JJA
ISN 0044	C	JG=J-1
ISN 0045	C	IF(YA.LT.YJ(J)) GO TO 203
ISN 0047	20	CONTINUE

ORIGINAL PAGE
OF POOR
QUALITY

```

ISN 0048      200 IF(YA.GE.YJ(JG+1)) GO TO 202
ISN 0050
ISN 0052      201 IF(YA.GE.YJ(JG))    GO TO 204
ISN 0053
ISN 0055      202 IF(YA.LT.YJ(JG))    GO TO 201
ISN 0056
ISN 0057      C   JG=JG+1
ISN 0059      203 IF(YA.GE.YJ(JG+1)) GO TO 202
ISN 0060      C   NCH=1
ISN 0061      204 CONTINUE
ISN 0063
ISN 0065      C   ACCEPT IF YJ(JG) LESS THAN OR EQUAL TO YA LESS THAN YJ(JG+1).

ISN 0067      C   LOCATE ZA
ISN 0068
ISN 0069      C   IF(ZA.EQ.ZK(KKA)) KG=KKA-1
ISN 0071      30  IF(ZA.EQ.ZK(KKA)) GO TO 303
ISN 0072      C   IF(INT.NE.0) GO TO 300
ISN 0074
ISN 0076      300 DO 30 K=2,KKA
ISN 0077      C   KG=K-1
ISN 0079      301 IF(ZA.LT.ZK(KG))    GO TO 303
ISN 0080      C   CONTINUE
ISN 0081      302 IF(ZA.GE.ZK(KG+1)) GO TO 302
ISN 0083      C   IF(ZK(KG) LESS THAN OR EQUAL TO ZA LESS THAN ZK(KG+1)).
ISN 0084      303 NCH=1
ISN 0085      304 CONTINUE
ISN 0086
ISN 0087      C   ACCEPT IF ZK(KG) LESS THAN OR EQUAL TO ZA LESS THAN ZK(KG+1).

ISN 0088      C   LOCATE LINE AND BOX
ISN 0089
ISN 0090      C   X1=XI(IG)
ISN 0091      Y1=YJ(JG)
ISN 0092      Z1=ZK(KG)
ISN 0093      X2=XI(IG+1)
ISN 0094      Y2=YJ(JG+1)
ISN 0095      Z2=ZK(KG+1)
ISN 0096      C   IF(X.NE.X1.OR.XDOT.GE.0.) GO TO 400
ISN 0097      TG=TG-1
ISN 0098      X2=X1
ISN 0099      X1=XI(IG)
ISN 0100      C   IF(Y.NE.Y1.OR.YDOT.GE.0.) GO TO 500
ISN 0101      JG=JG-1
ISN 0102      Y2=Y1
ISN 0103      Y1=YJ(JG)
ISN 0104      C   IF(Z.NE.Z1.OR.ZDOT.GE.0.) GO TO 600

```

ISN 0103 KG=KG-1
ISN 0104 Z2=Z1
ISN 0105 Z1=ZK(KG)

ISN 0106 C 600 PHI=VV(IG,JG,KG)
ISN 0107 IGOUT=IG
ISN 0108 JGOUT=JG
ISN 0109 KGOUT=KG
ISN 0110 RETURN
ISN 0111 END

```

COMPILER OPTIONS - NAME= MAIN,OPT=02,LINECNT=60,SIZE=0000K,
                   SOURCE,EBCDIC,NOLIST,NOECK,LOAD,MAP,NOEDIT,NOID,NOXREF

ISN 0002          SUBROUTINE POWER

C CURRENT DENSITIES AND POWER LOSS
C

ISN 0003          COMMON/BK/IIM,IIP,JJM,JJP,KK,NTOT,IV,JV,II,JJ,H,N,VP(30),
                  IXYZ(2080,3),VV(30,20,10),XP(30),XH(10),YP(20),YH(10),ZZ(10),
                  2XX(40),YY(30),ILX,IUX,KUK,MBC,MBD,VRF,NFPS,SKPRFL,SKPLST

ISN 0004          COMMON/CP/NPRINT,NPTS,MA,MB,ME,KMAX,XPT,YPT,AL1,BE1,EV,SMACH,
                  1 TVOLTS,CUR,XMETER

ISN 0005          COMMON/CD/PVOLTS,XMACH,DENST,NN,PARTCL(2),PART1(2),PART2(2)
ISN 0006          DIMENSION A(2)

ISN 0007          IF(NPTS.EQ.0.OR.MA.EQ.0) WRITE(6,997) XPT,YPT,AL1,BE1,EV
ISN 0009          997 FORMAT(/1X, 9HX AND Y =,2F10.5,20X,19HALPHA,BETA,ENERGY =,3F20.5)
ISN 0010          IF(NPRINT.EQ.0) WRITE(6,990)
ISN 0012          IF(NPRINT.EQ.1) WRITE(6,991)
ISN 0014          IF(NPRINT.EQ.2) WRITE(6,992)
ISN 0016          IF(NPRINT.EQ.3) WRITE(6,993)
ISN 0018          990 FORMAT(/38H NPRINT=0 MEANS NO TRAJECTORY PRINTING)
ISN 0019          991 FORMAT(/53H NPRINT=1 PRINT INDICES OF ESCAPING TRAJECTORIES ONLY)
ISN 0020          992 FORMAT(/56H NPRINT=2 PRINT FIRST AND LAST STEPS OF ALL TRAJECTORIES
ISN 0021          1S)
ISN 0022          993 FORMAT(/52H NPRINT=3 MEANS PRINT EVERY STEP OF ALL TRAJECTORIES)
ISN 0024          C
                  IF(TVOLTS.EQ.0.) RETURN
                  C
                  XMACH=SMACH.

ISN 0025          C NON-DIMENSIONALIZE THE POTENTIAL DISTRIBUTION. THEN RESTORE AT END.
ISN 0026          C
ISN 0027          DO 200 K=1,KK
ISN 0028          DO 200 J=1,JJ
ISN 0029          DO 200 I=1,II
                  VV(I,J,K)=VV(I,J,K)/TVOLTS
ISN 0030          200 CONTINUE
                  C DEFINE THE PANEL POINTS AT WHICH THE CURRENT AND POWER IS EVALUATED
                  C CASE OF A SINGLE POINT
                  C
                  IF(NPTS.EQ.0.OR.MA.EQ.0) COEFM = XMETER**2
                  C CASE OF MULTIPLE POINTS FOR INTEGRATION OVER PANEL SUB-AREAS
                  C

ISN 0032          JVH=1
ISN 0033          IVM=1
ISN 0034          IF(JV.GT.1) JVM=JV-1
ISN 0036          IF(IV.GT.1) IVM=IV-1
ISN 0038          NA=0
ISN 0039          NAREAS=IVM*JVH
ISN 0040          TPOWER=0.
ISN 0041          TCURNT=0.
ISN 0042          TAREA=0.
ISN 0043          NN=0
ISN 0044          DO 500 J=1,JVM
ISN 0045          DO 500 I=1,IVM
                  NA=NA+1

```

ORIGINAL PAGE
OF POOR
QUALITY

```

ISN 0047      NP=0
ISN 0048      IF(NPTS.EQ.0.OR.MA.EQ.0) GO TO 250
ISN 0050      PO = 0
ISN 0051      CU = 0
ISN 0052      A(1)=-1./SQRT(3.)
ISN 0053      A(2)=-A(1)
ISN 0054      GO TO 260
ISN 0055      250  CONTINUE
ISN 0056      JXMAX=1
ISN 0057      JYMAX=1
ISN 0058      KMAX=1
ISN 0059      GO TO 270
ISN 0060      260  JXMAX=2
ISN 0061      JYMAX=2
ISN 0062      CONTINUE
ISN 0063      DO 400 KY=1,KMAX.
ISN 0064      DO 400 KX=1,KMAX
ISN 0065      DO 400 JY=1,JYMAX
ISN 0066      DO 400 JX=1,JXMAX
ISN 0067      NP=NP+1
ISN 0068      NN=NN+1
ISN 0069      IF(NPTS.EQ.0.OR.MA.EQ.0) GO TO 300
ISN 0071      CX=(AC(JX)+FLOAT(2*KX-1-KMAX))/FLOAT(KMAX)
ISN 0072      CY=(AC(JY)+FLOAT(2*KY-1-KMAX))/FLOAT(KMAX)
ISN 0073      XPT=(XPC(I+1)-XPC(I))/2.*CX+(XPC(I+1)+XPC(I))/2.
ISN 0074      YPT =(YP(J+1)-YP(J))/2.*CY +(YP(J+1)+YP(J))/2.
ISN 0075      COEF =(XPC(I+1)-XPC(I))*(YP(J+1)-YP(J))
ISN 0076      AREA = COEF * XMETER**2
ISN 0077      COEFM = AREA/4.*FLOAT(KMAX**2)

C COMPUTE EACH CURRENT DENSITY AND MULTIPLY BY LOCAL POTENTIAL TO
C EVALUATE POWER DENSITY
ISN 0078      300  CALL DEN
ISN 0079      DENCUR=DENST*CUR
ISN 0080      POWDEN=PVOLTS*DENCUR
ISN 0081      IF(MA.EQ.0) GO TO 600
ISN 0083      XPTM=XPT*XMETER
ISN 0084      YPTM=YPT*XMETER
ISN 0085      XPM=XPC(I)*XMETER
ISN 0086      XPPM=XPC(I+1)*XMETER
ISN 0087      YPM=YP(J)*XMETER
ISN 0088      YPPM=YP(J+1)*XMETER

ISN 0089      995  FORMAT(6X,12HAT POINT NO.,I3,10H, WITH X.=,F10.5,13H METERS, Y =
1,F10.5,27H METERS, AND COEFFICIENT =,F10.5,14H SQUARE METERS)
ISN 0090      C
ISN 0092      994  IF(NPTS.GT.0.AND.MA.GT.0) WRITE(M,994) NA,XPM,XPPM,YPM,YPPM
ISN 0093      C
ISN 0094      FORMAT(15X,16H IN SUB-AREA NO.,I3,1X,17H8DUNDED BY X IN C,
1 F10.5,3H TO,F10.5, 9H) METERS,,4X,I3H AND BY Y IN C,
2 F10.5,3H TO,F10.5, 8H) METERS)
ISN 0095      C
ISN 0096      988  WRITE(M,995) NP,XPTM,YPTM,COEFF
ISN 0097      WRITE(M,988) PVOLTS,DENCUR,POWDEN,PARTCL
ISN 0098      FORMAT(6X,53HTHE VOLTAGE, CURRENT DENSITY, AND POWER DENSITY ARE =
1/6X,1PE16.4,6H VOLTS,4X,E16.4,23H AMP/(SQ-METER), AND,E16.4,
2 24H WATT/(SQ-METER), FOR,2A5//)
ISN 0099      IF(NPTS.EQ.0) GO TO 600

```

4 x 4 x 4 x 4 x 2,

[REDACTED]

*LTRJ = NN / (MA * MB * NE)*

NIMBZ = [REDACTED] : 3.2 :

LTRJCT = NN / NIMB

```

ISN 0098      CU = CU + COEFM*DENCUR
ISN 0099      PO = PO + COEFM * POWDEN
ISN 0100      CONTINUE
ISN 0101      AVCD = CU/AREA
ISN 0102      AVPD = PO/AREA
ISN 0103      C
ISN 0104      WRITE(M,986) NA,CU,PO,PARTCL
ISN 0105      WRITE(M,984) NA,AREA,AVCD,AVPD
ISN 0106      984   FORMAT( 1X,18HIN SUB-AREA NUMBER,I3,8H OF AREA,1PE16.4,15H SQUARE
                  1 METERS,/52H THE AVERAGE CURRENT DENSITY AND POWER DENSITY ARE =,
                  2 E16.4,19H AMP/(SQ-METER) AND,E16.4,16H WATT/(SQ-METER))
ISN 0107      986   FORMAT( /1X,18HIN SUB-AREA NUMBER,I3,28H THE CURRENT AND POWER ARE
                  1 =,1PE16.4,12H AMP,    AND,E16.4,14H WATTS,   FOR,2A5)
ISN 0108      C
ISN 0109      TAREA=TAREA + AREA
ISN 0110      TCURNT = TCURNT + CU
ISN 0111      TPOWER = TPOWER + PO
ISN 0112      500   CONTINUE
ISN 0113      C
ISN 0114      WRITE(M,982) TCURNT,TPOWER,PARTCL
ISN 0115      982   FORMAT(//1X,34HTOTAL CURRENT AND POWER LOSS ARE =,1PE16.4,
                  1 12H AMP,    AND,E16.4,13H WATT,   FOR,2A5)
ISN 0116      AVCD=TCURNT/TAREA
ISN 0117      AVPD=TPOWER/TAREA
ISN 0118      WRITE(M,980) TAREA,AVCD,AVPD
ISN 0119      980   FORMAT(1X,26HWITH A TOTAL PANEL AREA OF,1PE16.4,15H SQUARE METERS
                  1,/1X,51HTHE AVERAGE CURRENT DENSITY AND POWER DENSITY ARE =,
                  2 E16.4,19H AMP/(SQ-METER) AND,E16.4,16H WATT/(SQ-METER))
ISN 0120      C
ISN 0121      C
ISN 0122      RESTORE POTENTIAL DISTRIBUTION TO DIMENSIONAL VALUES
ISN 0123      C
ISN 0124      600   CONTINUE
ISN 0125      DO 700 K=1,KK
ISN 0126      DO 700 J=1,JJ
ISN 0127      DO 700 I=1,II
ISN 0128      VV(I,J,K)=VV(I,J,K)*TVOLTS
ISN 0129      700   CONTINUE
ISN 0130      RETURN
ISN 0131      END

```

COMPILER OPTIONS - NAME= MAIN,OPT=02,LINECNT=60,SIZE=0000K,
 SOURCE,EBCDIC,NOLIST,NODECK,LOAD,MAP,NOEDIT,NOIO,NOXREF
 ISN 0002 SUBROUTINE LIST(LST,IP)
 ISN 0003 COMMON/BK/IIM,IIP,JJM,JJP,KK,NTOT,IV,JV,II,JJ,H,N,VPC(30),
 1XYZ(2080,3),VV(30,20,10),XP(30),XMC(10),YP(20),YMC(10),ZZ(10),
 2XX(40),YY(30),ILX,IUX,KUK,MBC,MBD,VRF,NFPS,SKPRFL,SKPLST
 ISN 0004 COMMON/FLD/X(2080,2),COEF(2080,7),INDX(2080,6),SKPCO
 ISN 0005 DIMENSION KOUT(5),XOUT(5),YOUT(5),ZOUT(5)
 ISN 0006 DO 500 LINE=1,60
 ISN 0007 DO 200 NP=1,5
 ISN 0008 KP=LINE + (NP-1)*60 + (IP-1) * 300
 ISN 0009 IF(KP.GT.NTOT.AND.NP.EQ.1) RETURN
 ISN 0011 IF(KP.GT.NTOT) GO TO 300
 ISN 0013 NMAX=NP
 ISN 0014 KOUT(NP) = KP
 ISN 0015 IF(LST.EQ.1) XOUT(NP) = X(KP,1)
 ISN 0017 IF(LST.EQ.2) XOUT(NP) = XYZ(KP,1)
 ISN 0019 IF(LST.EQ.2) YOUT(NP)=XYZ(KP,2)
 ISN 0021 IF(LST.EQ.2) ZOUT(NP) = XYZ(KP,3)
 ISN 0023 200 CONTINUE
 ISN 0024 300 GO TO (400,450),LST
 ISN 0025 400 WRITE(M,1000) (KOUT(NP),XOUT(NP), NP=1,NMAX)
 ISN 0026 1000 FORMAT(5(I8,F16.8))
 ISN 0027 450 WRITE(M,3000) (KOUT(NP),XOUT(NP),YOUT(NP),ZOUT(NP),NP=1,NMAX)
 ISN 0028 3000 FORMAT(5(I8,3F6.2))
 ISN 0029 500 CONTINUE
 ISN 0030 500 RETURN
 ISN 0031 END
 ISN 0032

COMPILER OPTIONS - NAME= MAIN,OPT=02,LINECNT=60,SIZE=0000K,
 SOURCE,EBCDIC,NOLIST,NOECK,LOAD,MAP,NOEDIT,NOID,NOXREF

ISN 0002	C	SUBROUTINE RELAX POINT-SUCCESSIVE OVERRELAXATION METHOD COMMON/BK/IIM,ITP,JJM,JJP,KK,NTOT,IV,JV,II,JJ,M,N,VPC(30), 1XYZ(2080,3),VV(30,20,10),XP(30),XMC(10),YPC(20),YH(10),ZZ(10), 2XX(40),YY(30),ILX,IUX,KUK,MBC,MBD,VRF,NFPS,SKPRFL,SKPLST COMMON/FLD/X(2080,2),COEF(2080,7),INDX(2080,6),SKPCO	ORIGINAL PAGE IS OF POOR QUALITY
ISN 0003			
ISN 0004			
ISN 0005			
ISN 0006			
ISN 0007			
ISN 0008			
ISN 0009			
ISN 0010			
ISN 0011			
ISN 0012	200	IITR=0 IGO=1 ITR=ITR+1 DELTAM=0. DO 500 N=1,NTOT IF(X(N,2).EQ.1)GO TO 500 X1=X(N,1)	
ISN 0013	C	FN=COEF(N,1)/COEF(N,7) FS=COEF(N,2)/COEF(N,7) FE=COEF(N,3)/COEF(N,7) FW=COEF(N,4)/COEF(N,7) FU=COEF(N,5)/COEF(N,7) FD=COEF(N,6)/COEF(N,7)	
ISN 0014	C	NN=INDX(N,1) NS=INDX(N,2) NE=INDX(N,3) NW=INDX(N,4) NU=INDX(N,5) ND=INDX(N,6)	
ISN 0015	C	SUM=0. IF(NN.GT.0) SUM = SUM+FN*X(NN,1) IF(NS.GT.0) SUM = SUM+FS*X(NS,1) IF(NE.GT.0) SUM = SUM+FE*X(NE,1) IF(NW.GT.0) SUM = SUM+FW*X(NW,1) IF(ND.GT.0) SUM = SUM+FD*X(ND,1) IF(NU.GT.0) SUM = SUM+FU*X(NU,1)	
ISN 0016	C	X(N,1) = OMEGA*SUM+(1.-OMEGA)*X1 DELTA = ABS(X(N,1)-X1) IF(ABS(X1).GT.1.E-10) DELTA=ABS((X(N,1)-X1)/X1) IF(DELTAM.GT. DELTAM) DELTAM=DELTA CONTINUE IF(ITR.GT.ITMAX) WRITE(M,8888) ITR IF(ITR.GT.ITMAX) GO TO 700 FORMAT(//10H MORE THAN, I4,11H ITERATIONS) IPR=ITR/500 IF(IPR.LE.IPROLD) GO TO 600 IPROLD=IPR GO TO 800	
ISN 0017	C	600 IF(DELTAM.GT.EPS) GO TO 200	
ISN 0018	C	ITERATION FINISHED. PRINT AND EXIT.	

ISN 0061 C
ISN 0062 700 I60=2
ISN 0062 800 NFPP=(NTOT/300) +1
ISN 0063 DO 900 IP=1,NFPP
ISN 0064 WRITE(M,7777) ITR,EPS,DELTAM,OMEGA
ISN 0065 7777 FORMAT(1SH1SOLUTION AFTER,I6,2X,25HITERATIONS WITH TOLERANCE,
1 F12.8,8X,18HMAXIMUM DIFFERENCE,F12.8,8X,6HOMEGA=,F8.5)
ISN 0066 CALL LIST(1,IP)
ISN 0067 900 CONTINUE
ISN 0068 C
ISN 0069 1000 GO TO -600,1000),I60 IF(I60.EQ.1) GO TO 600
ISN 0070 RETURN
END

LEVEL 21.0 (JUN 74)

OS/360 FORTRAN H

DATE

COMPILER OPTIONS - NAME= MAIN,OPT=02,LINECNT=60,SIZE=0000K,
SOURCE,EBCDIC,NOLIST,NODECK,LOAD,MAP,NOEDIT,NOID,NOXREF

TSN 0002 SUBROUTINE FIND(I,J,K)
ISN 0003 COMMON/DK/IIM,IIP,JJM,JJP,KK,NTOT,IV,JV,II,JJ,N,N,VP(30),
1XYZ(2080,3),VV(30,20,10),XPC(30),XH(10),YP(20),YH(10),ZL(10),
2XX(40),YY(30),ILX,IUX,XUK,MBC,MBD,VRF,NFPS,SKPRFL,SKPLST
ISN 0004 IIJJ=II*JJ
ISN 0005 K=N/IIJJ+1
ISN 0006 IF(K .GE. 2 .AND. MOD(N,IIJJ) .EQ. 0) K=K-1
ISN 0008 NKIJ=N - IIJJ*(K-1)
ISN 0009 J=NKIJ/II+1
TSN 0010 IF(J .GE. 2 .AND. MOD(NKIJ,II) .EQ. 0) J=J-1
ISN 0012 I=NKIJ - II*(J-1)
ISN 0013 RETURN
ISN 0014 END

SYNTHESIS C JUN 14 3

OS/360 FORTRAN H

DATI

COMPILER OPTIONS - NAME= MAIN,OPT=02,LINECNT=60,SIZE=0000K,
SOURCE,EBCDIC,NOLIST,NODECK,LOAD,MAP,NOEDIT,NOID,NOXREF

ISN 0002 SUBROUTINE ARRAY
ISN 0003 COMMON/BK/IIM,IIP,JJM,JJP,KK,NDOT,IV,JV,II,JJ,R,N,VP(30),
1XYZ(2080,3),VV(30,20,10),XP(30),XH(10),YP(20),YH(10),ZZ(10),
2XX(40),YY(30),ILX,IUX,KUK,HBC,HBD,VRF,NFPS,SKPRFL,SKPLST
ISN 0004 COMMON/FLO/XC(2080,2),COEF(2080,7),INDX(2080,6),SKPCO
ISN 0005 COMMON/CCC/CN,CS,CE,CW,CU,CD,CC,NN,NS,NE,NW,NU,ND

C COEFFICIENT ARRAY = COEF(N,7), WHERE
COEF(N,1)=CN (NORTH=+Y NEIGHBOR)
COEF(N,2)=CS (SOUTH=-Y NEIGHBOR)
COEF(N,3)=CE (EAST=+X NEIGHBOR)
COEF(N,4)=CW (WEST=-X NEIGHBOR)
COEF(N,5)=CU (UP=+Z NEIGHBOR)
COEF(N,6)=CD (DOWN=-Z NEIGHBOR)
COEF(N,7)=CC (= CENTRAL POINT)

C SAVE COEFFICIENTS AND INDICES

ISN 0006 COEF(N,1)=CN
ISN 0007 COEF(N,2)=CS
ISN 0008 COEF(N,3)=CE
ISN 0009 COEF(N,4)=CW
ISN 0010 COEF(N,5)=CU
ISN 0011 COEF(N,6)=CD
ISN 0012 COEF(N,7)=CC

C
ISN 0013 INDX(N,1)=NN
ISN 0014 INDX(N,2)=NS
ISN 0015 INDX(N,3)=NE
ISN 0016 INDX(N,4)=NW
ISN 0017 INDX(N,5)=NU
ISN 0018 INDX(N,6)=ND
ISN 0019 IF(SKPCO.EQ.1) GO TO 20
ISN 0020 WRITE(M,1000) ND,CD,NS,CS,NW,CW,N,CC,NE,CE,NN,CN,NU,CU
JSN 0021 1000 FORMAT(/7(1X,1HC,I4,2H)=,1PE10.4))
ISN 0022 20 CONTINUE
ISN 0023 RETURN
ISN 0024 END
ISN 0025

COMPILER OPTIONS - NAME= MAIN,OPT=02,LINECNT=60,SIZE=0000K,
 SOURCE,EBCDIC,NOLIST,NODECK,LOAD,MAP,NOEDIT,NOID,NOXREF

```

ISN 0002      SUBROUTINE CUD(MP,C,A)
ISN 0003      COMMON/BK/IIM,IIP,JJM,JJP,KK,NTOT,IV,JV,II,JJ,M,N,VP(30),
               1XYZ(2080,3),VV(30,20,10),XP(30),XM(10),YP(20),YM(10),ZL(10),
               2XX(40),YY(30),ILX,IUX,KUK,HBC,M8D,VRF,NFPS,SKPRFL,SKPLST
ISN 0004      COMMON/CCC/CN,CS,CE,CW,CU,CD,CC,NN,NS,NE,NW,NU,ND
ISN 0005      NF(IX,JX,XX) = IX+II*(JX-1) + II*JJ*(KX-1)
ISN 0006      A=0.
ISN 0007      C=0.
ISN 0008      CALL FIND(I,J,K)
ISN 0009      IF(I .EQ. 1) GO TO 100
ISN 0011      IF(I .EQ. II) GO TO 200
ISN 0013      NH=NF(I+1,J,K)
ISN 0014      NL=NF(I-1,J,K)
ISN 0015      DX=XYZ(NH,1) - XYZ(NL,1)
ISN 0016      GO TO 300
ISN 0017      NH=NF(2,J,K)
ISN 0018      DX=XYZ(NH,1) - XYZ(N,1)
ISN 0019      GO TO 300
ISN 0020      NL=NF(II-1,J,K)
ISN 0021      DX=XYZ(N,1) - XYZ(NL,1)
ISN 0022      CONTINUE
ISN 0023      IF(J .EQ. 1) GO TO 400
ISN 0025      IF(J .EQ. JJ) GO TO 500
ISN 0027      NH=NF(I,J+1,K)
ISN 0028      NL=NF(I,J-1,K)
ISN 0029      DY=XYZ(NH,2) - XYZ(NL,2)
ISN 0030      GO TO 600
ISN 0031      NH=NF(I,2,K)
ISN 0032      DY=XYZ(NH,2) - XYZ(N,2)
ISN 0033      GO TO 600
ISN 0034      NL=NF(I,JJ-1,K)
ISN 0035      DY=XYZ(N,2) - XYZ(NL,2)
ISN 0036      600      A=DX*DY/4.
ISN 0037      IF(MP .EQ. 1) GO TO 700
ISN 0039      IF(MP .EQ. 2) GO TO 800
ISN 0041      RETURN
ISN 0042      NU=0
ISN 0043      IF(K .EQ. KK) RETURN
ISN 0045      NH=NF(I,J,K+1)
ISN 0046      NU=NH
ISN 0047      DZ=XYZ(NH,3) - XYZ(N,3)
ISN 0048      GO TO 900
ISN 0049      ND=0
ISN 0050      IF(K .EQ. 1) RETURN
ISN 0052      NL=NF(I,J,K-1)
ISN 0053      ND=NL
ISN 0054      DZ=XYZ(N,3) - XYZ(NL,3)
ISN 0055      C=A/DZ
ISN 0056      RETURN
ISN 0057      END
  
```

DATA MAINTENANCE IS
THE FLOOR QUALITY

COMPILER OPTIONS - NAME= MAIN,OPT=02,LINECNT=60,SIZE=0000K,
 SOURCE,ERCOIC,NOLIST,NOODECK,LOAD,MAP,NOEDIT,NOID,NOXREF

ISN 0002 SUBROUTINE CEW(CMP,C,A)

ISN 0003 COMMON/BK/IIM,IIP,JJM,JJP,KK,NTOT,IV,JV,II,JJ,M,N,VPC(30),
 1XYZ(2080,3),VV(30,20,10),XPC(30),XMC(10),YPC(20),YMC(10),ZZ(10),
 2XX(40),YY(30),ILX,IUX,KUK,XBC,MBD,VRF,NFPS,SKPRFL,SKPLST

ISN 0004 COMMON/CCC/CN,CS,CE,CW,CU,CD,CC,NN,NS,NE,NW,NU,ND
 NF(IX,JX,KX)= IX+ II*(JX-1) + II*JJ*(KX-1)

ISN 0005

ISN 0006

ISN 0007

ISN 0008

ISN 0009

ISN 0011

ISN 0013

ISN 0014

ISN 0015

ISN 0016

ISN 0017

ISN 0018

ISN 0019

ISN 0020

ISN 0021

ISN 0022

ISN 0023

ISN 0025

ISN 0027

ISN 0028

ISN 0029

ISN 0030

ISN 0031

ISN 0032

ISN 0033

ISN 0034

ISN 0035

ISN 0036

ISN 0037

ISN 0039

ISN 0041

ISN 0042

ISN 0043

ISN 0045

ISN 0046

ISN 0047

ISN 0048

ISN 0049

ISN 0050

ISN 0052

ISN 0053

ISN 0054

ISN 0055

ISN 0056

ISN 0057

 A=0.

 C=0.

 CALL FIND(I,J,K)

 IF(J.EQ.1) GO TO 100

 IF(J.EQ.JJ) GO TO 200

 NH=NF(I,J+1,K)

 NL=NF(I,J-1,K)

 DY=XYZ(NH,2) - XYZ(NL,2)

 GO TO 300

100 NR=NF(I,2,K)

 DY=XYZ(NH,2) - XYZ(N,2)

 GO TO 300

200 NL=NF(I,JJ-1,K)

 DY=XYZ(N,2) - XYZ(NL,2)

300 CONTINUE

 IF(K.EQ.1) GO TO 400

 IF(K.EQ.KK) GO TO 500

 NH=NF(I,J,K+1)

 NL=NF(I,J,K-1)

 DZ=XYZ(NH,3) - XYZ(NL,3)

 GO TO 600

400 NH=NF(I,J,2)

 DZ=XYZ(NH,3) - XYZ(N,3)

 GO TO 600

500 NL=NF(I,J,KK-1)

 DZ=XYZ(N,3) - XYZ(NL,3)

600 A=DY*DZ/4.

 IF(CMP.EQ.1) GO TO 700

 IF(CMP.EQ.2) GO TO 800

 RETURN

700 NE=0

 IF(I.EQ.II) RETURN

 NH=NF(I+1,J,K)

 NE=NH

 DX=XYZ(NH,1) - XYZ(N,1)

 GO TO 900

800 NW=0

 IF(I.EQ.1) RETURN

 NL=NF(I-1,J,K)

 NW=NL

 DX=XYZ(N,1) - XYZ(NL,1)

 C=A/DX

 RETURN

900 END

COMPILER OPTIONS = NAME= MAIN,OPT=02,LINECNT=60,SIZE=0000K,
 SOURCE,EBCDIC,NOLIST,NODECK,LOAD,MAP,NOEDIT,NOIO,NOXREF

ISN 0002 SUBROUTINE CNS(CP,C,A)
 ISN 0003 COMMON/BK/IIM,LIP,JJM,JJP,KK,NTDT,IV,JV,II,JJ,H,N,VPC(30),
 1XYZ(2080,3),VVC(30,20,10),XPC(30),XMC(10),YP(20),YM(10),ZZ(10),
 2XX(40),YY(30),ILX,IUX,KUK,HBC,MBD,VRF,NFPS,SKPRFL,SKPLST
 COMMON/CCC/CN,CS,CE,CW,CU,CD,CC,NN,NS,NE,NW,NU,NO
 NFC(IX,JX,KX)=IX+II*(JX-1)+II*JJ*(KX-1)

ISN 0004 A=0.
 ISN 0005 C=0.
 ISN 0006 CALL FIND(I,J,K)
 ISN 0007 IF(I.EQ.1) GO TO 100
 ISN 0008 IF(I.EQ.II) GO TO 200
 ISN 0009 NH=NFC(I+1,J,K)
 ISN 0010 NL=NFC(I-1,J,K)
 ISN 0011 DX=XYZ(NH,1) - XYZ(NL,1)
 ISN 0012 GO TO 300
 ISN 0013 NH=NFC(2,J,K)
 ISN 0014 DX=XYZ(NH,1) - XYZ(N,1)
 ISN 0015 GO TO 300
 ISN 0016 NL=NFC(II-1,J,K)
 ISN 0017 DX=XYZ(N,1) - XYZ(NL,1)
 ISN 0018 CONTINUE
 ISN 0019 IF(K.EQ.1) GO TO 400
 ISN 0020 IF(K.EQ.KK),GO TO 500
 ISN 0021 NH=NFC(I,J,K+1)
 ISN 0022 NL=NFC(I,J,K-1)
 ISN 0023 DZ=XYZ(NH,3) - XYZ(NL,3)
 ISN 0024 GO TO 600
 ISN 0025 NH=NFC(I,J,2)
 ISN 0026 DZ=XYZ(NH,3) - XYZ(N,3)
 ISN 0027 GO TO 600
 ISN 0028 NL=NFC(I,J,KK-1)
 ISN 0029 DZ=XYZ(N,3) - XYZ(NL,3)
 ISN 0030 A=DX*DZ/4.
 ISN 0031 IF(CMP.EQ.1) GO TO 700
 ISN 0032 IF(CMP.EQ.2) GO TO 800
 ISN 0033 RETURN
 ISN 0034 NN=0
 ISN 0035 IF(CJ.EQ.JJ) RETURN
 ISN 0036 NH=NFC(I,J+1,K)
 ISN 0037 NN=NH
 ISN 0038 DY=XYZ(NH,2) - XYZ(N,2)
 ISN 0039 GO TO 900
 ISN 0040 NS=0
 ISN 0041 IF(CJ.EQ.1) RETURN
 ISN 0042 NL=NFC(I,J-1,K)
 ISN 0043 NS=NL
 ISN 0044 DY=XYZ(N,2) - XYZ(NL,2)
 ISN 0045 C=A/DY
 ISN 0046 RETURN
 ISN 0047 END

COMPILER OPTIONS - NAME= MAIN,OPT=02,LINECNT=60,SIZE=0000K,
 SOURCE,EBCDIC,NOLIST,NOECK,LOAD,HAP,NOEDIT,NOID,NOXREF

TSN 0002 C
 SUBROUTINE FIELD

C CONSTRUCTION OF COEFFICIENTS (MATRIX ELEMENTS)
 C IN LINEAR DIFFERENCE EQUATIONS
 C SOLUTION BY OVEPRELAXATION

ISN 0003 COMMON/BK/IIM,IIP,JJM,JJP,KK,NTOT,IV,JV,II,JJ,M,N,YP(30),
 IXYZ(2080,3),VVC(30,20,10),XPC(30),XMC(10),YP(20),YHC(10),ZZ(10),
 2XX(40),YY(30),ILX,IUX,KUK,MBC,MBD,VRF,NFPS,SKPRFL,SKPLST

ISN 0004 COMMON/FLD/X(2080,2),CUEF(2080,7),INDX(2080,6),SKPC0

ISN 0005 COMMON/CCC/CN,CS,CE,CW,CU,CD,CC,NN,NS,NE,NW,NU,ND

ISN 0006 C
 INTEGER OO,ON//NORT//,OS//SOUT//,OE//EAST//,OW//WEST//,
 1 OU//UP //,OD//DOWN//
 C ASSUME ASYMPTOTIC MONPOLE AT INFINITY

ISN 0007 C
 ALPHAF(UUU)=ABSC(UUU/RS)

ISN 0008 C
 NDO=POSITIVE FOR DIAGNOSTIC OUTPUT
 NDO=0

ISN 0009 C
 WRITE(M,1000)

ISN 0010 1000 FORMAT(IH1/18HCFIELD CALCULATION)

ISN 0011 C
 WRITE(M,2000)

ISN 0012 2000 FORMAT(//1X,17HCOEFFICIENT ARRAY)

ISN 0013 X0=.5*XP(IV)

ISN 0014 Y0=.5*YP(JV)

ISN 0015 ZOLD=0.

ISN 0016 DO 600 N=1,NTOT

ISN 0017 RS=(XYZ(N,1)-X0)**2 +(XYZ(N,2)-Y0)**2 +XYZ(N,3)**2

ISN 0018 CALL FIND(I,J,K)

TSN 0019 IF(ZZ(K).LE.ZOLD.AND.N.GT.1) GO TO 200

TSN 0021 ZOLD=ZZ(K)

TSN 0022 WRITE(M,3000) K,ZZ(K)

ISN 0023 3000 FORMAT(//1X,2HZC,I2,2H)=,F6.3/
 1 12X,1HD,17X,1HS,17X,1HW,17X,1HC,17X,1HE,17X,1HN,17X,1HU)

ISN 0024 200 CC=0.

C MODIFICATION TO SOLVE HELMHOLTZ EQUATION USING LINEARIZED SPACE
 C CHARGE. HELM = DEBYE-LENGTH-LIKE PARAMETER. (ASSUMES POTEN-
 C TIALS ARE DIMENSIONLESS)

ISN 0025 C
 HELM=0.0

TSN 0026 VOLSQ=1.

ISN 0027 DO 300 MP=1,2

ISN 0028 CALL CNS(MP,C,AREA)

ISN 0029 IF (MP.EQ.1) OO=ON

ISN 0031 IF (MP.EQ.2) OO=OS

ISN 0033 IF (NDO.GT.0) WRITE (M,888) N,I,J,K,OO,AREA,C

ISN 0035 888 FORMAT(IX,18HN,I,J,K,OO,AREA,C=,I4,2X,3I3,1X,A5,1P2E16.4)

ISN 0036 CC=CC+C

ISN 0037 IF(C.GT.0.) GO TO 250

ISN 0039 YYY=XYZ(N,2)-Y0

ISN 0040 ALPHA=ALPHAF(YYY)

ISN 0041 IF (NDO.GT.0) WRITE (M,999) N,I,J,K,ALPHA

ISN 0043 999 FORMAT(IX,14HN,I,J,K,ALPHA=,I4,2X,3I3,1PE16.4)

```

ISN 0044      CC=CC+AREA*ALPHAF(YYY)
ISN 0045      IF(MP.EQ.1) CN=C
ISN 0047      IF(MP.EQ.2) CS=C
ISN 0049      300 CONTINUE
ISN 0050      VOLSQ=VOLSO*AREA
ISN 0051      DO 400 MP=1,2
ISN 0052      CALL CEW(MP,C,AREA)
ISN 0053      IF (MP.EQ.1) DD=OE
ISN 0054      IF (MP.EQ.2) DD=OW
ISN 0055      IF (NDO.GT.0) WRITE (M,888) N,I,J,K,DD,AREA,C
ISN 0056      CC=CC+C
ISN 0057      IF(CC.GT.0.) GO TO 350
ISN 0058      XXX=XYZ(N,1)-X0
ISN 0059      ALPHA=ALPHAF(XXX)
ISN 0060      IF (NDO.GT.0) WRITE (M,999) N,I,J,K,ALPHA
ISN 0061      CC=CC+AREA*ALPHAF(XXX)
ISN 0062      IF(MP.EQ.1) CE=C
ISN 0063      IF(MP.EQ.2) CW=C
ISN 0064      350 CONTINUE
ISN 0065      VOLSQ=VOLSO*AREA
ISN 0066      DO 500 MP=1,2
ISN 0067      CALL CUD(MP,C,AREA)
ISN 0068      IF (MP.EQ.1) DD=OU
ISN 0069      IF (MP.EQ.2) DD=OO
ISN 0070      IF (NDO.GT.0) WRITE (M,888) N,I,J,K,DD,AREA,C
ISN 0071      CC=CC+C
ISN 0072      IF(CC.GT.0..OR.(C.EQ.0..AND.MP.EQ.2))GO TO 450
ISN 0073      ALPHA=ALPHAF(XYZ(N,3))
ISN 0074      IF (NDO.GT.0) WRITE (M,999) N,I,J,K,ALPHA
ISN 0075      CC=CC+AREA*ALPHAF(XYZ(N,3))
ISN 0076      IF(MP.EQ.1) CU=C
ISN 0077      IF(MP.EQ.2) CD=C
ISN 0078      450 CONTINUE
ISN 0079      VOLSQ=VOLSO*AREA
ISN 0080      VOL=SQRT(VOLSO)
ISN 0081      IF(HELM.GT.0.) CC=CC+VOL/HELM**2
ISN 0082      CALL ARRAY
ISN 0083      500 CONTINUE
ISN 0084      VOLSQ=VOLSO*AREA
ISN 0085      VOL=SQRT(VOLSO)
ISN 0086      IF(HELM.GT.0.) CC=CC+VOL/HELM**2
ISN 0087      CALL ARRAY
ISN 0088      600 CONTINUE
ISN 0089      C
ISN 0090      CALL RELAX.
ISN 0091      RETURN
ISN 0092      END
ISN 0093
ISN 0094
ISN 0095
ISN 0096
ISN 0097
ISN 0098
ISN 0099
ISN 0100
ISN 0101

```

COMPILER OPTIONS - NAME= MAIN,OPT=02,LINECNT=60,SIZE=0000K,
SOURCE,EBCDIC,NOLIST,NODECK,LOAD,MAP,NOEDIT,NOID,NOXREF
ISN 0002 BLOCK DATA
ISN 0003 COMMON/CD/PVOLTS,XMACH,DENST,NN,PARTCL(2),PART1(2),PART2(2)
ISN 0004 REAL PART1//IONS:,/,/,PART2//ELEC/,TRON//
ISN 0005 END

Appendix B

Computer Programs: Electric Fields Produced by Cloud-to-Ground Lightning Flashes

The following four pages contain a listing of the computer programs written to compute the electric field produced on the ground as a function of time and distance from "ground zero" by the charges associated with a cloud-to-ground lightning flash. This program was written by Jerry L. Bohannon.

```

TITLE CLOUD-TO-GROUND SIMULATION
BATCH
LAE= STROKE
JBUG
IMPLICIT INTEGER*2 ( I-N )
DIMENSION RSI(2,10),RSIS(2,10)
DATA TPIE/5.56062E-11/,TIPIM/2.0E-7/
DATA ICARDS/''C'',ITERM/''T'',IY/''Y'',LN/''N''/
DATA IMA/X''1D15'',ICY/X''1D16'',IBEL/X''0707'',PBG/X''1E10''/
DATA IRD/X''1D11'',IGR/X''1D12'',IYE/X''1D13'',EBL/X''1D14''/
DATA IA7N/X''0E'',IA7F/X''0F'',NULL/X''00'',IHOMB/X''08''/
DATA IBGY/X''1E13''/
DATA RSI(1,1)/0.0/,RSI(2,1)/0.0/,RSI(2,10)/0.0/
DATA PIE/3.1415926/
DATA RH0/2.0E-9/
CROOT=1./3.
WRITE(14,1) :
FORMAT(14,1)
DO 1000 I=1,32000
100 K=1
WRITE(14,4) (IA7N,IMA,IBEL,IA7F
FORMAT(2A2,'LIGHTNING BOLT SIMULATION',ROI'',2A2)
) WRITE(14,11) IBL,IGR
L FORMAT(A2,'READ DATA FROM CARDS OR TERMINAL',A2)
READ(15,12) :IWHERE
FORMAT(A1)
:IF(IWHERE.EQ.1CARDS)GOTO 50
:IF(IWHERE.EQ.2ITERM)GOTO 70
WRITE(14,14) IRD,IGR
FORMAT(A2,'TRY AGAIN',A2)
GOTO 10
) READ(1,51,END=999) Y0,QCL,QL,VSL,IVRS,(RSI(L,J),I=1,2),J=2,9)
FORMAT(5(F6.0,2X)/8(2F10.0))
90 GOTO 90
WRITE(14,71) IMA
FORMAT(A2,'ENTER FLOATING POINT INITIAL CONDITIONS F6.0')
WRITE(14,75) IBL,ICY
FORMAT(A2,'INITIAL HEIGHT KM',A2)
READ(15,73) IY0
WRITE(14,76) IBL,ICY
FORMAT(A2,'CLOUD CHARGE , COUL',A2)
READ(15,73) IQCL
WRITE(14,72) IBL,ICY
FORMAT(A2,'STEPPED LEADER CHARGE COUL',A2)
READ(15,73) IQSL
FORMAT(F6.0)
WRITE(14,74) IBL,ICY
FORMAT(A2,'STEPPED LEADER VELOCITY E5 M/S',A2)
READ(15,73) IVSL
WRITE(14,77) IBL,ICY
FORMAT(A2,'RETURN STROKE VELOCITY E7 M/S',A2)
READ(15,73) IVRS
WRITE(14,80) IBL,ICY
FORMAT(A2,'ENTER 8 TIMES (MS) AND CURRENTS (KAMP) TO DEFINE THE RETURN STROKE 2F10.0',A2)
DO 82 J=2,9
READ(15,81) RSI(1,J),RSI(2,J)
IF(RSI(1,J).LT.0.)GOTO 78
CONTINUE

```

ORIGINAL PAGE IS
OF POOR QUALITY

```

81  :FORMAT(2F10_0)
90  VSL=VSL
RSI(1,10)=RSI(1,9)
DO 1002 J=1,10
RSIS(1,J)=RSI(1,J)
RSIS(2,J)=RSI(2,J)
RSIG1,J)=RSI(1,J)/1000.
PSI(2,J)=RSI(2,J)*1000.
1002 :CONTINUE
:QCL=-QCL
QSL=-QSL
!YOS=Y0
RAD=(0.75*ABS(QCL)/RH0/P[E])**CROOT
DO 1005 I=2,9
A=RSI(2,I)
B=RSI(2,I-1)
C=RSI(2,I+1)
IF(A.GT.B.AND.A.GT.C) IQ,T=I
1005 :CONTINUE
VRSS=VRS
00  VSL=-VSL*1.0E5
.Y0=Y0*1000.0
IVRS=VRS*1.0E7
.DTSL=1.0E-4
05  WRITE(14,110) IBL,ICY
10  FORMAT(A2,"WHAT IS RADIUS",A2)
READ(15,73) ID
WRITE(13,111) IRD,IBGY
11  FORMAT(2A2//1")
DO 1001 I=1,32000
001 K=I
WRITE(13,149)
149 FORMAT(1X,"SI UNITS//")
50  !WRITE(13,150) YOS,QCL,QSL,VSL,VRSS,RSIS,D
51  FORMAT(1X,"HEIGHT=",F7.10," KM/1X,""Q-CLOUD=","F7.1," C/
$1X,"Q-LEADER=","F6.1," C,"/1X,"V-LEADER=","F6.1," E5 M/S/"1X,
$"V-RETURN=","F6.1," E7. M/S/"1X," RETURN STROKE MS. KAMP"/
$1,(2F10_4//1"IX,"RADIUS=","F6.0," M"//1")
WRITE(13,152) IRG,IRD
52  FORMAT(1X,
$A2,"X="T",15X,"E",15X,"Q",16X,"H",A2)
T=0.0
SLRY2=1.0/(D*D+Y0*Y0)
SLRY=SQRT(SLRY2)
YC=Y0+RAD
SLRQC2=1.0/(D*D+YC*YC)
SLRQCL=SQRT(SLRQC2)*SLRQC2
DI=1.0/D
X=Y0
EMAX=0.0
CONTINUE
:SLRX2=1.0/(D*D+X*X)
SLRX=SQRT(SLRX2)
SLRX32=SLRX*SLRX2
E=QSL/TPIE/Y0*(SLRY-SLRY)+SLRCCL*YC/TPIE*(QCL-QSL+(1.-X/Y0))
IF(ABS(E).GT.ABS(EMAX)) EMAX=E
IF(ABS(E).LT.5.0E4) GOTO 211
WRITE(13,210) T,E,X
0  FORMAT(F16.7, F16.0, 16X, F16.1)

```

```

215 FORMAT(F16.7, F16.0, F16.15, F16.1, 110, F16.7, F16.0)
211 IF(ABS(E).LT.1.0E4.0R.X.GT.0.5E3) DTSL=1.0E-3
    T=T+DTSL
    IF(X.LT.50.) GOTO 50
    X=Y0+VSL*T
    IF(X.LT.0.0) GOTO 50:
    DTSL=1.0E-4 :
    GOTO 200
500 !CONTINUE
    T=T+DTSL
    WRITE(13,501)
501 FORMAT(1X,"   ")
    ESL=E
    QRC=QSL-QCL :
    PL=-QSL/Y0
    SLRY03=YC*SLRQCL
    KRNT=1
    RI=0.0
    ITR=0.0
    KOLD=0
    Q=0.0
10 !CONTINUE
    CALL CURENT(IRSI,Q,DT,TR,IRI,KRNT,KOLD)
    IF(RI.LE.0.0) GOTO 60
    T=T+DT
    Y=YRS*TR
    IF(Y.GT.Y0) GOTO 522
    P=Q/Y
    SLRYR=1.0/SQRT(D+D+Y*Y)
    E=ESL+P*(DI-SLRYR)/TPIE
    IF(ABS(E).GT.ABS(EMAX)) .EMAX=E
    IF(IOT.LT.KRNT.AND.ABS(E).LT.5.0E4) GOTO 510
    WRITE(13,215) T,E,Q,Y,KRNT,ITR,RI
    GOTO 510
22 !WRITE(13,501)
20 !CONTINUE
    P=Q/Y0
    IF(P.GT.PL) GOTO 572
    E=ESL+P*(DI-SLRY)/TPIE
    IF(ABS(E).GT.ABS(EMAX)) .EMAX=E
    IF(IOT.LT.KRNT.AND.ABS(E).LT.5.0E4) GOTO 521
    WRITE(13,215) T,E,Q,Y0,KRNT,ITR,RI
11 !CALL CURENT(IRSI,Q,DT,TR,IRI,KRNT,KOLD)
    IF(RI.LE.0.0) GOTO 60
    T=T+DT
    GOTO 520
2 !WRITE(13,501)
3 !CONTINUE
    QRS=Q+QSL
    IF(QRS.GT.QRC) GOTO 1600
    E=ESL+PL*(DI-SLRY)/TPIE+QRS*SLRY03/TPIE :
    IF(ABS(E).GT.ABS(EMAX)) .EMAX=E
    IF(IOT.LT.KRNT.AND.ABS(E).LT.5.0E4) GOTO 571
    WRITE(13,215) T,E,Q,Y0,KRNT,ITR,RI
1 !CALL CURENT(IRSI,Q,DT,TR,IRI,KRNT,KOLD)
    IF(RI.LE.0.0) GOTO 60
    T=T+DT
    GOTO 570
    WRITE(13,599) Q,EMAX

```

ORIGINAL PAGE IS
OF POOR QUALITY

```

79  FORMAT(//1X,"CRT= ",F10.14," C= 5X,"EMAX= ",E12.4," V/M")
80  WRITE(14,601) IBC,IBL,IGR,IBEL
81  FORMAT(2A2," DO YOU WANT ANOTHER RADIUS",2A2)
82  READ(15,12) :IAD
83  IF(IAD.EQ.1Y) GOTO 1.5
84  IF(IAD.EQ.1N) GOTO 650
85  WRITE(14,14) IRD,IGR,
86  GOTO 602
87  WRITE(14,651) IBL,IGR
88  FORMAT(A2," DO YOU WANT ANOTHER EVENT",A2)
89  READ(15,12) :IE
90  IF(IE.EQ.1YY) GOTO 13
91  IF(IE.EQ.1NN) GOTO 95,
92  WRITE(14,14) IRD,IGR
93  GOTO 652
94  WRITE(14,998) IRD
95  FORMAT(A2,"NO MORE CARDS")
96  WRITE(14,951) :MA,IGR
97  FORMAT(A2,"END OF PROGRAM",A2)
98  STOP 1
99  END
A8= CURENT
BUG
SUBROUTINE CURENT(RSI,Q,DT,TR,RI,KRNT,KOLD)
IMPLICIT INTEGER *2 (I-N)
DIMENSION RSI(2,100)
IF(KOLD.EQ.KRNT) GOTO 50
TAU=RSI(1,KRNT+1)-RSI(1,KRNT)
IF(TAU.LE.0.0) GOTO 1100
IF(TAU.LE.1.0E-5) DT=0.5E-6
IF(TAU.GT.1.0E-5.AND.TAU.LE.1.0E-4) DT=1.0E-5
IF(TAU.GT.1.0E-4.AND.TAU.LE.1.0E-3) DT=1.0E-4
IF(TAU.GT.1.0E-3.AND.TAU.LE.1.0E-2) DT=1.0E-3
IF(TAU.GT.1.0E-2.AND.TAU.LE.1.0E-1) DT=1.0E-2
IF(TAU.GT.1.0E-1) DT=0.025
DEL=(RSI(2,KRNT+1)-RSI(2,KRNT))/TAU
IF(QEQ.0.0) RI1=0.0
TRR=TR+DT
IF(TRR.GT.RSI(1,KRNT+1)) DT=RSI(1,KRNT+1)-TR
RI=RI+DELI+DT
RI2=RI
Q=Q+DT*(RI2+RI1)/2.
TR=TR+DT
KOLD=KRNT
IF(IR.GE.RSI(1,KRNT+1)) IKRNT=KRNT+1
RI1=RI2
RETURN
CONTINUE
RI=0.0
RETURN
END

```

Appendix C

Computer Output Listing: Cloud-to-Ground Lightning Flash Density

The following seven pages are the computed output from the program that calculates the lightning flash density (cloud-to-ground) from the monthly thunderstorm days using the Pierce Conversion. This program, written by Jerry L. Bohannon, uses the Normals, Means and Extremes data from "Local Climatological Data -- Annual Summaries for 1977" published by the National Oceanic and Atmospheric Administration, Environmental Data Service, Asheville, North Carolina (available also on magnetic tape).

```

      T03NCPOT [0]?
      ♦ AARF+HID COMPUTE POT HI

[1] A THIS FUNCTION COMPUTES THE ELECTRIC POTENTIAL IN A REGION AROUND
[2] A ONE BILLBOARD OF THE RESTERA, THE MEASUREMENT AREA STARTS 31.96 METERS
[3] A FROM THE LEFT HAND EDGE OF THE RECTANGA AND EXTENDS TO THE RIGHT 'AC' METERS,
[4] A THE BOTTOM OF THE MEASUREMENT AREA IS AT GROUND LEVEL, WHILE THE TOP
[5] A IS 'UP' METERS HIGH,
[6] A THE RESOLUTION IS CONTROLLED BY THE ARGUMENTS OF THE FUNCTION, THE
[7] A LEFT ARGUMENT SPECIFIES THE NUMBER OF COLUMNS IN THE OUTPUT, THE RIGHT
[8] A ARGUMENT IS THE NUMBER OF ROWS,
[9] A THE FORMAT OF THE OUTPUT IS AN ARRAY OF NUMBERS IN SCIENTIFIC NOTATION
[10] A WITH ONLY ONE SIGNIFICANT DIGIT PRINTED,
[11] POT+(HI,HID)/0
[12] DPF+1
[13] R+R+1
[14] LOOPH;H|+(0-1)xUP+HI-1
[15] R+1
[16] LOOPL;L1+31.96+(R-1)xAC+HID-1
[17] PCT[0|R]+L1 FIELD HI
[18] R+R+1
[19] +(R|HID)/LOOPL
[20] DPF+1
[21] +(0|HI)/LOOPH
[22] TRY+TRY+1
[23] DATA1#3#DT5.
[24] 'THIS IS RUH NUMBER ',(TRY),DATE
[25] 'THE CALCULATED VALUES OF THE ELECTRIC POTENTIAL, IN VOLTS, ARE SHOWN BELOW,'
[26]
[27]
[28] AARF+HID COMPUTE POT
[29] 5#DAY[201].
[30] DPF+10
[31] 'THE VECTOR OF LINE CHARGES USED IS,,, ','(LA),' COULOMBS PER METER,'
[32] 'THE SUM OF THE LINE CHARGES IS ','(++/LA),' COULOMBS PER METER,'
[33] 'THE TOP OF THE MEASUREMENT ARRAY IS ','(UP),' METERS HIGH,'
[34] 'THE RIGHT EDGE OF THE ARRAY IS ','(R|),' METERS FROM THE FIRST BILLBOARD,'
[35] 'THERE ARE ','(AC+HID),' COLUMNS PER METER, AND ','(UP+HT),' ROWS PER METER IN THE ARRAY,'
[36] 'RUH NO. ','(TRY),DATE
[37] DPF+1
[38] 5#DAY[201]
[39] +(SIGN=0)/0
[40] 'THE ARRAY BELOW SHOWS THE SIGN OF EACH OF THE NUMBERS IN THE ABOVE ARRAY,'
[41]
[42] XPOT
[43] 'THIS IS RUH NUMBER ',(TRY),DATE
?
```

PROTECT [0]9
9 MID PROTECT HI

[1] A THIS FUNCTION COMPUTES THE ELECTRIC POTENTIAL IN A REGION OF SPACE
[2] A DUE TO A CHARGED WIRE LOCATED SOME FIXED PERPENDICULAR DISTANCE FROM
[3] A THE TOP OF EACH BILLBOARD OF THE ANTENNA, THE MEASUREMENT AREA IS
[4] A EXACTLY THE SAME AS THAT USED IN ((COMPUFOT)), AS WITH ((COMPUFOT))
[5] A THE RESOLUTION IS DETERMINED BY THE ARGUMENTS OF THE FUNCTION,
[6] A THE FUNCTION DOES NOT PRINT ANY OUTPUT, THE OUTPUT IS CONTAINED IN
[7] A THE VARIABLE, ((PROT)), THIS VARIABLE WILL HAVE THE SAME DIMENSIONS AS
[8] A ((POT)), THE VARIABLE CONTAINING THE OUTPUT FROM ((COMPUFOT)),
[9] PROT(HI,WID)~0

[10] 01+R1+1

[11] A ((LOOPH)) COMPUTES ALL OF THE VERTICAL INDICES,

[12] LOOPH;H2-(01-1)*UP+HI-1

[13] R1+1

[14] A ((LOOPL)) COMPUTES THE HORIZONTAL INDICES AND CALLS ((FIELDW)),

[15] LOOPL;L2=31,96+(R1-1)*AC+4*ID-1

[16] PROT[S1][A1]+L2 FIELDW H2

[17] R1+R1+1

[18] +(R1*WID)/LOOPH

[19] 01+01+1

[20] +(01*HI)/LOOPH

[21] PROTECT

[22] TRY1-TRY1+1

[23] 'THIS IS FOR NUMBER ',(TRY1),' OF PROTECT',DATE

[24] DFPH10

[25] 'THE PROTECTING WIRE IS LOCATED ',(W1),' METERS FRONT THE'

[26] 'LEFT EDGE OF THE ARRAY, AND ',(S1XX1),' METERS FROM THE BOTTOM.'

9

```

?FIELD [0]?
? UHL+L FIELD H
[1] R THIS FUNCTION COMPUTES THE ELECTRIC POTENTIAL AT ANY POINT, (L,H)
[2] R IN THE SPACE AROUND THE ARRAY OF FIVE BILLBOARDS,
[3] R LI=15.93x^-1+N
[4] R H=(9.38x10)^-6x/LA
[5] S+3e32+9
[6] A=L-XJ
[7] I+1-
[8] UI+H/0
[9] BBLOOP;HH+=((H-SX/J)x2)+HA+(A-LI[I])x2
[10] DM=((H+SX/J)x2)+HA
[11] UI[I]+/-((LA+0.2x50)x2)(HH+DM)x0.5
[12] I+1+
[13] +(I(H+1))/BBLOOP
[14] UHL+=("100000xH)++/UI
    +

```

```

?FIELDW [0]?
? P+L FIELD H
[1] R THIS FUNCTION COMPUTES THE ELECTRIC POTENTIAL AT ANY POINT, (L,H),
[2] R DUE TO THE CHARGED PROTECTION WIRE ABOVE THE BILLBOARD, THIS WIRE IS
[3] R ASSUMED TO BE PARALLEL TO THE BILLBOARD AND LOCATED A PERPENDICULAR
[4] R DISTANCE, ((SPACE)), FROM THE TCF OF THE BILLBOARD,
[5] R THE CHARGE ON THE WIRE IS ((LW)),
[6] R LI+=15.93x^-1+N
[7] R H+=LW+LW
[8] R LONG+=12.24x23THTA+=30(+12,24)xSPACE
[9] R XJ1+=XJ1+LONGx20THTA+02-9
[10] S1+=9(02+9)+THTA
[11] R1+=L-XJ1
[12] I+1
[13] UI1+H/0
[14] LLOOP;WH1+=((H-S1xXJ1)x2)+HA1+(S1-LI1[I])x2
[15] DM1=((H+S1xXJ1)x2)+HA1
[16] UI1[I]+/-((LW+0.2x50)x2)(WH1+DM1)x0.5
[17] I+1+
[18] +(I(H+1))/LLOOP
[19] P+=UI
    +

```

ORIGINAL PAGE IS
OF POOR QUALITY

STATE	STATION	THUNDERSTORM DAYS (NO./YEAR)	GROUND STRIKE DENSITY (NO./YR./KM ²)
AL	BIRMINGHAM	59,71	13.87
AL	HUNTSVILLE	58,22	13.34
AL	MOBILE	79,78	27.07
AL	MONTGOMERY	92,18	15.44
AK	ANCHORAGE	1.13	0.39
AK	ANNETTE	1.45	0.60
AK	BARROW	0.07	0.08
AK	GARTER ISLAND	0.25	0.17
AK	BETHEL	1.39	0.51
AK	BETTLES	4.07	0.73
AK	BIG DELTA	2.50	0.41
AK	COLD BAY	0.05	0.02
AK	FAIRBANKS	5,12	0.33
AK	GULKAHA	4,70	0.76
AK	HOMER	0,32	0.15
AK	JUNEAU	0,32	0.24
AK	KING SALMON	1,31	0.49
AK	KODIAK	0,29	0.24
AK	KOTZEBUE	0,52	0.15
AK	MC GRATH	0,77	0.45
AK	NOME	0,42	0.16
AK	ST PAUL ISLAND	0,05	0.05
AK	SHEYMA ISLAND	0,15	0.10
AK	SUMMIT	5,00	0.22
AK	TALKEETNA	5,30	0.77
AK	UNAKLEET	1,20	0.48
AK	YAKUTAT	1,59	0.60
AZ	FLAGSTAFF	50,63	15.87
AZ	PHOENIX	23,03	4.00
AZ	TUCSON	39,84	13.29
AZ	WINSLOW	36,34	9.33
AZ	YUMA	7,26	1.43
AR	FORT SMITH	57,05	11.54
AR	LITTLE ROCK	56,97	11.51
AS	PAGO PAGO	26,09	3.73
CA	BAKERSFIELD	2,50	0.95
CA	BISHOP	13,24	2.21
CA	BLUE CANYON	11,83	1.57
CA	EUREKA	4,53	1.23
CA	FRESNO	5,43	1.37
CA	LONG BEACH	3,71	1.10
CA	LOS ANGELES (CITY)	6,21	1.43
CA	LOS ANGELES (LAX)	3,51	1.10
CA	MOUNT SHASTA	13,27	2.16
CA	OAKLAND	2,26	0.57
CA	RED BLUFF	0,70	1.52
CA	SACRAMENTO	4,76	1.27

STATE	STATION	THUNDERSTORM DAYS (NO./YEAR)	DESTRUCTION (NO./YEAR, km ²)
CA	SAN JOSE	4.22	1.14
CA	SAN DIEGO	2.70	2.76
CA	SAN FRANCISCO (CITY)	2.26	3.86
CA	SAN FRANCISCO (SFO)	2.12	3.65
CA	STOCKTON	3.11	1.01
CA	SANTA MARIA	2.32	0.87
CO	ALAMOSA	44.42	12.92
CO	COLORADO SPRINGS	59.69	22.43
CO	DENVER	41.33	11.02
CO	GRAND JUNCTION	34.32	6.36
CO	PUEBLO	40.32	10.99
CT	BRIDGEPORT	21.57	3.50
CT	MARTFORD	22.30	3.62
DE	WILMINGTON	31.03	5.73
DC	WASHINGTON (DCA)	29.07	5.18
DC	WASHINGTON (IAD)	27.13	4.60
FL	APALACHICOLA	70.19	22.94
FL	DAYTONA BEACH	79.61	27.25
FL	FORT MYERS	94.87	47.04
FL	JACKSONVILLE	63.94	20.20
FL	KEY WEST	62.65	19.86
FL	LAKELAND	69.50	48.50
FL	MIAMI	74.04	29.37
FL	ORLANDO	81.21	32.79
FL	ORLANDO (MC COY AFB)	78.82	30.37
FL	PENSACOLA	74.13	29.90
FL	TALLAHASSEE	56.37	30.05
FL	TAMPA	89.19	34.00
FL	WEST PALM BEACH	75.63	28.63
GA	ATHENS	51.52	13.00
GA	ATLANTA	53.19	11.87
GA	AUGUSTA	56.15	15.41
GA	COLUMBUS	56.71	15.61
GA	MACON	56.93	15.43
GA	ROME	51.42	15.67
GA	SAVANNAH	64.33	20.62
GU	TAGUAC	27.03	4.79
HI	HIL ^E	8.75	1.67
HI	HONOLULU	7.07	1.43
HI	KAHULUI	4.95	1.20
HI	LIHUE	8.51	1.64

STATE	STATION	THUNDERSTORM DAYS (NO./YEAR)	GRUNDY STRIKE DENSITY (NO./YR./KM ²)
ID	BELISE	14.84	2.34
ID	LEWISTON	15.75	2.45
ID	POCATELLO	23.11	6.32
IL	CARIB	52.77	13.98
IL	CHICAGO (MIDWAY)	40.54	7.63
IL	CHICAGO (O'HARE)	38.42	6.22
IL	MULINE	27.36	10.01
IL	MCRIA	46.41	10.26
IL	ROCKFORD	42.19	5.38
IL	SPRINGFIELD	50.00	10.79
IN	EVANSVILLE	45.73	5.87
IN	FORT WAYNE	41.00	7.87
IN	INDIANAPOLIS	44.69	8.37
IN	SOUTH BEND	42.89	8.64
IA	BURLINGTON	50.58	11.06
IA	DES MOINES	49.73	11.22
IA	DUBUQUE	44.93	9.20
IA	SIOUX CITY	45.38	10.46
IA	WATERLOO	41.70	8.51
KS	CONCORDIA	58.93	15.71
KS	DODGE CITY	53.53	14.32
KS	GOODLAND	45.74	13.69
KS	TOPEKA	57.58	14.14
KS	WICHITA	55.29	13.25
KY	LEXINGTON	48.76	10.22
KY	LOUISVILLE	45.40	9.13
LA	ALEXANDRIA	68.07	16.96
LA	BATON ROUGE	70.46	20.07
LA	LAKE CHARLES	76.88	22.59
LA	NEW ORLEANS	66.93	20.38
LA	SHREVEPORT	54.16	10.21
ME	CARIBOU	20.33	3.57
ME	PORTLAND	18.05	2.98
MD	BALTIMORE	28.44	5.10
MA	BOSTON	19.33	3.14
MA	NANTUCKET	20.27	3.09
MA	WORCESTER	21.27	3.51

STATE	STATION	THUNDERSTORM DAYS (NO./YEAR)	BIG BANG STRIKE DENSITY (NO./YR./KM ²)
MI	ALPENA	33.29	6.26
MI	DETROIT (DTT)	32.52	6.67
MI	DETROIT (DTA)	33.20	6.67
MI	FLINT	33.03	6.67
MI	GRAND RAPIDS	36.71	6.67
MI	HOUGHTON LAKE	38.54	6.67
MI	LANSING	34.17	6.67
MI	MARQUETTE	28.07	6.67
MI	MUSKEGON	37.34	6.67
MI	SAULT STE MARIE	29.44	6.67
MN	DULUTH	34.66	7.38
MN	INTERNATIONAL FALLS	31.42	5.67
MN	MINNEAPOLIS	36.79	7.41
MN	ROCHESTER	41.00	7.52
MN	SAINT CLOUD	35.76	7.54
MS	JACKSON	65.11	16.30
MS	HERIDAN	58.54	13.31
MO	COLUMBIA	51.50	10.40
MO	KANSAS CITY (MCI)	51.20	11.39
MO	KANSAS CITY (MKC)	49.50	10.59
MO	SAINT JOSEPH	50.35	13.70
MO	ST. LOUIS	44.55	8.61
MO	SPRINGFIELD	58.00	13.00
MT	BILLINGS	28.79	5.00
MT	GLASCOW	27.11	5.80
MT	GREAT FALLS	25.60	5.17
MT	HAVRE	21.60	3.80
MT	HELENA	33.81	3.32
MT	KALISPELL	22.75	3.90
MT	MILES CITY	28.48	6.00
MT	MISSOULA	23.61	4.36
NE	GRAND ISLAND	47.99	11.76
NE	LINCOLN (APT)	48.33	10.77
NE	LINCOLN (CITY)	49.33	11.99
NE	NORFOLK	50.20	13.11
NE	NORTH PLATTE	45.92	11.95
NE	OMAHA (CITY)	40.50	8.00
NE	OMAHA (EPPLY FIELD)	48.60	11.20
NE	SCOTTSBLUFF	43.56	11.93
NE	VALENTINE	45.22	12.74
NV	ELKO	20.72	3.47
NV	ELY	32.00	6.75
NV	LAS VEGAS	14.37	3.00
NV	RENO	13.54	2.00
NV	WINNEMUCCA	14.30	2.24

ORIGINAL
OF POOR QUALITY

STATE	STATION	THUNDERSTORMS DAYS (NO./YEAR)	THUNDERSTORMS DENSITY (NO./YEAR/1000 ²)
NH	CONCORD MT WASHINGTON	20.47 100.33	7.47 2.74
NJ	ATLANTIC CITY	20.47	4.36
NJ	NEWARK	20.47	4.46
NJ	TRENTON	33.22	0.53
NM	ALBUQUERQUE	42.34	11.13
NM	CLAYTON	54.11	17.03
NM	RUSSELL	32.00	0.30
NY	ALBANY	27.04	5.20
NY	BINGHAMTON	31.42	5.94
NY	BUFFALO	30.74	5.10
NY	NEW YORK (CITY)	19.47	3.16
NY	NEW YORK (JFK)	22.32	3.56
NY	NEW YORK (LA GUARDIA)	24.24	4.01
NY	ROCHESTER	29.24	5.21
NY	SYRACUSE	29.39	5.43
NC	ASHEVILLE	49.00	12.18
NC	CAPE HATTERAS	44.75	9.23
NC	CHARLOTTE	41.89	9.35
NC	GREENSBORO	46.57	11.50
NC	RALEIGH	45.67	10.67
NC	WILMINGTTON	40.12	10.08
ND	FARGO	32.33	5.28
ND	BISMARCK	33.58	7.99
ND	WILLISTON	26.77	5.05
OH	AKRON	40.41	3.13
OH	CINCINNATI (ABOVE OBS)	50.41	11.51
OH	CINCINNATI (APT)	44.33	8.01
OH	CLEVELAND	36.42	8.03
OH	COLUMBUS	42.46	8.53
OH	DAYTON	40.32	7.03
OH	TOLEDO	40.00	3.11
OH	MANSFIELD	30.78	7.73
OH	YOUNGSTOWN	35.86	8.68
OK	OKLAHOMA CITY	50.08	10.54
OK	TULSA	32.20	11.21
OR	ASTORIA	7.07	1.32
OR	BURNS	13.86	2.03
OR	EUGENE	14.50	1.60
OR	MCACHAM	15.70	1.82
OR	MEDFORD	8.02	1.03

STATE	STATION	THUNDERSTORM DAYS (NO./YEAR)	GND STRIKE DENSITY (NO./YR./K.M. ²)
OR	PENOLETON	9.90	1.64
OR	PORTLAND	9.50	1.46
OK	SALEM	8.50	1.38
OK	SEXTON SUMMIT	8.70	1.20
PA	ALLEN TOWN	32.82	6.31
PA	AVOCA	31.05	6.56
PA	ERIE	33.36	6.91
PA	HARRISBURG	32.79	6.34
PA	PHILADELPHIA	26.81	4.66
PA	PITTSBURG	36.23	6.53
PA	WILLIAMS PORT	34.20	7.11
PR	SAN JUAN	36.73	7.92
RI	BLOCK ISLAND	16.79	2.68
RI	PROVIDENCE	20.42	3.27
SC	CHARLESTON	56.45	10.60
SC	COLUMBIA	54.27	14.73
SC	GREER	43.37	9.54
SD	ABERDEEN	35.08	8.13
SD	HURON	40.34	9.63
SD	RAPID CITY	42.42	12.17
SD	SIOUX FALLS	43.09	10.23
TN	BRISTOL	45.50	10.55
TN	CHATTANOOGA	56.11	13.95
TN	KNOXVILLE	47.63	10.36
TN	MEMPHIS	52.93	10.28
TN	NASHVILLE	53.42	12.42
TN	OAK RIDGE	52.81	12.71
TX	ABILENE	41.73	7.65
TX	AMARILLO	45.81	12.25
TX	AUSTIN	40.81	6.71
TX	BROWNSVILLE	31.34	3.72
TX	CORPUS CHRISTI	30.70	4.69
TX	DALLAS-FT WORTH (DFW)	45.12	8.04
TX	DALLAS (LOVE FIELD)	40.15	6.62
TX	DEL RIO	35.36	6.30
TX	EL PASO	35.59	6.99
TX	HOUSTON	57.50	17.92
TX	LUBBOCK	45.32	10.12
TX	MIDLAND-ODESSA	36.46	6.76
TX	PORT ARTHUR	34.17	10.71
TX	SAN ANGELO	30.60	6.32
TX	SAN ANTONIO	36.30	6.74
TX	VICTORIA	45.13	9.91

STATE	STATION	THUNDERSTORM DAYS (NO./YEAR)	WINDSTRIKE DENSITY (NO./YEAR/KM ²)
TX	WACO	45.44	7.82
TX	WICHITA FALLS	48.69	4.30
TT	JOHNSTON ISLAND	4.07	1.17
TT	KOROR ISLAND	36.55	5.46
TT	KWAJALEIN ISLAND	39.75	1.78
TT	MAJURO ATOLL	16.52	2.55
TT	PONAPE ISLAND	26.04	3.97
TT	TRUK ATOLL	19.42	2.52
TT	WAKE ISLAND	6.93	1.30
TT	YAP ISLAND	16.03	2.46
UT	MILFORD	32.00	7.33
UT	SALT LAKE CITY	35.29	6.24
UT	WENDOVER	29.00	5.77
VT	BURLINGTON	24.94	4.03
VA	LYNCHBURG	40.50	3.13
VA	NORFOLK	37.07	7.46
VA	RICHMOND	38.75	7.05
VA	ROANOKE	37.80	6.13
WA	OLYMPIA	4.65	1.24
WA	SEATTLE (APT)	7.27	1.60
WA	SEATTLE (CITY)	5.06	1.43
WA	SPokane	10.50	1.74
WA	STAMPEDE PASS	7.29	1.29
WA	WALLA WALLA	11.25	1.51
WA	YAKIMA	6.90	1.25
WV	DECKLEY	45.71	10.27
WV	CHARLESTON	43.37	9.42
WV	ELKINS	44.33	10.33
WV	HUNTINGTON	44.35	9.57
WV	PARKERSBURG	44.00	9.91
WI	GREEN BAY	34.79	6.49
WI	LA CROSSE	40.16	5.20
WI	MADISON	40.62	7.96
WI	MILWAUKEE	35.91	6.40
WY	CASPER	34.26	7.85
WY	CHEYENNE	49.86	15.41
WY	LANDER	31.71	7.05
WY	SHERIDAN	35.50	6.03

DATA IS
POOR QUALITY